IMPACTS OF PARTIAL-RETENTION HARVESTING WITH NO BUFFER ON THE THERMAL REGIME OF A HEADWATER STREAM AND ITS RIPARIAN ZONE

by

Steven Martin Guenther

B.Sc. (Hon's) University of Toronto 2004

A THESIS SUBMITTED IN PARTIAL FULFILLMENT

OF THE REQUIREMENTS FOR THE DEGREE OF

MASTER OF SCIENCE

in

The Faculty of Graduate Studies

(Geography)

UNIVERSITY OF BRITISH COLUMBIA

April 2007

ABSTRACT

The temperatures of stream water and the stream bed influence biogeochemical processes and the growth and distribution of fish and macro-invertebrate species in streams. While numerous studies have examined the effects of various harvesting practices on stream temperature, none has estimated the effects on bed temperature, or conducted heat budget analysis before and after harvest to assess the mechanisms that control the magnitude of post-harvest stream heating.

In this study, we analyzed data from a paired-catchment experiment involving both control and treatment streams and pre- and post-harvest monitoring. The partial retention harvesting resulted in removal of 50% of the basal area along 300 m of the channel in the treatment catchment. Stream temperature, bed temperature, riparian microclimate and stream hydrology were monitored in the treatment stream both before and after harvest. Daily maximum stream temperatures increased by up to over 7 °C during summer. Effects on winter temperatures were relatively small. Summer bed temperatures increased by as much as 6 °C, with greatest warming in areas of down-welling flow into the stream bed. Heat budgets were estimated for two reaches of a headwater stream before and after partial retention harvesting. Heat budget components responded in variable ways to the logging treatment depending on the reach, date, and weather. Incoming solar radiation was the largest input of energy into the stream following harvesting, while latent heat, hyporheic heat, groundwater heat, and bed heat exchanges tended to reduce the amount of daytime stream heating after harvest. These results will assist in understanding and predicting the spatial and temporal variability in stream temperature response to forest harvesting.

TABLE OF CONTENTS

LIST OF TABLES

LIST OF FIGURES

ACKNOWLEDGEMENTS

This research was made possible with the support of many people. Many thanks go to my supervisor Dan Moore, whose guidance, expertise, open door policy, and level of excellence through this project have given me a bench mark to aspire to. Additional thanks go to Markus Weiler for his helpful comments on drafts of this thesis. This research was made possible only with the extensive help in the field by Takashi Gomi, Francis Wu, Jackie Ngai, Jenn Todd, Elisa Scordo, Ian Redden, Dani Ramos, Matt Bauer, Pamela O, and Ritter. I have to specifically thank Takashi Gomi whose work in setting up the research sites gave me the opportunity to work on this extensive data set. Special thanks go to my wife Pam who was an unending source of support through the duration of this degree.

CHAPTER ONE

INTRODUCTION

1.1 SIGNIFICANCE OF STREAM TEMPERATURES AND THE IMPACTS OF FORESTRY PRACTICES

Stream temperature plays a critical role in stream ecology. It influences dissolved oxygen concentrations, rates of biochemical and biological processes, and can control species distributions for both invertebrates and fish [*Beschta et al.*, 1987; *Vannote and Sweeney*, 1980]. Stream temperature is particularly important in relation to cold-water species such as salmonids. Increases in stream temperature reduce the survival of salmonid ova [*Crisp*, 1988] and can interfere with the survival and abundance of salmonid food sources, such as macro-invertebrates [*Crisp*, 1990; *Vannote and Sweeney*, 1980]. In addition to temperature of surface water in a channel, the amount of water exchange in the substrate of the stream channels and its temperature is vital to the survival and spawning success of most salmonid species [*Alexander and Caissie*, 2003; *Curry and Devito*, 1996; *White et al.*, 1987].

It has been recognised for decades that many forestry practices, such as streamside clear-cutting, can cause increases in stream temperature over the summer months [*Johnson and Jones*, 2000; *Levno and Rothacher*, 1967; *Titcomb*, 1926]. Documented increases in summer maximum temperature have ranged up to 13 °C [*Moore et al.*, 2005b]. This influence has generated significant concern about the potential negative influences of forest harvesting on stream ecology, respiration rates as well as nutrient dynamics and transport into downstream systems [*Allen*, 1995; *Findlay*, 1995]. In British Columbia and throughout the Pacific Northwest, a particular concern is the impact that logging-related stream temperature increases have on salmonid populations [*Beschta et al.*, 1987; *Curry et al.*, 2002].

The conventional approach to minimising the impact of forestry practices on stream temperatures is the retention of linear buffer strips along the stream [*Brown*, 1970; *Gomi et al.*, 2006; *Macdonald et al.*, 2003]. However, linear buffer strips are highly susceptible to windthrow, which can render them ineffective. Alternatives to linear buffers are variable retention logging practices, which may have similar benefits to stream temperature with a reduced susceptibility to blowdown or windthrow. As of the late 1990's partial retention logging approaches have been implemented in British Columbia [*Beese et al.*, 2003]. Variable retention

logging practices involve leaving standing trees as patches or as single trees, and will hereafter be called patch retention and dispersed retention, respectively. Similar to linear buffers, variable retention logging has the potential to mitigate seasonal increases of headwater stream temperatures but may be less susceptible to the effects of wind. Partial retention logging approaches can also reduce the opportunity costs for timber companies by not restricting access to portions of the basin, as can occur with continuous linear buffers.

While the use of linear buffer strips to minimize logging-related stream heating has received significant attention in the literature [*Bourque and Pomeroy*, 2001; *Brown*, 1970; *Gomi et al.*, 2006; *Macdonald et al.*, 2003], only one study appears to have tested the ability of a partial retention technique to protect stream temperature, and that was on only one stream [*Macdonald*, 2003]. Therefore further research is warranted to investigate whether partial retention logging approaches are able to minimize seasonal stream temperatures.

1.2 APPROACHES TO QUANTIFYING STREAM TEMPERATURE REPONSE TO FOREST HARVESTING

Two empirical approaches have been used to quantify the effects of stream temperature response to forest practices: (1) spatial comparisons with no pre-harvest data, and (2) studies involving pre- and post-harvest monitoring. The spatial comparison approach involves monitoring temperatures for streams with different amounts of forest harvesting within their catchments, and uses a space-for-time substitution to infer the effects of harvesting [*Burton and Likens*, 1973; *Mellina et al.*, 2002; *Storey and Cowley*, 1997; *Zwieniecki*, 1999]. A major drawback to this approach is that inherent differences in temperature regimes among the study catchments can confound the identification of treatment effects.

Studies involving pre- and post-harvest monitoring are most efficient when some method is employed to control for climatic variations between the pre- and post-harvest years [*Loftis et al.*, 2001]. Some studies have used air temperature data as a covariate [*Curry et al.*, 2002; *Holtby*, 1982]. However, there is often significant scatter in the relation between stream temperature and air temperature, reducing the statistical power of the approach. A more powerful approach is the use of control streams, which remain untreated through the study period. Although some studies have used ANOVA to analyse the post-harvest response for the treatment streams [*Feller*, 1981; *Johnson and Jones*, 2000; *Macdonald et al.*, 2003], many studies used a paired-catchment analysis, which involves fitting a regression between each treatment stream and a control stream using the pre-treatment data; this regression is then used in the post-harvest

period to predict what temperatures would have been had the treatment not been applied [*Feller*, 1981; *Gomi et al.*, 2006; *Harris*, 1977; *Johnson and Jones*, 2000; *Macdonald et al.*, 2003; *Moore et al.*, 2005c]. The differences between the observed post-harvest temperatures and those predicted using the pre-harvest regression constitute estimates of the change associated with the logging treatment. Harris [1977] followed the standard approach of analysing stream temperature metrics computed at an annual time step to avoid potential problems with autocorrelation.

An important limitation to our ability to assess the biological significance of stream temperature changes is that most studies examined metrics, such as summer maximum temperature, that may not be biologically significant, especially in cases where temperatures do not approach or exceed thresholds for mortality. Sullivan *et al.* [2000] and Nelitz *et al.* [2006] argued that the use of a bio-energetic approach may provide a sounder basis for assessing risks to organisms, and that metrics such as the maximum weekly average temperature (MWAT) may be an appropriate metric. Furthermore, there is some suggestion that temperatures between autumn and spring may be important in relation to growth and development of stream organisms [*Holtby*, 1988; *Leggett and Carscadden*, 1978].

Moore *et al.* [2005c] and Gomi *et al.* [2006] pioneered the use of time series regression to allow the analysis of daily time series while explicitly accounting for autocorrelation in the residuals. This approach allows forestry-related stream temperature changes to be estimated on a daily basis, providing more information on the seasonal and interannual variations in temperature response. For example, Gomi *et al.* [2006] found that maximum treatment effects occurred in late spring/early summer, rather than in late summer, when annual temperature maxima normally occur. The use of daily time series also allows calculation of metrics such as MWAT and the effect of forest harvesting on them.

While the approaches described above allow the effects of forest harvesting on stream temperature to be estimated, they do not provide any information on what processes were responsible. This topic is addressed in the next section.

1.3 FACTORS CONTROLLING STREAM TEMPERATURE RESPONSE TO FOREST PRACTICES

Stream temperatures reflect the influences of a variety of energy fluxes, which can be classed as being atmospheric or terrestrial. Atmospheric energy exchanges include solar radiation, longwave radiation, sensible heat, and latent heat. Terrestrial fluxes include bed heat conduction, heat from groundwater discharge, and hyporheic heat exchanges. Heat budgets have

been used to understand stream temperature dynamics in a variety of settings; however most of these studies were not conducted in the context of forest harvesting [*Evans et al.*, 1998; *Webb and Zhang, 1997*]. The earliest heat budget study focused on forest harvesting was conducted by Brown [1969]; since then, only Story *et al.* [2003], Johnson [2004] and Moore *et al.* [2005c] appear to have estimated heat budgets for forestry-influenced streams.

Sensible and latent heat exchanges can be determined using empirical wind functions employing measurements of air temperature, humidity and wind speed [*Brown*, 1969; *Evans et al.*, 1998; *Johnson*, 2004; *Moore et al.*, 2005c; *Webb and Zhang*, 1997]. This approach may result in significant errors since wind in an incised stream channel or under intact forest can often be near or below stall speeds for typical anemometers [*Story et al.*, 2003]. In such cases, some data logger systems record the stall speed, even though the true wind speed was lower, resulting in over-estimates of the sensible and latent heat exchanges. Even with this bias, studies in clear cuts found sensible and latent heat exchanges were small and even one order of magnitude lower than incident solar radiation [*Brown*, 1969; *Johnson*, 2004; *Moore et al.*, 2005c].

The determination of incoming solar radiation in forested environments and their complicated shade regimes is a significant challenge. Webb and Zhang [1997] used a light meter to determine the fraction of incoming light between a site that is covered by tree canopy and one that is not. However, the estimation of shading cannot be represented by a constant fraction of open-site solar radiation because it varies with the sun's movement and changes in cloud cover. Several modelling studies have used geometric calculations of shade based on tree height, terrain angles, and stream width [e.g., *Rutherford et al.*, 1997; *Sridhar et al.*, 2004]. However, these approaches are difficult to apply to dispersed retention harvesting, which should result in more complex patterns of sky blockage. Moore *et al.* (2005c) addressed this problem using hemispheric photographs of the canopy to model the transmission of both direct and diffuse radiation based on the spatial distribution of canopy gap fraction. These analyses were used in conjunction with measurements of direct and diffuse radiation made in a clear cut to model the direct and diffuse radiation reaching the stream surface. This approach also accounts for bank shading and any other obstruction that shades the stream channel by blocking the transmission of solar radiation.

Hydrologic and bed processes can influence the thermal regime of streams. Hyporheic exchange appears to influence stream temperature patterns in both space and time [*Alexander and Caissie*, 2003; *Johnson*, 2004] though only three studies appear to have estimated the associated heat exchange [*Cozzetto et al.*, 2006; *Moore et al.*, 2005c; *Story et al.*, 2003]. Story *et*

al. (2003) found that hyporheic exchange was quantitatively an important process in driving downstream cooling under forest cover below a cut block. Moore *et al.* (2005c) showed that hyporheic exchange appeared to play a secondary, though still important, role within a clear cut, acting to suppress daytime heating. However, estimates of hyporheic exchange flows, and their associated heat exchanges, is subject to considerable uncertainty [*Kasahara and Wondzell*, 2003; *Moore et al.*, 2005c; *Story et al.*, 2003].

Bed heat conduction tends to suppress daytime heating and nocturnal cooling [*Brown*, 1969; *Moore et al.*, 2005c]. Previous studies suggest that bed heat conduction in a clearcut has the potential to be between 10 and 25% of the net radiation of a stream for step-pool units [*Moore et al.*, 2005c] and [*Brown*, 1969] bedrock channel substrates, respectively. Bed heat conduction depends on the thermal properties of the stream bed and also on the vertical temperature gradients within the bed, which in turn depend on the influence of groundwater discharge [*Silliman and Booth*, 1993; *Story et al.*, 2003]. Therefore, the magnitude of bed heat conduction should depend on the local hydrologic context of the stream reach or channel unit.

Groundwater is typically cooler than stream water in summer/daytime and warmer in winter/night-time [*Bogan et al.*, 2003; *Webb and Zhang*, 1997]. Groundwater discharge thus acts to reduce diurnal and seasonal temperature fluctuations. There is mixed evidence about the role of groundwater on stream temperature response to forest harvesting. Where streams have warm sources, such as lakes or wetlands, groundwater discharge can result in downstream cooling, even as a stream flows through a clear cut [*Mellina et al.*, 2002]. However, there is also a widespread belief that shallow groundwater warms in logged basins due to reduced transpiration and increased solar radiation at the soil surface, and that the associated advection of heat by discharge into a stream can contribute to post-logging stream warming [*Bourque and Pomeroy*, 2001; *Brosofske et al.*, 1997; *Hartman and Scrivener*, 1990; *Hewlett and Fortson*, 1982].

1.4 BED TEMPERATURE RESPONSE TO LOGGING AND THE IMPACTS ON THE BENTHIC ENVIRONMENT

While the impacts of logging on stream temperatures are clear, the impacts on the benthic environment are still not understood. Only two studies have examined benthic temperatures in a forestry context, and neither used a before/after approach to quantify the increases in the post-logging period [*Ringler and Hall*, 1975; *Curry et al.*, 2002].

Water exchange between the channel and the stream bed, called hyporheic exchange, is argued to be as vital a component as the temperature of the stream to the survival and abundance

of most salmonid species [*Alexander and Caissie*, 2003; *Curry and Devito*, 1996; *White et al.*, 1987]. Hyporheic exchange is largely controlled by the geomorphic features of the stream channel, such as riffle-pool and step-pool sequences which help force water into the substrate at the top of a riffle or step feature and allow water to remerge in a pool [*Brunke and Gonser*, 1997; *Findlay*, 1995; *Harvey and Bencala*, 1993; *Hill et al.*, 1998; *Kasahara and Wondzell*, 2003].

Water in the hyporheic zone is a mixture of stream and groundwater, and the hyporheic water temperature is determined to a large extent by the amounts of each of the two components and their respective temperatures [*Alexander and Caissie*, 2003; *Hendricks and White*, 1991; *Silliman and Booth*, 1993; *White et al.*, 1987]. Further research has observed that areas of upwelling hyporheic flow have water temperatures related to groundwater and downwelling flow is similar to that of surface water temperatures [*Bilby*, 1984; *Malard et al.*, 2001; *Moore et al.*, 2005c]. Based on this existing knowledge, a reasonable hypothesis is that the response of benthic temperatures to forest harvesting should depend on the local hydrologic environment, in particular whether upwelling or downwelling flow occurs.

1.5 RESEARCH QUESTIONS AND THESIS ORGANIZATION

The literature review above has identified a number of gaps in our understanding of stream temperature response to forest harvesting, and these form the context for the current study. The specific research questions are provided below.

(1) To what extent can a dispersed retention logging treatment that removes 50% of the standing timber in the basin protect a headwater stream from temperature changes? How do treatment effects vary in relation to short-term weather conditions, and the effects of seasonal and inter-annual climatic variations?

(2) What are the temperature changes of the stream bed after logging, and do the temperature changes vary with patterns of hyporheic exchange and groundwater discharge?

(3) Which energy processes control the changes in summer stream temperatures? Can the complex shade environment associated with partial-retention harvesting be adequately characterised using fish-eye canopy photography? How important are the terrestrial processes relative to the better-studied atmospheric processes?

This study addressed these questions at Griffith Creek, a headwater stream located in the Malcolm Knapp Research Forest. The study is part of a broader, interdisciplinary experiment on the ecological effects of alternative riparian management strategies [*Kiffney et al.*, 2003]. The study is unique in that it combines a traditional paired-catchment approach, with data collection before and after harvest and the inclusion of a control stream, with a process-focused heat budget study. It employs the time-series regression approach for developing pre-harvest regressions, to maximize the information available in the daily time series data.

The remainder of the thesis is organized as follows. Chapter Two describes the study site, field monitoring program and methods of data analysis. Chapter Three provides an overview of the hydroclimatic context of the study period, with a specific focus on microclimatic conditions over Griffith Creek both before and after harvest. Chapter Four applies the paired catchment approach to quantify stream temperature response and address question (1). Chapters Five and Six respectively address questions (2) and (3). Chapter Seven summarizes the main conclusions from the three components of the study and identifies topics for further research.

CHAPTER TWO

METHODS

2.1 STUDY AREA

The study was conducted in the University of British Columbia Malcolm Knapp Research Forest. It is one component of a broader experiment on the effects of alternative riparian management strategies on stream and riparian ecology. While the broader experiment currently involves 13 streams subjected to a range of treatments (plus 3 control streams), this study focused on one treatment stream, Griffith Creek. This section provides background to the study area and describes the characteristics of the catchments and streams included in the study.

2.1.1 Physiography and Climate

The University of British Columbia Malcolm Knapp Research Forest (MKRF) is located approximately 60 km east of Vancouver in the Lower Mainland of British Columbia, Canada. This area has a maritime climate exhibiting relatively dry summers and wet mild winters. Mean annual precipitation varies between 2000 and 2500 mm over the study catchments, with the fall and spring periods (between October and April) receiving approximately 70% of the total annual precipitation. Precipitation falling as snow only accounts for approximately 15% of the annual precipitation amounts due to the low elevation and relatively warm maritime climate.

Soils in the forest consist of highly permeable shallow podzols formed in glacial till of approximately 1 m in depth. The soil is underlain by relatively impermeable compacted basal till or granitic bedrock [*Hutchinson and Moore*, 2000]. The forest prior to logging consisted of mature second growth trees approximately 30 to 40 m tall, with a canopy cover greater than 90%. Tree species are dominated by three types, western hemlock (*Tsuga heterophylla*), western red cedar (*Thuja picata*), and Douglas fir (*Pseudo-tsuga menziesii*), from most to least abundant, respectively.

2.1.2 Study Streams

The treatment stream, Griffith Creek, is a first order stream with a basin area of 10 ha. Three streams remained untreated throughout the study to serve as experimental controls (East, Mike, and Spring Creeks); these have similar basin areas, with the largest being 20 ha (see

Figure 2.1 for locations of streams). All streams produce surface flow throughout their length for most of the year and exhibited southerly aspects. A 300 m study reach was designated in Griffith Creek. The 0 m location is the lowest point of the 300 m study reach, and is equipped with a V-notch weir. The 300 m location is the furthest upstream location to produce surface flow in the driest portion of the year. The elevation of Griffith Creek from weir to headwaters ranges from 365 to 405 m above sea level.

The headwater portion of Griffith Creek is characterized by steep channel gradients of approximately 20% in an incised channel, which decreases in steepness in the downstream direction to less than 7% slope. Bed materials change in composition from large cobbles in the headwaters to sand downstream and increasing amounts of organic matter in lower 150 m of the primary study reach.

Two study reaches were designated in Griffith Creek for detailed study of the hydrology and thermal regime. The "Low" Reach was located at approximately the 100 m location of Griffith's primary study reach and was 20 m in length. The "Mid" Reach was 30 m in length and was located at approximately the 180 m location of the Griffith Creek primary study reach (Figure 2.1). Both reaches were instrumented with piezometers and thermocouple nests (see relevant sections for details); in addition, the Low Reach was equipped with a meteorological station directly above the stream.

2.1.3 Logging Treatment

The logging treatment that was applied to Griffith Creek's catchment involved dispersed retention of single spaced trees within the basin including the riparian zone, with 50% of the basal area being removed from within the cut block. Smaller stems were removed, leaving the larger stems for harvest at a later date. Logging started in September, 2004, and was completed by the end of November, 2004. The forest remained intact for the top 80 m of Griffith Creek because logging was not feasible in the upper portion of the basin (Figure 2.1). Timber was removed using skidders on the east side of Griffith Creek, and by high-lead cable yarding on the west side, due to the steeper slopes.

2.2 FIELD MEASUREMENTS

2.2.1 Stream temperature

Stream temperature in MKRF was recorded with Onset 32K StowAway TidbiT temperature probes which are accurate to ±0.2°C. Each stream involved in this study at MKRF

was equipped with one temperature probe at the lower boundary of the cut block, and for the control streams at an equivalent downstream distance (≈ 300 metres downstream from its headwater). Griffith Creek was also equipped with three additional data loggers at approximately 100 m intervals upstream of the lower boundary. All temperature loggers were placed in pools of the streams to ensure data loggers were submerged in water year round and equipped with solar shields, made of perforated 5 cm diameter white PVC pipe, to ensure only water temperature was measured. Data collection began 2 years prior to timber harvesting to ensure enough data was collected to fit the pre-logging regressions in the paired-catchment design.

2.2.2 Bed temperature

Bed temperature data were collected at the Low and Mid Reaches of Griffith Creek. Measurements were made using copper-constantan thermocouples with measurement precisions of ±0.2°C and were recorded using Campbell Scientific 21X data loggers and multiplexers. Temperatures were scanned every 10 s and averaged every 10 minutes. Thermocouples were installed in the bed using wooden stakes to which the thermocouples were attached, referred to as thermocouple nests, which were driven into the stream bed. Nests were installed so that depths of thermocouples were either 1, 5, 10, 15, and 30 cm or 1, 5, 10, and 20 cm below the stream bed. Bed temperature data collection started in fall 2003 at the Mid Reach, while the Low Reach was instrumented in February, 2004. Both sites recorded bed temperatures until 11 September 2004, when data loggers were removed for timber harvesting, and data loggers were reinstalled on 23 March 2005. Thermocouple nests were not moved between the pre- and post-treatment periods.

2.2.3 Discharge

Discharge was measured at the lower and upper boundaries of the study reaches and occasionally at additional locations within the reaches throughout the summer of 2005. The method employed was a constant rate NaCl dilution gauging method outlined in Moore [2005a]. A WTW electrical conductivity (EC) and temperature probe was used to measure the EC of the stream water before the injection began (EC_{bg}) and when the EC reached a plateau value (EC_{ss}). Discharge (Q) was calculated as:

[2.2.3.1] $$Q = \frac{q}{k\left(EC_{ss} - EC_{bg}\right)}$$

where q is the injection rate of the salt solution, and k is the slope of the linear relation between relative concentration (RC) and EC. The coefficient k was derived by adding 10 ml of the injection solution to 1 L of stream water, creating a secondary solution. This secondary solution was then added in 10 ml increments to a 1 L volume of stream water; EC was measured after each addition of secondary solution. RC then can be calculated as

$$[2.2.3.2] \qquad RC = \frac{RC_{\text{sec}} \Sigma y}{(V_c + \Sigma y)}$$

where, Σy is the cumulative amount of secondary solution added, and V_o is the volume of stream water (L), RC_{sec} is the relative concentration of the secondary solution and can be calculated as

$$[2.2.3.3] \qquad RC_{\text{sec}} = \frac{X}{V_o + X}$$

where X and V_o are the volume (L) of injection solution and stream water used to make the secondary solution, respectively.

Rating curves using a power-law relation were fitted between the measured discharges and the stream stage at the time of measurement; stream stage was measured continuously at a stilling well installed at the 0 m location of Griffith Creek. Under suitable conditions (i.e., complete tracer mixing within the dilution reach), discharge measurements based on constant-rate salt injection can be accurate within ±5% of the calculated value [Moore, 2005a].

2.2.4 Hydraulic gradients

2.2.4.1 Piezometers and installation

Hydraulic gradients within the stream bed were measured using two types of piezometers: 6 mm internal diameter plexiglas piezometers (0.60 m in length), and 12 mm internal diameter aluminium drive point piezometers (0.65 m in length). Both types had a 0.05 m perforated section at the bottom of the pipe. Aluminum piezometers were driven into the stream bed to the desired depth while plexiglas piezometers were installed using a steel drive rod with a steel sheath around it. The drive rod and sheath were driven into the stream bed to the desired depth, the drive rod was withdrawn, and the piezometer was dropped into the sheath. Once the piezometer was in place, the sheath was also removed from the stream bed.

2.2.4.2 Measurement

Hydraulic head levels were measured using an electronic beeper to determine the height of the water inside the piezometers. Stream water height along the piezometer was also

measured. These measurements were made on a weekly basis throughout the summers of 2004 and 2005. Accuracy is approximately ± 5 mm for each hydraulic head measurement.

2.2.4.3 Calculations and errors

Hydraulic gradients (*HG*) were calculated using equation [2.2.4.1]:

[2.2.4.1] $$HG = \frac{\Delta h}{L}$$

where Δh is the difference in hydraulic head between two points, and L is the distance between head measurements, equal to the depth of the piezometer screen within the bed. Piezometers were installed to depths of at least 20 cm. The depth of the piezometer screen was calculated by subtracting the length of tube protruding above the bed from the distance from the top of the piezometer tube to the mid-point of the screen. The piezometer depth is accurate to approximately ± 5 mm.

Relative errors in calculated hydraulic gradients were calculated as:

[2.2.4.2] $$\frac{\delta HG}{HG} = \frac{\delta(h_2 - h_1)}{(h_2 - h_1)} + \frac{\delta L}{L}$$

where δHG is the error in hydraulic gradient, $\delta(h_2 - h_1)$ is the error in the hydraulic head difference (10 mm), δL is the error in the piezometer depth (5 mm), and h_1 and h_2 are the hydraulic head measurements. The highest error in the term $\frac{\delta L}{L}$ is 0.025 (for a depth of 20 cm, which was among the shallowest depths for piezometers). Thus, the largest relative error in the calculated hydraulic gradients is

[2.2.4.3] $$\delta HG_{\max} = \frac{dh}{dl} \cdot \frac{10}{dh} + HG \cdot 0.025 = 0.05 + HG \cdot 0.025$$

Therefore, the errors for hydraulic gradients of 0.05 and 0.5 are 0.05 and 0.06, respectively. Considering the magnitudes of possible errors in hydraulic gradients, all values of hydraulic gradient less than 0.05 in magnitude are considered neutral.

2.2.5 Hydraulic conductivity

2.2.5.1 Method

Hydraulic conductivity (K) was measured 6 times throughout the summer of 2005 in 6 Plexiglas piezometers located in the stream in both the Low and Mid reaches to capture a range of flow conditions throughout the summer. A version of the two point falling head test outlined

by Baxter *et. al.* [*2003*] was used due to the high K of the stream substrate, which meant that water levels fell too quickly to make multiple measurements. The piezometer was filled to overflowing by pouring water into the top to create a positive head gradient, then the time taken for the head to fall to the stream water level was recorded. The initial head was thus the top of the piezometer tube, and the second point was the stream water level.

2.2.5.2 Error Assessment

Errors for K were assessed using an approximate 68% confidence interval (CI) around the geometric mean for each piezometer. These were calculated as:

[2.2.5.1] $$CI = 10^{mean(\log K) \pm s_e}$$

where s_e is the standard error and calculated using equation [2.2.5.2]

[2.2.5.2] $$s_e = \frac{sd(\log K)}{\sqrt{n}}$$

where *sd* is the standard deviation of the logarithm (base 10) of the *K* values, and *n* is the number of observations.

2.2.6 Meteorological measurements

Measurements of wind speed, air temperature, and relative humidity were made at two locations in MKRF starting in the summer of 2003. A meteorological site was established directly over the water of Griffith Creek within the Low Reach. The second meteorological site was located approximately 1 km away in a clear cut area that was logged in 2002, called control met site (see figure 2.1 for location of Griffith Creek and control met site). At both sites measurements were made using a Met One Anemometer (wind speed), and a Campbell Scientific CS-500 temperature and humidity probe, that were recorded with a Campbell Scientific CR10X data logger every minute and averaged every 10 minutes.

2.2.7 Solar radiation

Solar radiation was measured at the control met site starting in the summer of 2003. Two Kipp and Zonen CM-6B pyranometers were scanned every second and averaged every 10 minutes. One of the pyranometers measured total incoming shortwave radiation while the other measured only diffuse radiation with the use of a shadowband that was adjusted every few days throughout the summer months. Five additional CM-3 pyranometers were installed directly above Griffith Creek to calibrate and assess errors of solar radiation modelling. At each location

where a pyranometer was installed in Griffith Creek, a hemispherical photograph was taken of the forest canopy that was shading the pyranometer (see additional details in next section).

2.2.8 Canopy photography

Along the study reaches of Griffith Creek, hemispheric images of the forest canopy above the stream were taken every 3 m once each in the summers of 2004 and 2005. All hemispheric canopy images were oriented to north using a compass and levelled with a fish eye level to ensure the images took a picture of the canopy directly above the stream. These images were analyzed using Gap Light Analyzer software [*Frazer et al.*, 1999], to determine the gap fraction distribution, which was used for modelling incident solar radiation at the stream.

Hemispheric canopy images were taken using a digital camera using auto focus and automated light settings to optimize the image quality. These settings resulted in varying hues of blues and white for gaps, which was problematic when setting the colour thresholds in GLA to determine gaps in the canopy. Best results were obtained when hemispheric images were pre-processed using Photoshop to render all sky fields to the colour white. This procedure allowed for more precise gap fraction analysis because the sky was analyzed uniformly as a gap, compared to the hues of blue and white, which behaved differently with varying threshold levels. Thresholds needed to be significantly higher (less gap) than visual interpretation would suggest to achieve modelled below-canopy radiation values that matched measured data.

2.2.9 Stream geometry measurements

Measurements of stream geometry were conducted for both of the study reaches in the summers of 2004 and 2005. A longitudinal reference line was set up along the study reaches of Griffith Creek. At 1 m intervals perpendicular to the reference line, stream cross sections were measured. Cross sections were established by measuring depths where the channel cross section changed shape and the distance from the stream bank.

2.2.10 Evaporation

To verify the evaporation rates calculated using the Penman equation (Equation 2.3.6.4) described below, four Plexiglas evaporation pans were installed in the stream water of Griffith Creek. The evaporation pans were transparent to minimize heating of the water in the pans (see Figure 2.2 for diagram of evaporation pan). The pans were connected to a Mariotte reservoir,

which maintained a constant water level within the pan. Evaporation from the pan resulted water being drawn from the reservoir.

The four evaporation pans were located along approximately 100 m of the stream, between the Low and Mid Reach. During each visit in the field, when no precipitation was occurring, evaporation pans were measured in the morning and once or twice throughout that day, approximately every 4 hr, to determine the evaporation rates. Temperature of the water in the evaporation pan and the stream water surrounding it were also measured to calculate vapour pressure accurately.

2.2.10.1 Evaporation calculation and error

Evaporation (E) was calculated using equation [2.2.10.1]

[2.2.10.1] $$E = (\Delta h \cdot a)/(A \cdot \Delta t)$$

where Δh is the change in height of the reservoir, a the internal area of the reservoir less the area of the air tube (254 mm^2), A is the area of the pan ($1.8 \cdot 10^4$ mm^2) and Δt is the change in time (s). The error then can be calculated as

[2.2.10.2] $$\frac{\delta E}{E} = \frac{\delta h}{\Delta h} + \frac{\delta a}{a}$$

The measurement error of h can be assumed to be 1 mm, which then makes δh = 2 mm, and an average value for Δh was 5 mm over a 4 hr period. Error of the reservoir area can be calculated using equation [2.2.10.3]

[2.2.10.3] $$\delta a = 2\pi r_2 \cdot \delta r_2 + 2\pi r_1 \cdot \delta r_1$$

where r_1 is the external radius of the air tube and r_2 the internal radius of the reservoir. The measurement error of the radii are 0.05 mm for each measurement, which then makes δa = 4 mm^2. Since an average measurement period was 4 hr, then an estimate of the error can be assumed to be approximately 6.0 10^{-4} mm h^{-1}.

2.3 DATA ANALYSIS

2.3.1 Treatment effect calculations

Treatment effect is defined as the change in a system's response, in this case stream temperature, which is caused by a specific treatment such as partial retention logging. The analysis involved fitting a regression relation using pre-harvest temperature data from a treatment stream as the predictor variable and temperature data from a control stream as the

response variable. After harvest, the pre-harvest regression was used to predict what the temperature in the treatment stream should have been had logging not occurred. The difference between the observed and predicted temperatures is an estimate of the treatment effect.

One challenge in fitting the pre-harvest regressions is that the residuals are temporally autocorrelated, *i.e.* the residual on a given day is correlated to the residual of the preceding day or possibly days. Temporal autocorrelation violates the assumption of independence required by ordinary least squares regression. Therefore, Generalized Least Squares (GLS) regression analysis was employed using the statistical package S-Plus. Generalized Least Squares regression does not require that the residuals be independent. The fitted model was:

[2.3.1.1] $$y_t = \beta_o + \beta_1 x_t + \beta_2 \sin(2\pi j / T) + \beta_3 \cos(2\pi j / T) + \varepsilon_t$$

where y_t and x_t are the temperatures of the treatment and control stream respectively, β_o, β_1, β_2, and β_3 are regression coefficients, j is the Julian calendar day, and T is the number of days per year (365.25). The terms $\sin(2\pi j / T)$ and $\cos(2\pi j / T)$ were added to the model as sinusoidal seasonal trends to help account for any seasonality in the residuals [*Moore*, 2005c; *Watson*, 2001]. The error term in the model (ε_t) was modelled as an autoregressive process to the order "k" using equation 2.3.1.2.

[2.3.1.2] $$\varepsilon_t = \rho_1 \varepsilon_{t-1} + \rho_2 \varepsilon_{t-2} + \ldots.. + \rho_k \varepsilon_{t-k} + u_t$$

where ρ_i is the autocorrelation between error terms at a time lag of "i" days, ε_{t-i} is the error term "i" days before day "t", u_t is a random disturbance that is assumed to have a Gaussian distribution, and k is determined by analyzing the number of days which are significantly autocorrelated to the stream temperature that is being calculated using Equation 2.3.1.1.

Treatment effect (T_e) can then be calculated as:

[2.3.1.3] $$T_e = y_t - \hat{y}_t$$

where y_t and $\hat{y}_t$ are the measured and predicted temperatures of the treatment stream on day t.

2.3.1.1 Stream temperature

Temperature data were summarised from 10 min intervals to daily minimum, maximum, and mean temperatures for all temperature loggers. Treatment effects for stream temperatures were calculated for all four temperature loggers in Griffith Creek. Regressions were fitted using each of the three control streams (Mike, Spring and East Creeks). The fitted regression with the lowest standard error of the residuals (Mike Creek) was then used for calculating the treatment effect. To assess the stability of the pre-harvest regression, regressions were also fitted for

temperatures in the other two control streams (East Creek and Spring Creek) using Mike Creek temperature as a predictor variable. These "control-control" regressions were fitted using data from the pre-harvest period, then applied for the post-harvest period. Under the null hypothesis of no treatment effect (true in the case of a control-control regression), the distribution of residuals for the post-harvest period should not differ statistically from those for the pre-harvest period.

2.3.1.2 Bed temperature

To assess the effect of the logging on the bed temperatures, the same regression analysis was applied to bed temperatures collected in Griffith Creek. No bed temperatures were recorded in a control stream; therefore, the control stream temperature of Mike Creek was used as the independent variable. Bed temperatures were also summarized from 10 min intervals to daily minimum, maximum, and mean variables prior to regression analysis.

2.3.2 Principal component analysis (PCA)

Although PCA does not appear to have been applied previously to stream bed temperatures, it is widely used in meteorology, climatology and hydrology to reduce the size of data sets and to find underlying patterns [*Bao et al.*, 2002; *Jolliffe*, 1990; *Mantua et al.*, 1997; *Termonia*, 2001]. It is particularly useful for exploring data sets comprising time series measured at multiple locations, which is the structure of the bed temperature data set. PCA has also been used in studies of flora and fauna species in streams in relation to different hydrological and geomorphological factors [*Bornette and Amoros*, 1991; *Brittain et al.*, 2001; *Shieh and Yang*, 2000].

Bed temperature data were collected at 10 minute intervals at multiple depths and locations in the stream bed at both the Low and Mid Reaches of Griffith Creek. Given the differences in hydrological processes between the two reaches, PCA was applied separately to the two reaches, using the statistical package S-Plus. The PCA involved the correlation matrix, not the covariance matrix. Eigenvalues of near or greater than 1 were considered significant, and PC scores for the significant PC's were plotted against time to determine the structure of variance represented by each PC.

2.3.3 Cross correlation analysis

Cross correlation analysis was conducted on bed temperatures to determine their relations with stream and groundwater temperatures in both reaches in the pre- and post-logging periods. Bed, stream, and groundwater temperatures were assembled for two-day periods for each study reach under both clear and cloudy skies for both the pre- and post-logging periods. Each bed temperature measurement was cross-correlated to groundwater and stream temperatures, respectively, using the statistical package R [*Ihaka and Gentleman*, 1996]. The maximum correlation coefficients for each cross correlation were recorded, along with the lag associated with the maximum cross-correlation.

2.3.4 Hyporheic exchange estimation

Hyporheic exchange rates were estimated from physical measurements made in the field. The assumption was made that hyporheic exchange is direct from step to pool and no water travels further than the immediate downstream pool. If this is assumed then F_{hyp} can be defined as:

[2.3.4.1] $$F_{hyp} = A_{\inf} \cdot q_z / L_{s-p}$$

where A_{inf} is the infiltration area of the step (m^2), q_z is the rate of infiltation ($m^3\ s^{-1}$) and L_{s-p} is the distance between step and pool (m). The infiltration area and the length between step and pool were estimated from piezometer measurements in the field, while q_z was calculated using one of two methods. The first uses Darcy's Law:

[2.3.4.2] $$q_z = K_{sat} \cdot \Delta h / \Delta z$$

where q_z is the flux rate of water infiltrating the bed ($m\ s^{-1}$), K_{sat} is the saturated hydraulic conductivity in step-pool sections of the streams, and $\Delta h / \Delta z$ is the vertical hydraulic gradient in the infiltration area of the step. This method is complicated by two factors. First is the assumption that the medium through which the water is moving should be homogenous, which cannot necessarily be assumed. Secondly, the measurement of hydraulic conductivity in this environment is difficult due to the relatively high conductivity values and the uncertainties involved in using a two point method. Therefore, a second method can be used, as described by equation 2.3.4.3, which does not require these two assumptions to hold.

[2.3.4.3] $$q_z = \phi v$$

where ϕ is the effective porosity of the material and v is the vertical velocity of the water infiltrating the stream bed. The effective porosity values were assumed to be 0.30, which is

typical for sands and gravels [*Freeze and Cherry, 1979*]. Velocities of down-welling locations identified using hydraulic head measurements were calculated using the lag between the 1 and either the 5 or 10 cm thermocouples located in these steps. Therefore, velocities were calculated using equation 2.3.4.4.

[2.3.4.4] $$v = (\Delta z)/\tau_{\max}$$

where Δz is the difference in depth (m) between the thermocouples, and $\tau_{\max}$ is the time lag between the two thermocouple maximum daily temperatures.

2.3.5 Stream geometry calculations

Reach-average width and depth were calculated from the stream geometry measurements for use in the heat budget calculations. Firstly, the average depth for each cross section $(\overline{d_i})$ was calculated

[2.3.5.1] $$\overline{d_i} = \sum_{l=1}^{n}\left[(w_{l-1} - w_l)\cdot d_{l-1}\right] + \left[(w_{l-1} - w_l)\cdot(d_l - d_{l-1})\cdot 0.5\right]$$

where w_l and d_l are the distance from a stream bank and the corresponding depth in metres, respectively. Reach average width $(\overline{w})$ was calculated as:

[2.3.5.2] $$\overline{w} = \frac{1}{n}\sum_{i=1}^{n} w_i$$

where n is the number of cross-sections measured, and w_i are the individual width measurements (m). Average depth of the study reach was calculated using Equation 2.3.5.3:

[2.3.5.3] $$\overline{d} = \frac{1}{n\overline{w}}\sum_{i=1}^{n}\left(w_i\overline{d_i}\right)$$

where $\overline{d}$ is the reach average depth (m).

2.3.6 Heat budget calculations

To quantify the relative contribution of the processes within the stream that are contributing to the changes in stream temperature a heat budget approach was applied to the two study reaches of Griffith Creek in both the pre- and post-logging period. Two-day periods in July and August consisting of at least one day of cloudless sky and little discharge variability were used for the analysis. The heat budget that was used is a combination heat budget and water balance model from Moore *et al.* [*2005c*].

$$[2.3.6.1] \qquad \frac{\Delta < T >}{\Delta t} = \frac{F_{us}(T_{us} - T_{ds})}{w_s L d_*} + \frac{Q^* + Q_e + Q_h + Q_c + Q_{gw} + Q_{hyp}}{\rho c_p d_*}$$

where the term $\frac{\Delta < T >}{\Delta t}$ is the change in the spatial mean water temperature (°C) over time, F_{ds} is the downstream discharge ($m^3\ s^{-1}$), T_{us} and T_{ds} are the stream temperatures at the upstream and downstream boundaries of the reach (°C), w_s is the mean water surface width (m), and L and d_* are the length and average depth of the study reach (m). Q^* is the net radiation ($W\ m^{-2}$), Q_e the latent heat exchange ($W\ m^{-2}$), Q_h is the sensible heat flux from air to water ($W\ m^{-2}$), Q_c is the bed heat conduction ($W\ m^{-2}$), Q_{gw} the energy exchange from ground water inflow ($W\ m^{-2}$), Q_{hyp} is the energy exchanged from hyporheic exchange ($W\ m^{-2}$), ρ is the water density ($kg\ m^{-3}$), and c_p the specific heat of the water ($J\ kg^{-1}\ K^{-1}$). Each component of the heat budget will be explained in detail below.

2.3.6.1 Net radiation

Net radiation (Q^*) is one of the more complicated processes to quantify in forested environments. Since the banks of the stream and the trees shade the stream channel at different times of the day, the most appropriate method to accurately determine the actual amount of radiation that is reaching the stream channel is to use a model. The model of net radiation can be expressed in two components shortwave and longwave radiation. The shortwave (K^*) component can be expressed as:

$$[2.3.6.2] \qquad K^* = (1-\alpha)[D_t g_t + S_t f_v]$$

where α is the albedo, D_t and S_t are the direct and diffuse components of incident solar radiation at time (t), respectively ($W\ m^{-2}$), g_t is the canopy gap fraction at the sun's position at time (t). Longwave radition (L^*) was expressed as:

$$[2.3.6.3] \qquad L^* = [f_v \varepsilon_a + (1-f_v)\varepsilon_f]\sigma(T_a + 273.16)^4 - \varepsilon_w \sigma(T_w + 273.16)^4$$

where ε_a, ε_f, ε_w are the emissivities of the atmosphere, foliage, and water, σ is the Stefan-Boltzmann constant ($5.67\ 10^{-8}\ W\ m^{-2}\ K^{-4}$), and T_a and T_w represent the temperature of the air and water (°C), respectively. Emissivity values of 0.95 were used for both foliage and water, atmospheric emissivity was calculated using the Idso [1981] equation. The sky view factor is represented by f_v, and is calculated using:

$$[2.3.6.4] \qquad f_v = \frac{1}{\pi}\int_0^{2\pi}\int_0^{\pi/2} g^*(\theta, a_s)\cos\theta \cdot \sin\theta \cdot d\theta \cdot da_s$$

where $g^*(\theta,a_s)$ is the gap fraction as a function of zenith and azimuth angles, and θ and a_s are the zenith and azimuth angles respectively. Net radiation was then calculated as:

[2.3.6.5] $$Q^* = K^* + L^*$$

Solar radiation was modeled using 5° increments of both zenith and azimuth angles. Modeled radiation values were then compared to measured values over Griffith Creek in both the pre- and post-logging periods to calibrate the hemispheric images defining the amount of radiation penetrating the canopy.

2.3.6.2 Latent heat

The latent heat exchange, Qe, is expressed using a Penman equation from Webb and Zhang [1997]:

[2.3.6.6] $$Q_e = 285.9(0.132 + 0.143u_a)(e_a - e_w)$$

where u_a is the wind speed (m s^{-1}), and e_a and e_w refer to the vapour pressures (kPa) of the air and water, respectively. Saturation vapour pressure (e_{sat}) was calculated as a function of air or water temperature (T) as follows:

[2.3.6.7] $$e_{sat} = 0.6108 \cdot 10^{7.5 \cdot T/(T+237.3)}$$

The vapour pressure at the water surface was assumed to equal e_{sat}, while the actual vapour pressure of the air (e_a) was calculated using equation 2.3.6.8:

[2.3.6.8] $$e_a = \left(\frac{RH}{100}\right) e_{sat}$$

where RH is the relative humidity measured at the riparian meteorological site in Griffith Creek the stream.

2.3.6.3 Sensible heat

The sensible heat flux from the air to the water, Q_h, is computed as:

[2.3.6.9] $$Q_h = [\gamma(T_a - T_w)/(e_a - e_w)]Q_e$$

where γ is the psychometric constant of 0.622 kPa°C^{-1}, using an average value of atmospheric pressure of 98.0 kPa, and T_a and T_w are the temperatures (°C) of the air and water respectively. The terms e_a, e_w, and Q_e are the same as described above.

2.3.6.4 Bed heat conduction

Bed heat conduction, Q_c, was calculated using Fourier's law as:

[2.3.6.10] $$Q_c = K_c(T_b - T_w)/(0.04m)$$

where K_c is the thermal conductivity (W m^{-2} °C^{-1}), and T_b and T_w are bed temperatures at depths of 0.05 and 0.01 m, respectively (°C). The thermal conductivity was assumed to equal 2.6 W m^{-1} K^{-1}, based on estimates provided by Lapham [*1989*] using a porosity value of 0.30, which is typical for sands and gravels [*Freeze and Cherry, 1979*].

2.3.6.5 Heat transfer associated with hyporheic exchange

Energy exchange with the hyporheic zone can be expressed as:

[2.3.6.11] $$Q_{hyp} = \frac{\rho c_p F_{hyp}(T_{hyp} - <T>)}{w_s}$$

where F_{hyp} is the hyporheic exchange (m^3 s^{-1} m^{-1}), T_{hyp} is the temperature of the hyporheic zone in °C, and $<T>$ is the spatial mean water temperature (°C). Hyporheic exchange was determined using physically derived hyporheic exchange values described above. Hyporheic temperatures T_{hyp} were measured using thermocouples at 0.01 m depths located in up-welling zones of the stream.

2.3.6.6 Groundwater heat

Groundwater contribution (Q_{gw}) to the heat budget can be expressed as:

[2.3.6.12] $$Q_{gw} = \frac{\rho c_p F_{gw}(T_{gw} - T_{us})}{w_s}$$

where the terms T_{gw} and T_{us} are temperatures of the groundwater and the upstream boundary of the sub-reach (°C). These temperatures were acquired by identifying seepage zones and measuring these water temperatures. F_{gw} is the groundwater inflow rate (m^3 s^{-1} m^{-1}) and is computed as the difference in discharge between the upstream (F_{us}) and downstream (F_{ds}) discharges (m^{3}s^{-1}), measured using constant-rate salt dilution. The groundwater inflow rate is then calculated as:

[2.3.6.13] $$F_{gw} = \frac{F_{ds} - F_{us}}{L}$$

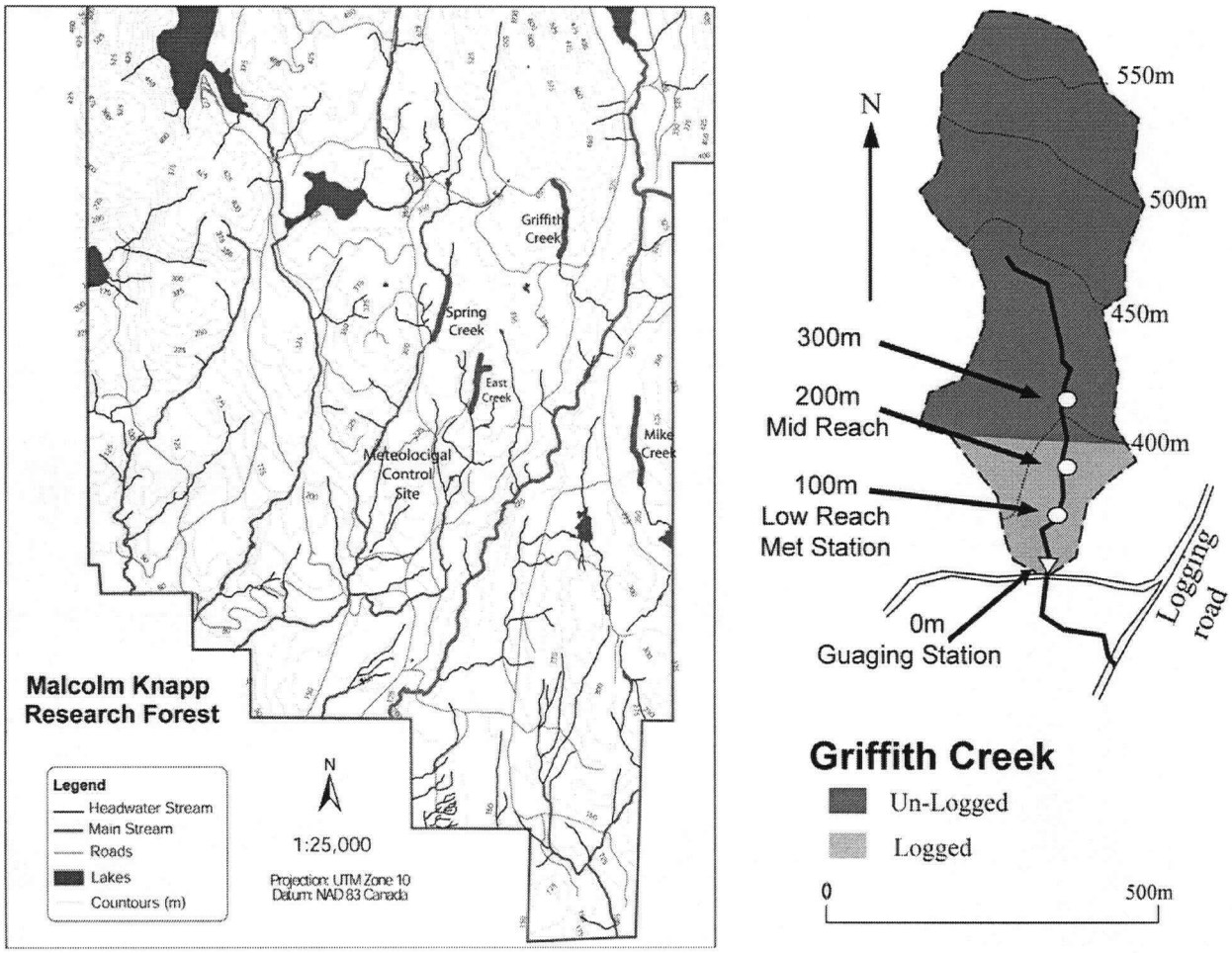

Figure 2.1 Map of Malcolm Knapp Research Forest (left) showing the location of study streams and control meteological site, and map of Griffith Creek (right) showing temperature loggers, meteorological site, study reaches, and gauging station.

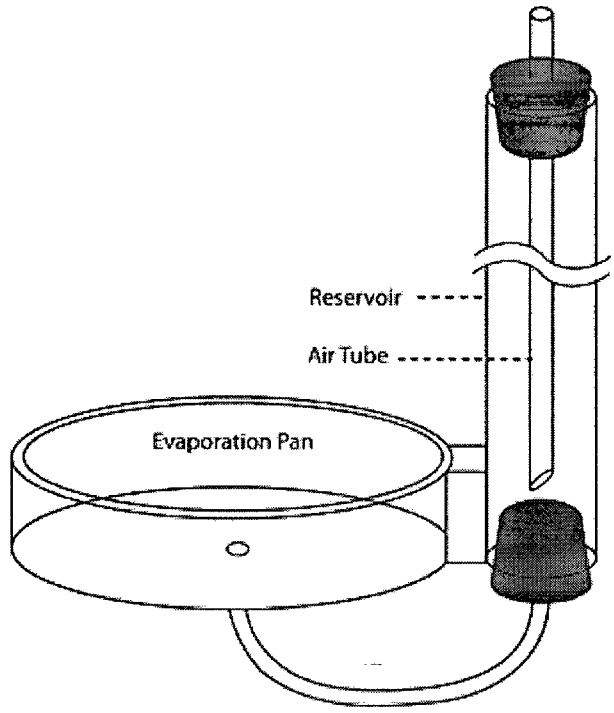

Figure 2.2 Diagram of Plexiglas evaporation pan. Internal radii of evaporation pan and mariotte reservoir are 73.1 and 9.5 mm, respectively, and external radius of air tube is 3.15 mm.

CHAPTER THREE

HYDRO-CLIMATIC CONDITIONS DURING THE STUDY PERIOD

3.1 STUDY PERIOD HYDROCLIMATE

Air temperatures were similar among the summers from 2002 to 2006 (Figure 3.1), with the pre- and post-logging periods showing similar ranges of minimum, mean, and maximum temperature (Table 3.1). Summer precipitation varied by almost a factor of five among years, with the driest and wettest summers occurring during the pre-logging period.

Stream discharge for Griffith Creek and an un-logged control stream, East Creek, varied similarly over the study period (Figure 3.1). Discharge at East Creek was approximately an order of magnitude greater than at Griffith Creek, consistent with the difference in drainage area. Summer mean discharge at East Creek generally varied in concert with summer total precipitation, with the exception of 2004, which had the highest precipitation but lower streamflow than in 2005 (Table 3.1). However, 2004 had the highest summer mean air temperatures, likely resulting in greater evapotranspiration. Maximum stream temperature at East Creek generally followed mean air temperature, with the coolest conditions in 2002 and the warmest in 2004.

Overall, the post-logging period was climatologically within the range of variability observed during the pre-logging summers, so that the pre-harvest regression relations should be valid during the post-harvest period. Based on East Creek temperatures, it appears that 2004 had the most extreme conditions for stream heating, so that the post-logging stream temperature changes may not be as extreme as could have occurred under drier conditions.

3.2 POST-LOGGING CHANGES IN THE RIPARIAN ZONE

3.2.1 Canopy cover

Following the 50% partial retention logging treatment, canopy closure decreased by 13.0% and 14.5% for the Low and Mid Reaches, respectively, resulting in canopy closures of 81.5% for both reaches. Paired pre- and post-harvest hemispherical canopy photographs from the same locations over Griffith Creek show that the predominant reduction in shade occurred at low zenith angles, so that increases in solar radiation reaching the stream would mainly occur near noon of each day (Figures 3.2 and 3.3). Figure 3.4 shows the relatively open canopy in the

post-logging period within the Griffith Creek basin, with large amounts of sunlight reaching the ground.

3.2.2 Wind speed

Mean July-August wind speeds at the control site were about 1.6 m s^{-1} in the pre-harvest period, compared to 1.1 m s^{-1} in the post-harvest period. Prior to harvest, wind speeds in the riparian zone were often near the stall speed of 0.447 m s^{-1} and showed little correlation with wind speeds at the open site ($r^2 = < 0.01$) (Figure 3.5). After harvest, riparian wind speeds increased and showed greater correlation with wind speeds in the open ($r^2 = 0.65$).

3.2.3 Air temperature

Scatterplots of July and August daily minimum temperatures between the Griffith Creek riparian meteorological station and the control station show no clear difference between the pre- and post-harvest periods, and the regression lines indicate close to a 1:1 relation between the two sites (Figure 3.6). The regression fits became stronger after logging, with r^2 increasing from 0.77 in the pre-logging period to 0.88 in the post-logging period.

The scatterplots and regression lines for daily maximum air temperature show that there were no logging-related increases in the riparian zone of Griffith Creek when temperatures at the control station were near 15 °C, but increases exceeded 2 °C when control temperatures were greater than 25 °C (Figure 3.6). Regression fits strengthened from the pre-logging to the post-logging period, with r^2 increasing from 0.90 to 0.97. The post-logging regression line was roughly parallel to the 1:1 line, with Griffith Creek riparian temperatures being approximately 2 °C lower than the control site temperatures. The Griffith Creek riparian site is approximately 200 m higher in elevation than the control site, which accounts for an approximate 1.3 °C difference using a typical environmental lapse rate of 0.65 °C/100 m elevations. The remaining difference between the sites could reflect the effects of shading and possibly some influence of the stream.

3.2.4 Humidity

Relative humidity and vapour pressure were approximately 10% and 1.5 kPa lower after harvesting, respectively (Figure 3.7). The regression lines for both relative humidity and vapour pressure had r^2 values of 0.86 for the pre-logging period. For the post-logging period, r^2 remained 0.86 for vapour pressure but increased to 0.96 for relative humidity. These reductions in the humidity of the riparian microclimate are likely related to the increases in wind speed

causing increased ventilation in the riparian zone, and thus a greater coupling with broader airmass characteristics and a decrease in the local influence of the stream.

3.2.4. Evaporation

Both measured and calculated evaporation from Griffith Creek increased significantly in the post-logging period (Figure 3.8). The pre-logging period was characterized by low to no evaporation, with 17 calculated and 5 measured values (out of a total of 30) indicating no evaporation or condensation occurring on the stream. In the post-logging period, evaporation rates increased dramatically with no condensation occurring and maximum rates of 9.6 10^{-3} and 9.5 10^{-3} mm/hr for calculated and measured values, respectively.

The substantial scatter in the relation between measured and calculated evaporation is likely due, in part, to spatial variability in the conditions driving evaporation at each pan, which may have differed from those measured at the riparian meteorological station. Thus, the data used in the Penman calculations may not have been representative of conditions at the pans, which were located in pools along a 100-m reach. In addition to the scatter is a tendency for the Penman equation to overestimate evaporation. One possible source of this bias is the fact that the riparian wind speeds were frequently below the anemometer's stall speed, and the default value of 0.447 m s^{-1} would have overestimated wind speed and, thus, calculated evaporation. Another possible source of bias is the lack of correction for atmospheric stability, which would have occurred given that daytime summer air temperatures were generally greater than stream temperature. Overall, however, the Penman evaporation was in the right order of magnitude.

3.2.5. Overview of changes in riparian microclimate

The effect of logging appears to have increased ventilation of the riparian zone, thus coupling it more strongly to the regional climate and disconnecting it from the local influence of the stream. Increased ventilation is clearly evident in the increased wind speed in the post-harvest period, and is also evidenced by the stronger relations between riparian and control climatic elements for the post-logging period. The end result of harvesting was increased solar radiation, daily maximum air temperature and wind speed, with decreased humidity, both relative and absolute. The effects of these changes in riparian microclimate on stream temperature will be the focus of Chapter 6.

Table 3.1 Climate data (total precipitation and air temperature) at MKRF Headquarters and discharge and stream temperature from East Creek and Griffith Creek for July and August.

Variable	Year				
	2002	2003	2004	2005	2006
Air T_{max} (°C)	32.0	32.5	35.0	31.0	35.5
Air T_{mean} (°C)	17.7	18.7	19.5	18.1	18.2
Air T_{min} (°C)	7.0	8.0	9.0	9.0	8.5
Days ≥ 30 (°C)	6	5	2	3	4
Precipitation (mm)	57.4	26.8	194.7	159.4	44.2
Q_{mean} Griffith (Ls^{-1})	NA	NA	0.72	1.15	0.21
Q_{mean} East (Ls^{-1})	6.34	3.29	7.91	11.03	4.01
East T_{max} (°C)	13.9	15.2	15.5	14.2	15.0

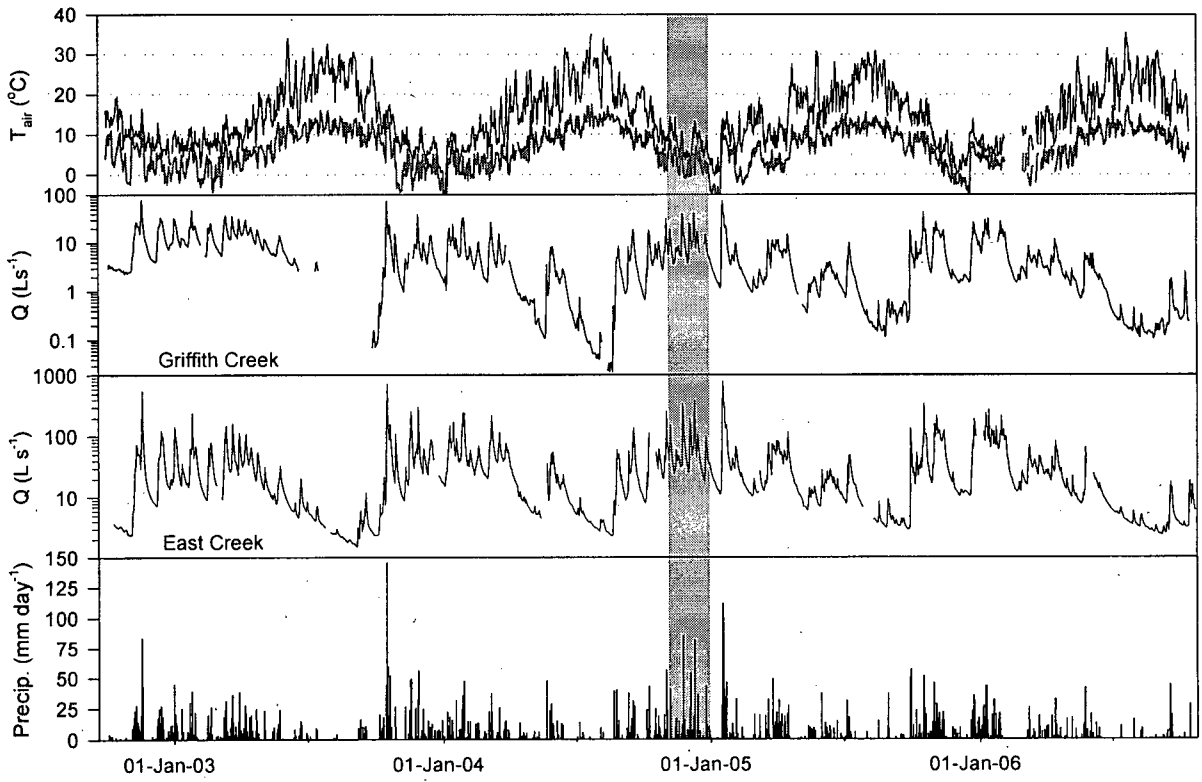

Figure 3.1 Weather and streamflow from October 2002 to October 2006. From top to bottom: daily maximum and minimum air temperature, Griffith Creek discharge, daily total precipitation. The shaded portion indicates the period of logging.

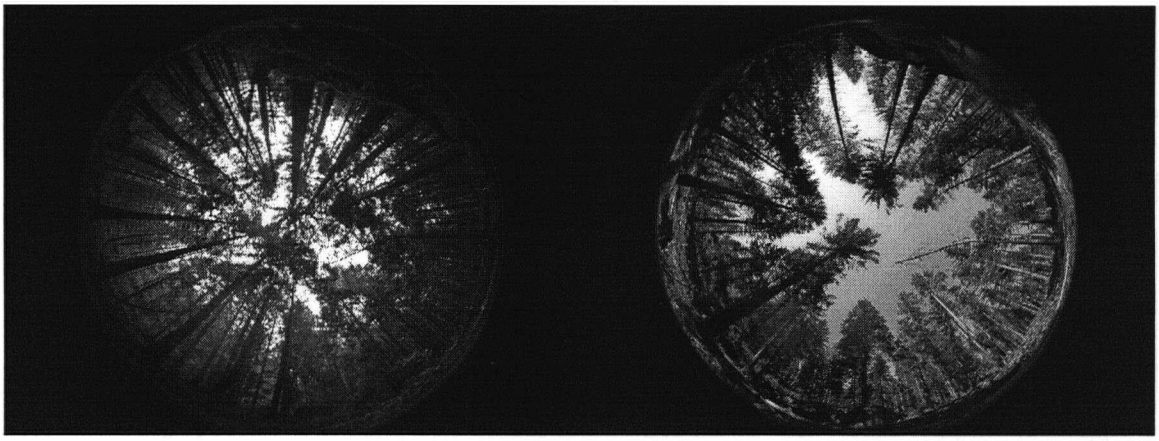

Figure 3.2 Pre- (left) and post-logging (right) hemispheric photographs from the same location of Griffith Creek Low Reach taken in 2004 and 2005, respectively.

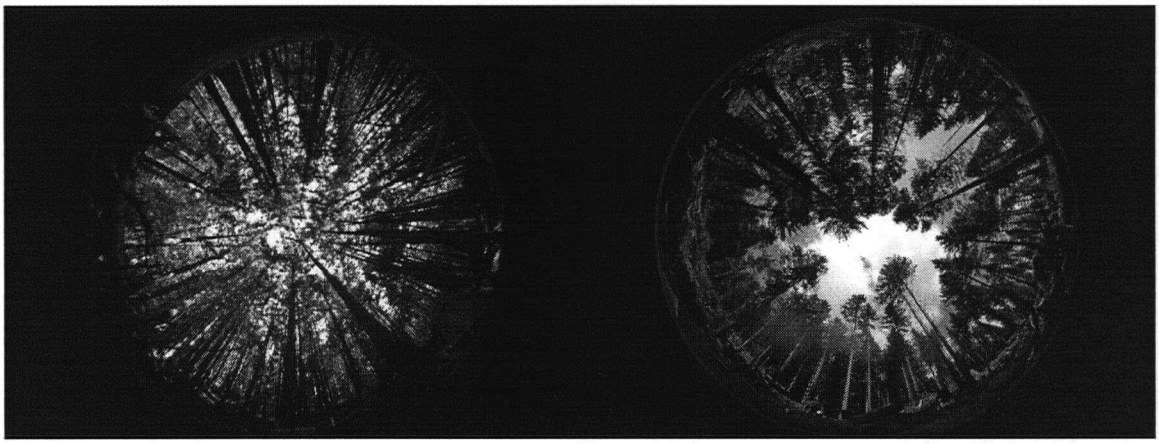

Figure 3.3 Pre- (left) and post-logging (right) hemispheric photographs from the same location of Griffith Creek Mid Reach taken in 2004 and 2005, respectively.

Figure 3.4 Griffith Creek catchment in summer 2005, following 50% removal of basal area.

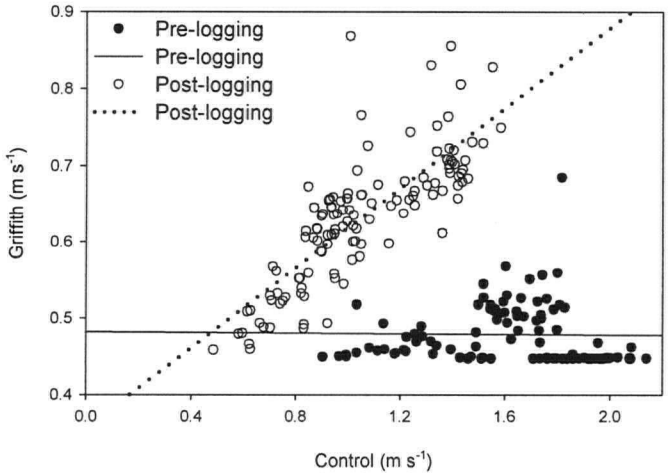

Figure 3.5 Pre- and post-logging relations between daily mean wind speed at the Griffith Creek riparian station and a control meteorological site less than 1 km away, for the months of July and August. Data span the years 2003 to 2006, with the later two years being post-logging data from Griffith Creek. Regression lines for the pre- and post-harvest periods are shown.

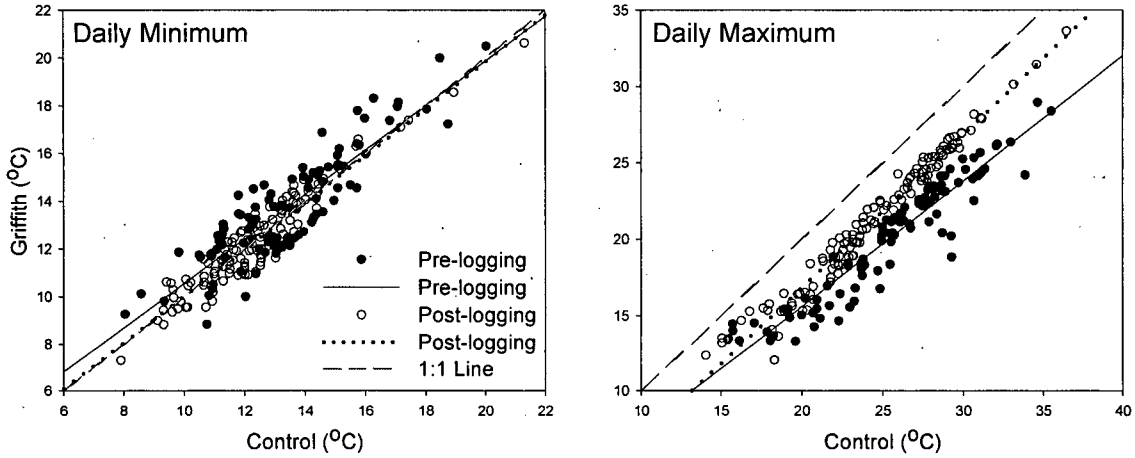

Figure 3.6 Pre- and post-logging relations between daily maximum and minimum air temperature for Griffith Creek and a control meteorological site less than 1 km away, for the months of July and August. Data span the years 2003 to 2006, with the later two years being post-logging data from Griffith Creek. Regression lines for the pre- and post-harvest periods are shown.

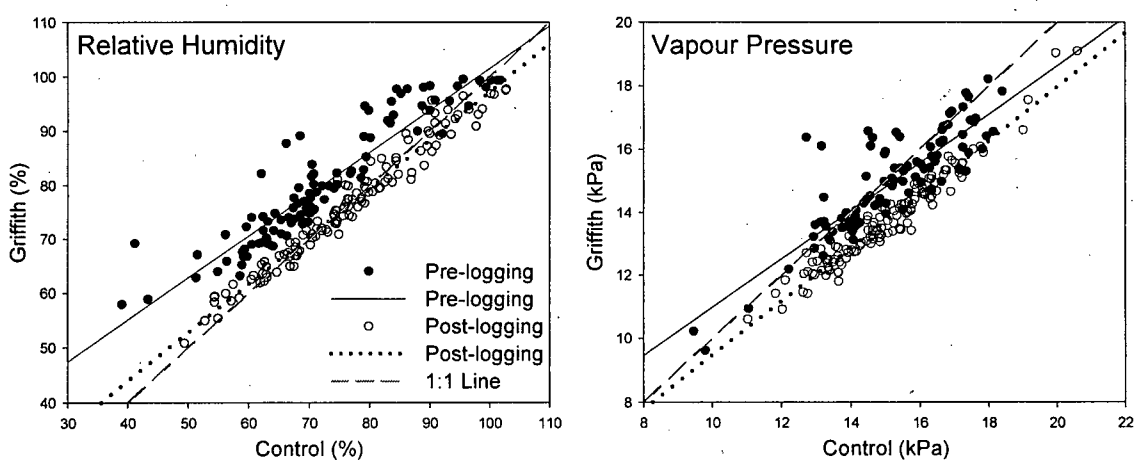

Figure 3.7 Pre- and post-logging relations between relative humidity and vapour pressure at Griffith Creek and a control meteorological site less than 1 km away, for the months of July and August. Data span the years 2003 to 2006, with the later two years being post-logging data from Griffith Creek. Regression lines for the pre- and post-harvest periods are shown.

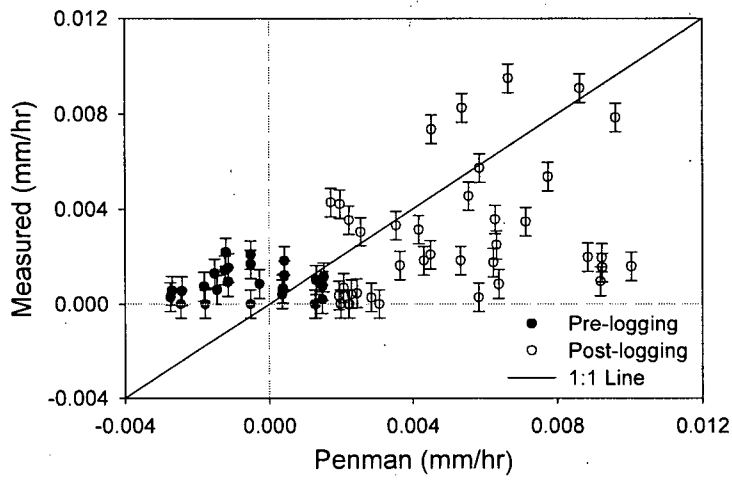

Figure 3.8 Relations between calculated and measured evaporation from Griffith Creek. Filled and open symbols are for pre- and post-logging periods, respectively. Evaporation was measured and calculated in the summers of 2004 and 2005. The solid line represents the 1:1 line with dashed lines as the 0.0 mm/hr evaporation rates for visual reference. Error bars represent the maximum possible measurement error for the evaporimeters.

CHAPTER FOUR

STREAM TEMPERATURE RESPONSE TO A DISPERSED RETENTION LOGGING TREATMENT

4.1 INTRODUCTION

It has been recognised for decades that traditional forestry practices, such as clear-cutting, cause increases in stream temperature over the summer months as a result of decreased shade and increased solar radiation reaching the water surface. [*Johnson and Jones*, 2000; *Levno and Rothacher*, 1967; *Titcomb*, 1926]. Linear buffer strips are the traditional method for mitigating stream temperature increases; however, they are highly susceptible to windthrow, which can render them ineffective. Alternatives to linear buffers are partial retention logging approaches which have been implemented since the late 1990's in British Columbia [*Beese et al.*, 2003]. However, only one study by Macdonald *et al.* [2003] has been conducted to date on the effects of partial retention logging on the stream environment.

In this study the effects of a dispersed retention logging treatment on stream temperature will be assessed using a paired-catchment pre/post-logging analysis. The effectiveness of this logging treatment will be assessed by calculating the treatment effect in the post-logging period. Additionally, the contribution of air temperature and discharge on treatment effect will be assessed using regression analysis for the spring and summer seasons of the two post-logging years.

4.2 STREAM TEMPERATURE PATTERNS

Throughout the pre-logging period, stream temperatures for Griffith Creek and the unlogged control stream (Mike Creek) varied similarly (Figure 4.1). The control stream was slightly warmer with mean and maximum pre-logging temperatures of 9.1 °C and 17.2 °C, compared to Griffith Creek, which showed mean and maximum temperatures of 8.9 °C and 16.7 °C. During the post-logging period, Griffith Creek exhibited a distinctly different temperature signature in the summer months compared to the un-logged control. Diurnal variations increased dramatically with fluctuations of up to 5 °C compared to the control stream, which showed fluctuations of approximately 1.5 °C for the same period in the summer of 2006. The post-logging mean and maximum temperatures also changed, with mean temperatures of 8.5 °C and

9.0 °C and maximum temperatures of 16.8 °C and 20.5 °C for the control and Griffith Creek, respectively. Minimum temperatures did not change between logging periods with temperatures ranging close to 0.0 °C for both streams.

4.3 RESULTS OF PAIRED-CATCHMENT ANALYSIS

4.3.1 Pre-harvest regressions

Generalised least-squares (GLS) regressions were fitted for the pre-harvest period, using Mike Creek as the control, for temperatures measured at sites along Griffith Creek. Regressions were also fitted for two other control streams (East and Spring Creeks), also using Mike Creek as the predictor. The paired-catchment analysis for stream temperature found significant residual autocorrelation for all three temperature metrics. Daily maximum temperatures required residual autocorrelation for lags of 1 day for all four locations in Griffith Creek and the two un-logged control streams. Mean daily temperature required 2 days of residual autocorrelation for Griffith Creek and 3 days for East and Spring Creeks. For minimum daily temperature, two locations had significant lag-1 autocorrelation, three had significant lag-2 autocorrelation and East Creek had significant lag-5 autocorrelation (Table 4.1). Degrees of freedom for the pre-logging regression were between 760 and 796, and standard errors of the residuals ranged from 0.27 to 0.49 °C.

To assess the stability of the pre-harvest regressions, relations were fitted for two un-logged control streams (East Creek and Spring Creek) using the control for Griffith Creek, Mike Creek, as the predictor. Relations were fitted using data from the pre-harvest period, then applied in the post-harvest period. If the pre-harvest regressions are stable, the deviations for the post-harvest period for East and Spring Creeks should be similar to those for the pre-harvest period. As shown in Figure 4.2, most of the deviations for the post-harvest period lie within two standard errors of the residual. The minor deviations outside the predicted range are most noticeable for daily maximum temperatures and are reasonably absent in the daily minimum temperatures. Spring Creek generally showed more deviation outside the prediction range than did East Creek. Overall, the paired-catchment analysis should be capable of identifying treatment effects that exceed 1 °C. Further evidence for stability of the pre-harvest regressions for Griffith Creek is the pattern of deviations from 0 m (bottom end of cut block) to 300 m (80 m upstream of cut block). The deviations for the 300 m logger, which should exhibit no change due to logging, are similar between the pre- and post-harvest periods, as expected (Figures 4.3 to 4.5).

4.3.2 Logging effects on daily maximum temperatures

Treatment effects in the post-logging summers varied with location (Figure 4.3). While the 300 m location, located above the cut block, showed little to no response, all three downstream locations showed significant increases in both of the post-logging summers. Increases were higher in 2006 compared to 2005, with increases of almost 7 °C at the 200 m location in the 2006 summer compared to 5 °C in 2005. The 100 and 0 m locations did not show increases as high as the 200 m location, but overall showed a greater number of days that temperature increased by at least 5 °C (Figure 4.4). Treatment effect tended to increase with downstream distance for spring and summer periods. However, in summer the logger at 200 m (the most upstream logger within the cutblock) recorded the greatest treatment effect and the 100 m logger showed greater probability to exceed 3.5 °C than the other loggers. Winter treatment effects did not appear significant and no longitudinal pattern was present. Almost all winter treatment effects were within the two times the standard error of the residual bounds.

Time series of observed and predicted maximum temperatures at the 0 m logger are shown in Figure 4.5. There is little apparent logging effect from late autumn through winter, with notable warming beginning in early spring and extending to late summer/early autumn. The largest treatment effects occurred in spring and not during the period of seasonal peak temperatures. Figure 4.5 shows that, while predicted temperatures without logging would have been expected to exceed 15 °C only during one warming event each year, that value was exceeded several times each year after logging. In fact, in 2006, maximum temperatures exceeded 20 °C during two warming events

4.3.3 Logging effects on daily mean temperatures

The paired-catchment analysis for mean daily temperatures revealed similar responses to those for daily maximum temperatures, though smaller in magnitude (Figure 4.6, Figure 4.7). At the 300 m location, increases in mean daily temperature were only noticeable in the summer of 2006. The three downstream locations showed post-logging temperature increases in the summer of 2005, and even greater increases in 2006. The greatest increases in daily mean temperatures occurred at the 200 m and 0 m locations.

The summer and spring months showed similar responses for the two lower loggers but not for the 200 m logger, which increased in treatment effect in the summer compared to the spring. During winter, the mean responses tended to be negative, suggesting increased cooling after harvest. However, the mean responses were small and possibly not statistically significant.

4.3.4 Logging effects on daily minimum temperatures

In contrast to daily maximum and mean temperatures, only small deviations occurred in the summers following logging, with maximum increases of 2.2 °C (Figure 4.8). Post-logging changes in minimum winter temperatures tended to be negative, possibly reflecting increased heat loss via longwave radiation, though the changes were small and did not vary with downstream distance, suggesting that they may not be statistically significant (Figure 4.9). In the summer period the greatest increases in daily minimum temperature occurred at the 200 m location; however, the 0 and 100 m locations showed greater warming than the 200 m location in both spring and summer periods.

4.4 METEOROLOGICAL AND HYDROLOGICAL CONTROLS ON TREATMENT EFFECT

To explore the relative effects of meteorological conditions and streamflow on the magnitude of post-logging temperature changes, the treatment effect for daily maximum temperature at the Griffith Creek 0 m location was analyzed using GLS regression analysis. Treatment effect was regressed against daily maximum air temperature and the logarithm of daily mean discharge for the spring and summer months, respectively, of both post-logging years. Significant autocorrelation of the residuals from the generalized least squares regression was 1 day for both seasons. Scatterplots for both seasons showed that the relationships were stronger for the spring season compared to the summer period for both air temperature and the logarithm of discharge (Figure 4.10).

Treatment effect was negatively correlated with discharge and positively correlated with daily maximum air temperature for both seasons (Table 4.2). The regression coefficients for air temperature were greater in the spring season than in the summer. This indicates that a change in treatment effect (°C) that would be associated with a 1 °C change in daily maximum air temperature would be 0.24 °C in spring and 0.16 °C in summer. Discharge regression coefficients indicate that a doubling or halving of discharge would change the treatment effect by 0.26 °C in the spring and 0.14 °C in the summer seasons.

4.5 DISCUSSION

4.5.1 Stream temperature response to logging

The paired catchment analysis showed similar results, standard errors of the residuals, and significant orders of residual autocorrelation to those reported by Moore *et al.* [2005c] and Gomi

et al. [2006] for other sites in Malcolm Knapp Research Forest. Daily maximum and mean temperatures increased notably during spring and summer at the three temperature loggers located within the cutblock. Spring and summer means of the post-logging deviations from the regression analysis showed that even though increases in temperature were similar for the three locations in the cutblock, the 0 m and 100 m loggers responded with more seasonal warming than the 200 m location. The 300 m temperature logger, located above the cutblock with the forest canopy still intact, did not respond significantly using any of the temperature variables in the post-logging summers.

Comparison of the four temperature loggers suggests that downstream distance was only a significant control on the mean seasonal response, reflecting the overall heat accumulation of the stream, and not on maximum temperature changes. Temperatures generally increased substantially between the 300 m and 200 m locations and then showed only minor variation in the remaining downstream direction. This spatial pattern of warming is consistent with studies at A Creek in Malcolm Knapp Research Forest, where daily maximum temperatures increased dramatically over the first 50-100 m downstream of the cut block edge, then alternately warmed and cooled over distances of 10's of metres [*Moore et al.*, 2005c].

The variations in the temperature responses, especially for seasonal maximum changes, are likely a result of local controls on stream temperature, such as lateral inflow or hyporheic discharge. To ensure that temperature loggers remained submerged during summer low flows they were placed in pools. Pools have been found to be locations of mixing of stream water with water from the hyporheic zone [*Bilby*, 1984; *Moore et al.*, 2005c; *Story et al.*, 2003], which is typically cooler than stream water during the daytime in summer. Temperature variation within pools of the Griffith Low Reach exceeded 2 °C on occasion, similar to the results of Moore *et al.* [2005c], who reported variations of water temperature in pools up to 3 °C. The effect of discharging hyporheic water may contribute to the slight variations in response between the three downstream temperature loggers, particularly during the low flows experienced in 2006.

4.5.2 Relative effects of meteorology and streamflow

Treatment effect was positively related to daily maximum air temperature and showed a negative relation to the logarithm of discharge, similar to findings for another site in the Malcolm Knapp Research Forest (*Moore et al.*, 2005b). Treatment effects were more sensitive to changes in air temperature and discharge in spring than in summer. This seasonal contrast is likely a result of the energetic feedbacks associated with the higher temperatures in summer: as stream

temperature increases, heat losses by outgoing longwave radiation and evaporation increasingly tend to offset heat gains by solar radiation [*Mohseni et al.*, 1998]. A contributing factor to decreased sensitivity in summer is heat storage in the stream bed. On cooler days in the summer, heat could be conducted from the bed to the stream, suppressing stream cooling. The larger value of the lag-one autocorrelation coefficient in the summer compared to spring supports the suggestion that day-to-day carryover of heat via storage in the bed tends to suppress stream temperature responsiveness.

4.5.3 Efficacy of dispersed retention logging for mitigating stream warming

Research on clearcut logging has shown that in most cases maximum temperature responses vary from less than 4 °C to as high as 13 °C [*Feller*, 1981; *Gomi et al.*, 2006; *Harris*, 1977; *Johnson and Jones*, 2000; *Moore et al.*, 2005c]. To mitigate these stream temperature increases, linear buffers have been used, with effective mitigation depending on the buffer width and type. Gomi *et al.* [2006] showed in the southern coast region of BC that a 10 m buffer allowed increases in daily maximum temperature of up to 4.4 °C, while Macdonald *et al.* [2003] found that buffer widths of 20 m with merchantable timber removed from the buffer strip allowed daily maximum temperature increases up to 3 °C in central BC. Full-retention 30 m buffers were shown in two studies to be effective, with maximum summer temperatures increasing by only 2.2 °C or less [*Gomi et al.*, 2006; *Harris*, 1977].

The results presented here suggest that dispersed retention of 50% throughout the cut block is not effective at mitigating stream temperature increases in the post-logging summers. Increases of at least 5.5 °C are similar to the increases reported following clearcut logging, such as at A Creek in Malcolm Knapp Research Forest, where daily maximum temperatures increased by up to 5 °C [*Gomi et al.,* 2006]. The increases at the 200 m temperature logger, which is located approximately 20 m below the cut block boundary, show that even a decrease in the canopy closure created by a 50% dispersed retention causes significant temperature increases in a short downstream distance.

It is difficult to assess the effectiveness of the 50% partial retention harvesting relative to studies employing other treatments, as the inherent sensitivities of a stream to warming will vary among sites, particularly due to differences in stream depth, stream-groundwater interactions and bank shading. For example, while the 50% removal of basal area produced marked warming, it is possible that much greater warming might have occurred with clearcut logging. One approach to

comparing the 50% partial retention harvesting to alternative strategies is via heat budget modelling, using different shading scenarios to represent effects of different treatments. This approach will be employed in Chapter 6.

4.5.4 Biological and ecological implications

Even though forest harvesting can produce marked warming, potentially lethal temperatures for salmonids are rarely reached, especially for the time periods that are required to harm fish [*Beschta et al.*, 1987; *Curry et al.*, 2002]. However, Curry *et al.* [2002] suggested that forestry practices which change stream temperatures may have detrimental effects on the spawning success of some species.

The primary concerns for non-fish-bearing headwater streams such as Griffith Creek are not on the fishes themselves but on the food sources for fish such as macroinvertebrates, which may affect fish downstream of the logged catchment. Increases in stream temperature are generally accepted to affect the distribution and abundance of macroinvertebrates in the benthic zone of streams [*Vannote and Sweeney*, 1980; *Ward and Stanford*, 1992]. However, the relation between changes in thermal regime and invertebrate response is complex, and cannot be represented using simple thresholds for mortality or morbidity. For example, diurnal fluctuations of 10 °C (i.e., ± 5 °C around the mean) decreased the mean temperature required to cause lethal results on mayfly *Deleatidium autumnale* to 22 °C from 24 °C [*Cox and Rutherford*, 1999]. Research conducted on changes in macroinvertebrate communities after logging has shown that effects are either not detectable on longer time scales or are short lived, persisting on the order of < 5 years [*Herlihy et al.*, 2005; *Hutchens et al.*, 2004]. This time scale is roughly consistent with the time required for thermal recovery associated with regrowth of riparian vegetation following logging, which occurred or was at least underway within 5 to 10 years after harvest in many studies [*Moore et al.*, 2005b].

Griffith Creek showed increased daily fluctuations of up to 5 °C and maximum temperatures of 20.5 °C in the post-logging period. Based on the results presented by Cox and Rutherford [1999], mortality of mayfly would not be expected to occur in Griffith Creek. However, it is unclear whether the results of Cox and Rutherford [1999], based on studies in New Zealand, are applicable at Griffith Creek, especially to species other than mayflies. Furthermore, the temperature changes could affect growth and/or development rates and thus the timing of emergence and/or condition of invertebrates at emergence, both of which could have broader ecological impacts.

Overall, the effects of logging on macroinvertibrate communities has not been adequately addressed in the literature. Some of the questions that need to be understood are: What is the impact of logging on the benthic thermal environment? How does hydrologic interaction contribute to the change in the benthic environment? Do spatial patterns develop in the distribution of macroinvertebrate communities in relation to hyporheic exchange zones? These questions will be addressed in Chapter 5.

Table 4.1 Results of the generalized least squares regression analysis for Griffith Creek at four sites located 0 to 300 m upstream of the lower edge of the cut block, and for two unlogged control streams (East Creek and Spring Creek). All regressions use Mike Creek as the control. s_e is the residual standard error for the pre-logging regression, d.f. is the pre-logging degrees of freedom, and k is the order of the residual autocorrelation.

Location	Daily Maximum			Daily Mean			Daily Minimum		
	s_e (°C)	d.f.	k	s_e (°C)	d.f.	k	s_e (°C)	d.f.	k
0 m	0.36	796	1	0.29	796	2	0.33	796	2
100 m	0.30	784	1	0.27	784	2	0.32	780	1
200 m	0.29	785	1	0.28	785	2	0.34	785	2
300 m	0.36	760	1	0.32	760	2	0.37	760	1
East	0.32	788	1	0.33	789	3	0.49	789	5
Spring	0.39	791	1	0.39	791	3	0.44	791	2

Table 4.2 Results of generalized least squares regression analysis of daily maximum treatment effect ($TE_{w\ max}$) as a function of the logarithm of mean daily discharge (log Q) and daily maximum air temperature ($T_{a\ max}$). The fitted model is $TE_{w\ max} = b_0 + b_1 \log Q + b_2 T_{a\ max} + e$.

Season	b_0 (p value)	b_1 (p value)	b_2 (p value)	R^2_{adj}	s_e	N	$\hat{\rho}_1$
Spring	-1.874 (<.001)	-0.856 (0.047)	0.242 (<.001)	0.73	0.83	115	0.57
Summer	-1.405 (0.006)	-0.470 (0.211)	0.162 (<.001)	0.47	1.05	124	0.79

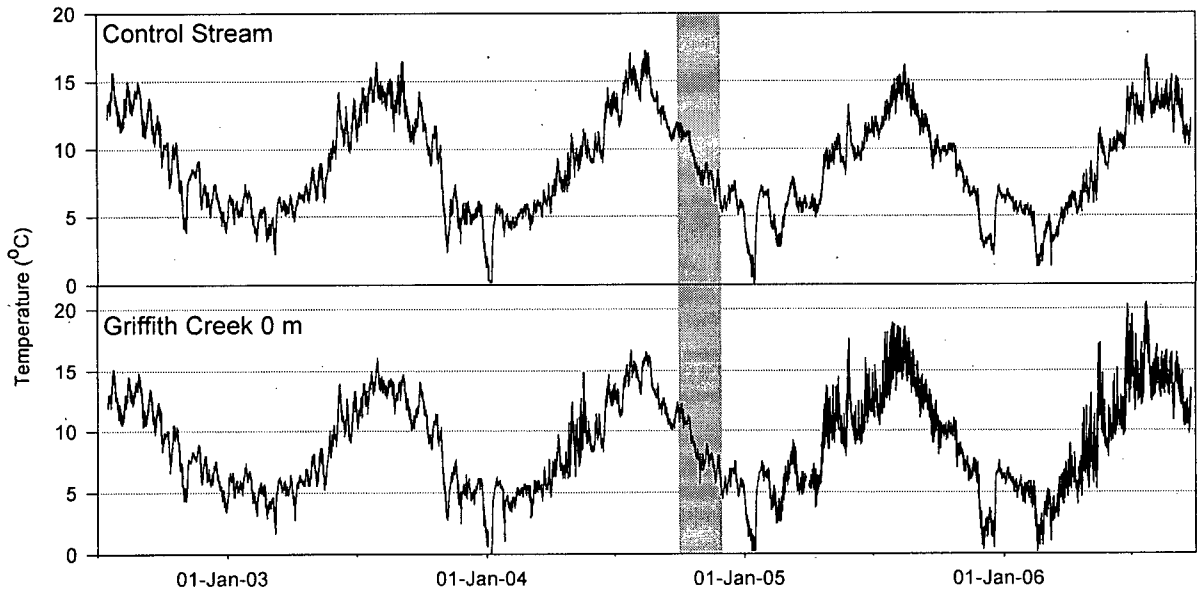

Figure 4.1 Observed 10 minute interval stream temperatures for the control stream (Mike Creek) and Griffith Creek from 16 July 2002 to 24 September 2006. Shaded area indicates the logging period (September – November 2004).

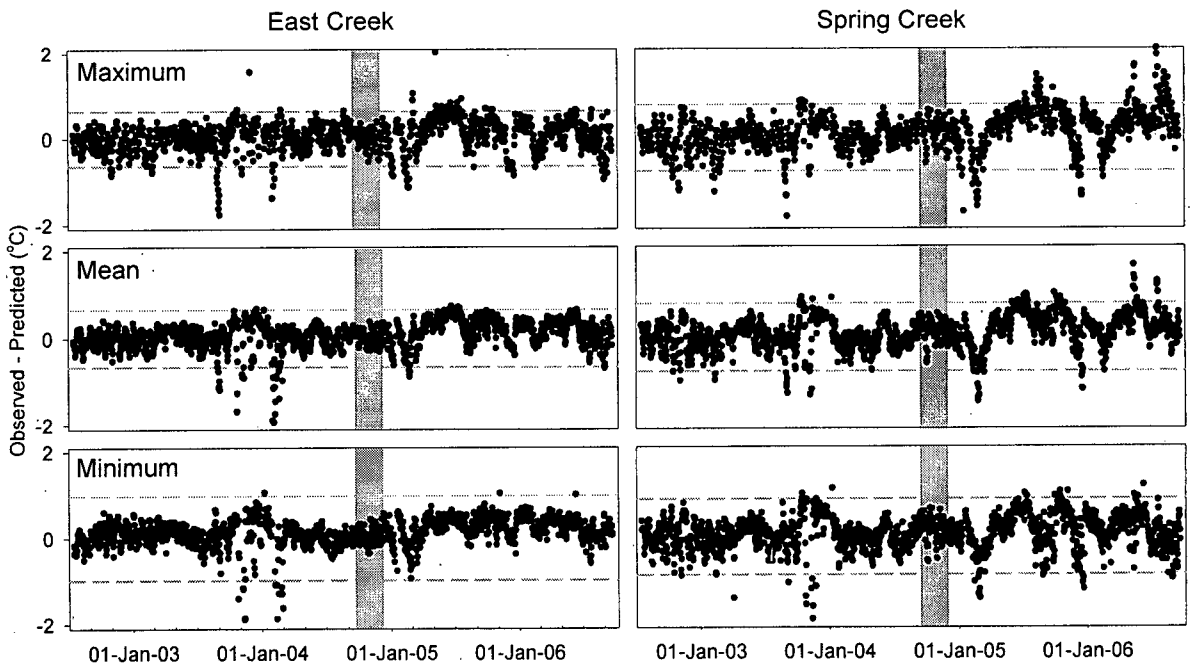

Figure 4.2 Deviations between observed and predicted daily maximum, mean, and minimum temperatures for two unlogged control streams using temperatures at Mike Creek (a third control stream) as the predictor variable. For the post-harvest period, the deviation is an estimate of the effect of harvesting. Shaded area indicates the logging period (September – November 2004). Horizontal dashed lines indicate 2 times the standard error of residuals from the pre-logging regression.

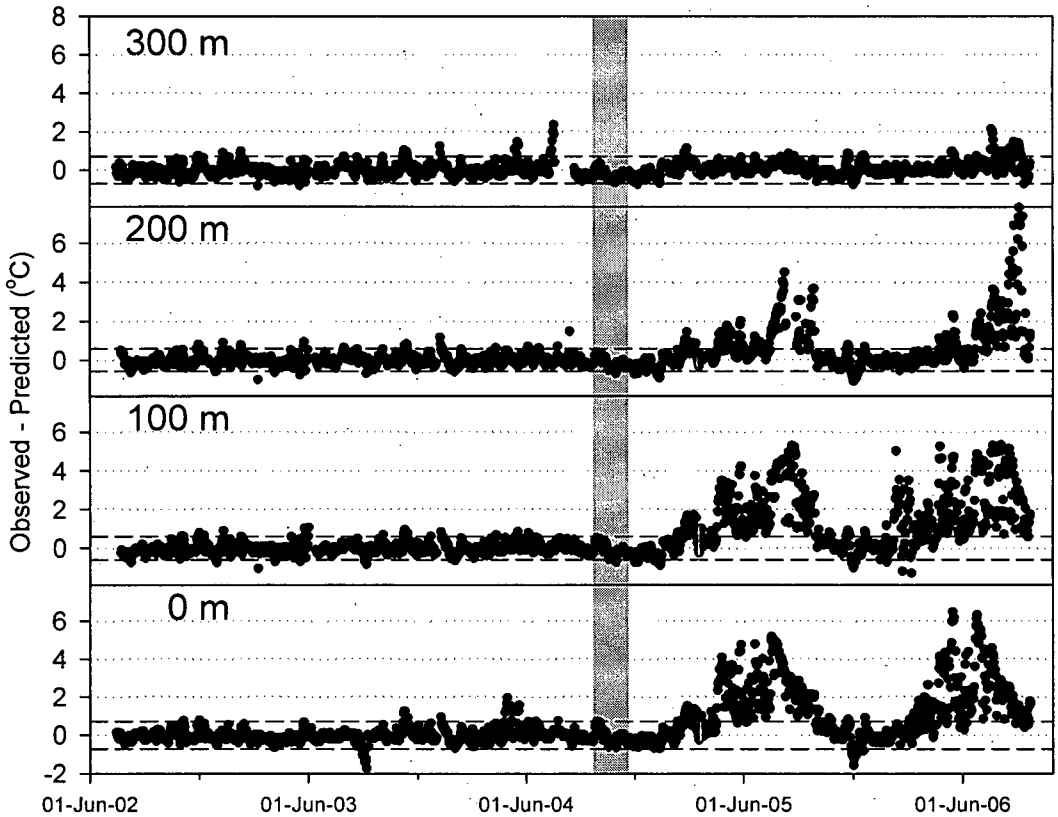

Figure 4.3 Deviations between observed and predicted daily maximum temperature at four locations along Griffith Creek. Distances are measured from the downstream end of the cut block. The 300 m logger is 80 m upstream of the cutblock. For the post-harvest period, the deviation is an estimate of the effect of harvesting. Shaded area indicates the logging period (September – November 2004). Horizontal dashed lines indicate 2 times the standard error of residuals from the pre-logging regression.

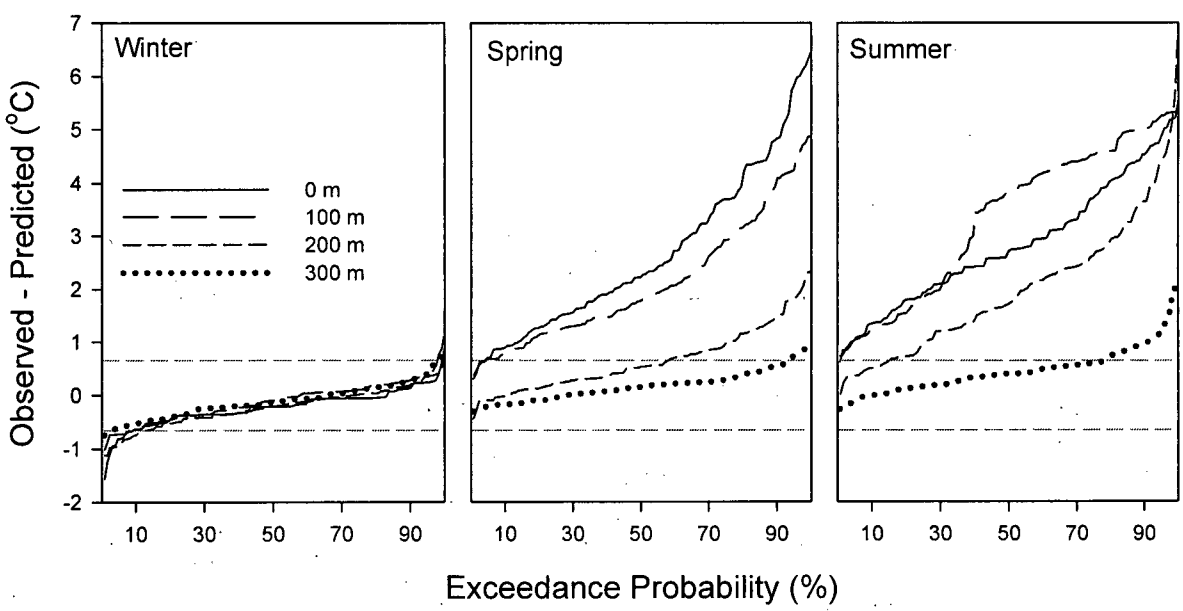

Figure 4.4 Exceedance probability curves for four locations in Griffith Creek for treatment effects for daily maximum temperatures for both post-logging years Winter (December – January), Spring (May - June), and Summer (July - August) periods. Horizontal dashed lines indicate 2 times the standard error of residuals from the pre-logging regression.

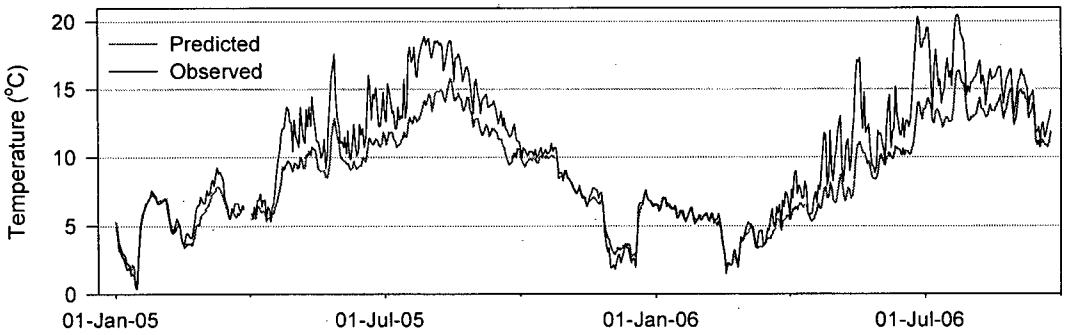

Figure 4.5 Predicted and observed daily maximum stream temperatures for the Griffith Creek 0 m logger from January 2005 to October 2006.

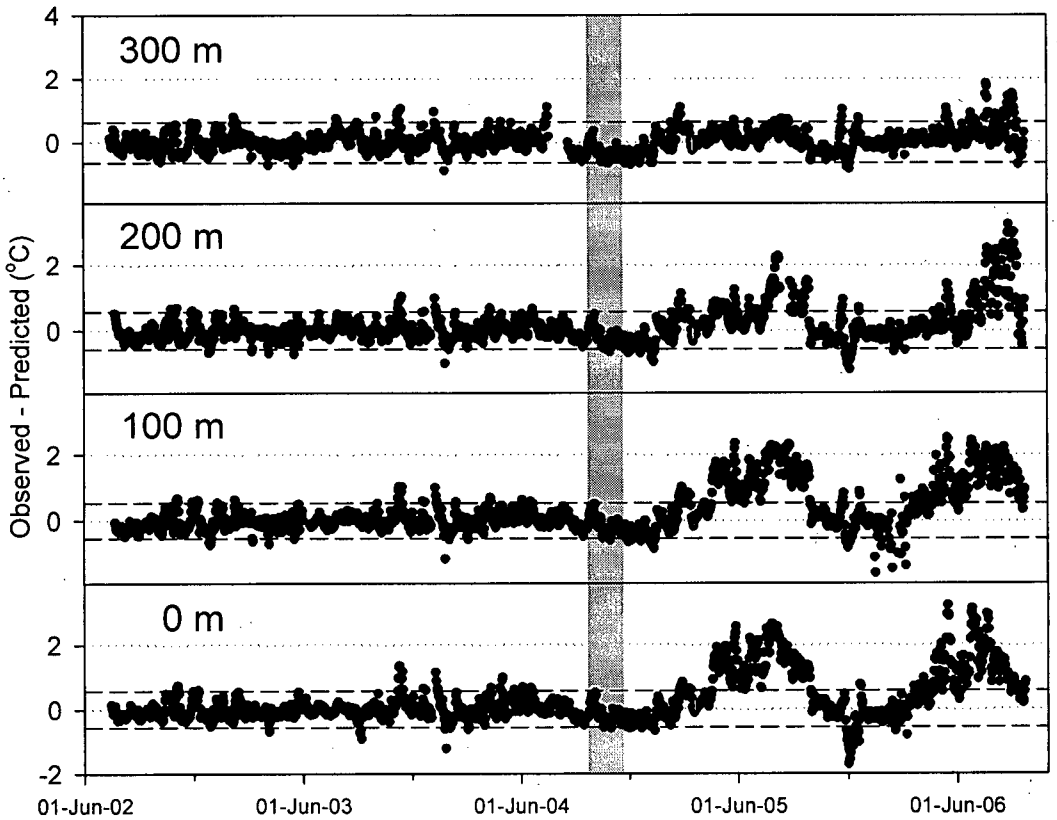

Figure 4.6 Deviations between observed and predicted daily mean temperature at four locations along Griffith Creek. Distances are measured from the downstream end of the cut block. The 300 m logger is upstream of the cutblock. For the post-harvest period, the deviation is an estimate of the effect of harvesting. Shaded area indicates the logging period (September – November 2004). Horizontal dashed lines indicate 2 times the standard error of residuals from the pre-logging regression.

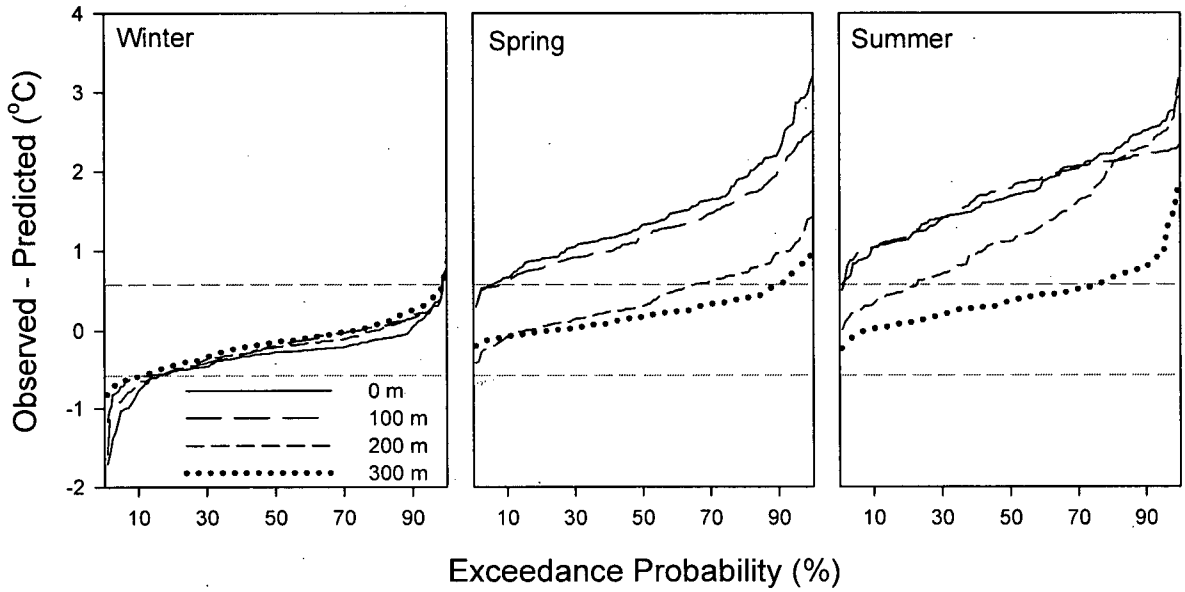

Figure 4.7 Exceedance probability curves for four locations in Griffith Creek for treatment effects for daily mean temperatures for both post-logging years Winter (December – January), Spring (May - June), and Summer (July - August) periods. Horizontal dashed lines indicate 2 times the standard error of residuals from the pre-logging regression.

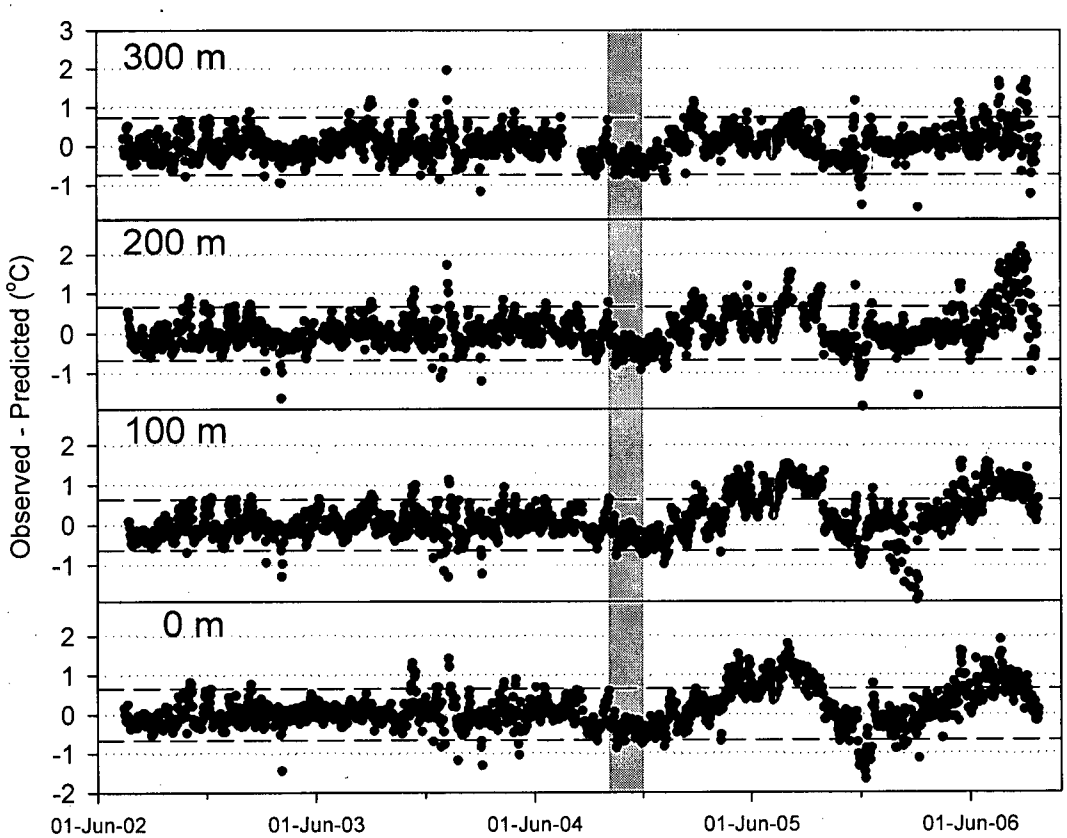

Figure 4.8 Deviations between observed and predicted daily minimum temperature at four locations along Griffith Creek. Distances are measured from the downstream end of the cut block. The 300 m logger is upstream of the cutblock. For the post-harvest period, the deviation is an estimate of the effect of harvesting. Shaded area indicates the logging period (September – November 2004). Horizontal dashed lines indicate 2 times the standard error of residuals from the pre-logging regression.

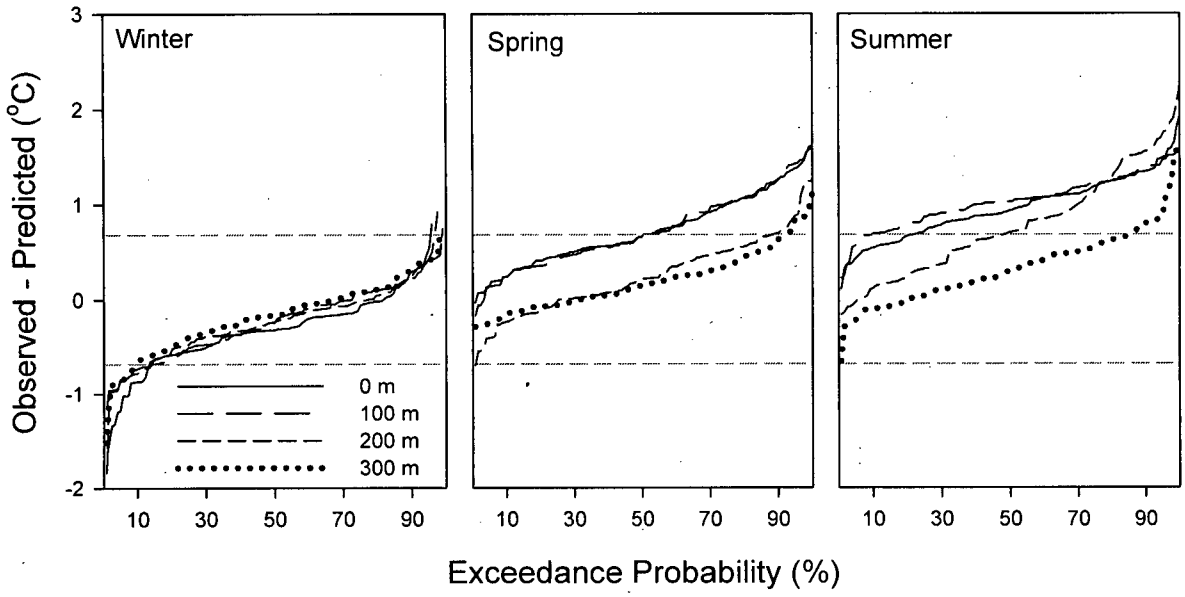

Figure 4.9 Exceedance probability curves for four locations in Griffith Creek for treatment effects for daily minimum temperatures for both post-logging years Winter (December – January), Spring (May - June), and Summer (July - August) periods. Horizontal dashed lines indicate 2 times the standard error of residuals from the pre-logging regression.

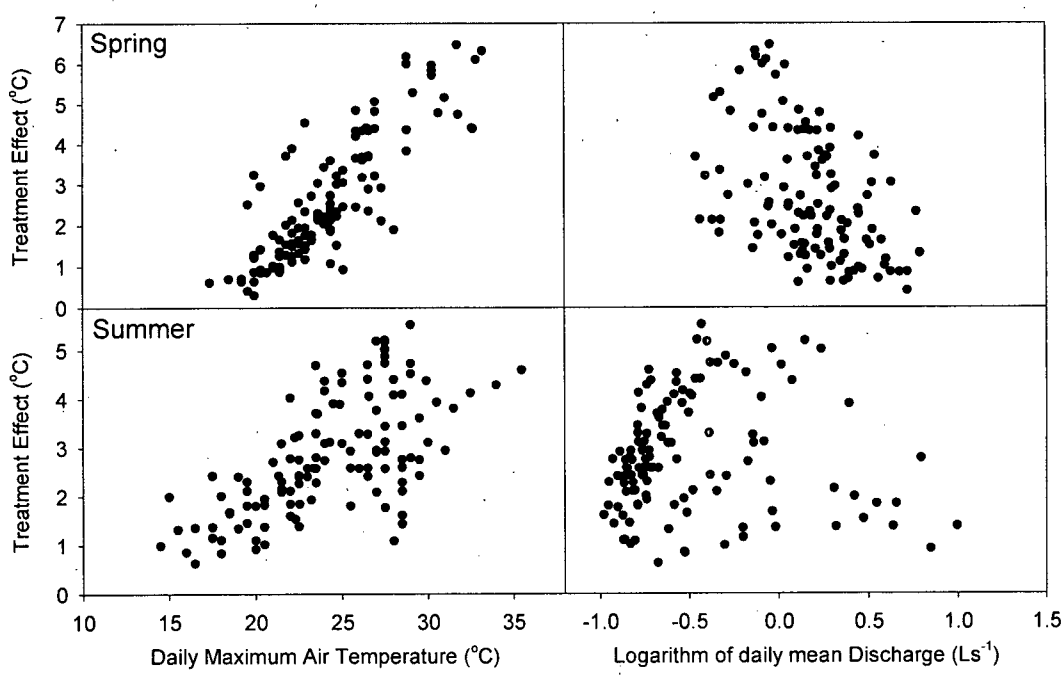

Figure 4.10 Scatterplots of daily maximum treatment effect for Griffith Creek 0 m temperature logger versus daily maximum air temperature and the logarithm of daily mean discharge for Spring (May and June) and Summer (July and August) periods of 2005 and 2006.

CHAPTER FIVE

HYDROLOGY AND THERMAL REGIME OF THE STREAM BED

5.1 INTRODUCTION

Although many studies have addressed the temperature response of stream water after logging [e.g., *Gomi et al.*, 2006; *Johnson and Jones*, 2000; *Levno and Rothacher*, 1967; *Titcomb*, 1926] and temperature patterns of water in the hyporheic zone [e.g., *Bilby*, 1984; *Malard et al.*, 2001; *Moore et al.*, 2005c], there is a significant gap in the literature relating to responses of bed temperature after forestry practices. Only two studies have addressed the impact of logging on the benthic environment and neither used a before-after approach to quantify the increases in the post-logging period [*Ringler and Hall*, 1975; *Curry et al.*, 2002].

This chapter addresses these knowledge gaps by documenting the changes in bed temperature patterns in a headwater stream before and after harvest. Data for both hyporheic flow directions and long term bed temperature profiles will be used to assess if hyporheic-exchange-induced bed temperature patterns are present in forested headwater streams and how they are affected by logging.

5.2 LOW REACH RESULTS

5.2.1 Discharge and lateral inflow

Measured discharge varied from 10.0 to 0.17 L s^{-1} throughout the summer of 2005 (Table 5.1). The reach generally gained flow, with changes of -5.9% to 15.3% between the upper and lower boundaries. The apparent losses could have been caused by measurement error, which is likely on the order of ± 5% for each measurement, or up to ± 16% error for the difference. There does not appear to be any systematic relation between lateral inflow and stream discharge. On four occasions, additional discharge measurements were conducted to assess the locations of lateral inflow in the reach. In all but one measurement no discharge was gained above the S2 location and greater than 50% of the lateral inflow entered below S3 (see Figure 5.1 for locations).

5.2.2 Hydraulic gradients and conductivity

Locations of hyporheic exchange flow into and out of the stream bed were inferred using hydraulic gradients between piezometers and the stream surface. The Low Reach is characterized by 3 step-pool sections which resulted in the identification of 3 distinct down-welling and up-welling zones (Figure 5.1). Down-welling (DW) zones were easier to define based on the hydraulic gradients and represented a larger proportion of the stream channel, while up-welling zones were smaller in comparison. Step units within the study reaches, all of which were located above woody debris, exhibited generally large negative hydraulic gradients (flow into the stream bed), as high as -0.74 at a depth of 25 cm below the stream bed (Appendix A and B). Up-welling sites were found in pools below steps in only a small zone directly downstream of the woody debris. These areas exhibited lower magnitudes of hydraulic gradients compared to their down-welling counterparts, ranging between 0 and 0.23. Since up-welling zones were relatively weak and the measurement uncertainty was ± 0.05, all up-welling sites and these with gradients of magnitudes equal to or less than 0.05 were considered as up-welling or neutral (UW/N) zones.

Spearman correlations calculated between hydraulic gradients and discharge exhibited more positive correlations than negative in both study period summers (Appendix A and B). Critical values of the Spearman correlations for the pre- and post-logging periods were 0.738 for $n = 8$ and 0.490 for $n = 17$, respectively. This indicates that two relationships in 2004 and 3 in 2005 were statistically significant, which is greater than amount expected from an alpha value of 0.05 under the null hypothesis (i.e. 1 significant correlation). Therefore, the pattern between hydraulic gradient and discharge is positive but not strong.

Furthermore, between the pre- and post-logging periods there were no noticeable changes between hydraulic gradients in piezometers, except for P3 and P6, which changed from weak DW to UW/N. Piezometer P6 still showed DW flows in the post-logging summer; however, the values were within the measurement error and therefore considered UW/N. After completion of logging piezometer P3 was replaced and the change in direction of hydraulic gradient may be attributed to not being able to replace it in the exact location and depth as the preceding year.

Hydraulic conductivity values from the post-harvest summer showed no systematic difference between UW/N and DW locations (Table 5.2). Values ranged between $1.1 \cdot 10^{-3}$ and $1.7 \cdot 10^{-7}$ m s^{-1}, with the geometric means of each piezometer ranging between $4.0 \cdot 10^{-4}$ and $6.7 \cdot 10^{-6}$ m s^{-1}.

5.2.3 Seep temperatures and bed temperature patterns at step-pool sequences

Seep temperatures measured at 50 cm depth showed diurnal changes of less than 0.2 °C and were lower than stream and bed temperatures for the two warm sunny days shown in the pre-logging summer (Figure 5.2). Bed temperatures at 10 cm depth at DW zones were approximately 1.0 - 1.5 °C higher than the bed temperatures of the UW/N zone (Figure 5.2). Stream temperature had a similar diurnal pattern to the DW sites but was approximately 1 °C warmer than the up-welling neutral sites and 0.5 °C cooler than the DW sites. Daily maximum temperatures were reached by stream water earliest followed by DW zones and UW/N zones, respectively. Stream water temperature was measured 1 m downstream of S1D which likely resulted in UW water mixing with stream water and causing the lower temperature compared to the DW bed temperatures.

In the post-logging summer, seep temperatures showed similar patterns to the pre-logging summer with temperatures ranging between 13 and 14 °C. Differences in bed temperatures between DW and UW/N zones were greater following logging, with DW zones being up to 2 °C warmer than UW/N zones. Stream temperatures were higher than DW bed temperatures in the post-logging summer, opposite to the pattern in the pre-logging summer. Stream temperature reached its daily maximum earliest in the day followed by DW and UW/N sites. Overall maximum temperatures increased in the post harvest summer, and diurnal temperature variations of both stream and bed temperatures increased compared to the pre-harvest summer.

Mean summer bed temperatures (measured 13 July to 12 September, 2004, and 10 July to 9 September, 2005) varied with depth and hydrologic setting (i.e., DW vs UW/N) (Figure 5.3). Temperature differences between hydrologic settings at a given depth were about 0.5 °C for all depths except for the 1 cm depth in the post-logging year, when differences between the hydrologic settings were 0.2 °C. Between the pre- and post-logging summers, temperatures increased by approximately 0.2 °C in both hydrologic settings. The largest increase occurred at the UW/N sites at 1 cm depth, which increased by 0.4 °C in the post-logging summer.

5.2.4 Paired-catchment analysis of bed temperature response to logging

Residuals from the pre-harvest regression for daily maximum temperatures exhibited the most persistent autocorrelation, with significant autocorrelation for lags of 3 or 2 days, while daily minimum and mean temperatures involved 1 - 2 days of lag (Table 5.3). Based on the difference between observed and predicted temperatures for the post-harvest period, daily maximum stream temperatures in the study reach increased by up to 5.5 °C (Figure 5.4). Daily

maximum bed temperatures showed varied responses to the logging treatment depending on their position in the stream. At UW/N sites, bed temperatures increased up to 2 °C at 20 cm depth and up to 3 °C at the 1 cm depth. Areas of the stream bed which exhibited DW flows showed bed temperature responses more closely related to that of the stream temperature. However, the number of days that DW sites reached these increases was fewer compared to those of the stream. Increases were highest near the surface, with increases at the 1 cm depth reaching 6 °C, while the 15 cm bed temperature depth responded with increases of slightly greater than 3 °C.

Table 5.3 summarizes the mean values of the pre- and post-logging treatment effects calculated from the regression analysis using daily maximum, mean, and minimum temperatures. For maximum daily temperatures, post-logging temperature increases were largest near the surface and decreased with depth. Areas exhibiting DW flows showed larger increases when compared to their equivalent depths in the UW/N zones. Daily mean temperatures showed the same pattern of increases as daily maximum temperatures, only with smaller increases at equivalent depths and hydrologic setting. Small post-logging increases were found for daily minimum temperatures, with small (and likely insignificant) temperature decreases in the 10 and 20 cm thermocouple depths of the UW/N site.

5.2.5 Principal component analysis

Principal component (PC) analysis was applied to bed temperatures at the Low Reach from 13 July to 12 September, 2004, and 10 July to 9 September, 2005, and resulted in sample sizes of 8830 and 7138 in the pre- and post-logging summers, respectively. The first two PC's accounted for 95.7 and 3.5% of the total variance in the pre-logging summer and 83.3 and 11.6% in the post-logging summer. Eigenvalues of the first two PC's were 5.1 and 1.0 in the pre-logging period and 4.7 and 1.8 in the post-logging summer, respectively. Since the first two PC scores accounted for at least 95% of the variance in the data sets and eigenvalues were less than 1.0 past the second PC, no other PC's were considered in the analysis. Time series of the PC scores (Figure 5.5) show that the first PC in each year accounted for the variation of the seasonal temperature pattern and included some portion of the diurnal pattern, while the second PC explained variation in the diurnal cycle among locations.

Ordination of the first two PC loadings revealed similar patterns in both years (Figure 5.6). Loadings on PC 2 separated the shallow DW sites (most negative PC 2) from the deeper UW/N sites, and the deepest DW site (most positive PC 2). The loadings on PC 1 were inversely related to the absolute value of the PC 2 loading. The ordination could be interpreted as

representing a gradient of temperature patterns reflecting surface influence (negative PC 2) to those reflecting a dominant subsurface signature (positive PC 2). This hypothesis is explored further in the next section. Ordination based on site does not show a systematic longitudinal thermal pattern with the second principal component, in contrast to that found for depth and hydrologic setting.

5.2.6 Cross correlation analysis

Cross correlation analysis was conducted on bed temperatures for two consecutive clear and cloudy sky days in the pre-and post-logging periods (Appendix C). Stream temperature and seep temperatures were used as independent variables representing surface-dominated and subsurface temperature signals, respectively. The time step was 10 minutes. Cross-correlations with stream temperature decreased with depth and those with seep temperature increased with depth (Figure 5.7). This was true in both the pre- and post-logging periods and under both clear and cloudy conditions. The lag associated with maximum cross-correlation showed an inverse relation with the correlation coefficient and decreased with increasing correlation (Appendix C).

In the pre-logging period under clear sky conditions, cross-correlations with stream temperature decreased less rapidly with depth at DW sites (S1U, S2U, and S3U) compared to their UW/N counterparts (S1D, and S3D). For example, cross-correlations at 15 to 20 cm depth remained near or above 0.8 at DW sites, but dropped below 0.5 for UW/N sites. The opposite pattern held for cross-correlations with seep temperature for clear days. During cloudy conditions, cross-correlations with both stream and seep temperatures were relatively high at all depths, exceeding 0.77. There was no clear distinction between UW/N and DW sites under cloudy sky conditions.

The post-logging period showed broadly similar patterns to those for the pre-logging period although with less variation with depth and among sites. Under clear skies, cross-correlations with stream temperature were similar to those in the pre-logging period, while, cross-correlations with seep temperatures generally increased relative to pre-harvest conditions for depth less than 20 cm. Under cloudy conditions, cross-correlations showed more variation in the post-logging period compared to the pre-logging period. Cross-correlations with both seep and stream temperatures did not differ greatly between clear and cloudy conditions in the post-logging period, with the exception of reduced variation and slightly higher correlations in the cloudy-day correlations with seep temperature. Hydrologic setting was not as significant a control

on correlations compared to the pre-logging period, with only the clear-sky correlations using stream temperature showing deviations for UW/N sites.

5.3 MID REACH RESULTS

5.3.1 Discharge and lateral inflow

The Mid Reach is characterized by a more complicated geomorphic pattern compared to the Low Reach, with no clearly identifiable step-pool sections. Measured discharge ranged from 0.15 to 8.99 $L \cdot s^{-1}$ (Table 5.4). Calculated lateral inflow was always positive and ranged from 1% to 54% of the downstream discharge. Estimated errors were on the order of ± 11% for the percent groundwater contribution. The percentage of flow associated with lateral inflow to the reach tended to be higher at lower flows. The additional discharge measurements at the mid-reach L5 location showed that, in almost all cases except for the 24 October measurement, more than half of the lateral inflow was acquired above the L5 location (see Figure 5.8).

5.3.2 Hydraulic gradients and conductivity

Hydraulic gradients throughout the reach exhibited no clear pattern with channel morphology, particularly step-pool units (Figure 5.8). This reach exhibited fewer strong DW zones and a greater proportion of UW/N zones compared to the Low Reach (Appendix D and E). Four piezometers changed direction of hydraulic gradient between the pre- and post-logging periods (1, 4, 9, and 10), all of which were replaced after logging. The change in direction of hydraulic gradient may be attributed to not being able to replace them in the exact location and depth as the preceding year. Hydraulic gradients at 25 cm depth ranged from -0.65 (DW flow) to 0.13 (UW/N). However, the majority of the piezometers showed low hydraulic gradients throughout the study period, relative to those at the Low Reach. Hydraulic gradients at Mid Reach showed generally more positive Spearman correlations with discharge in both study periods (Appendix D and E). Mid Reach Spearman correlations showed similar numbers of significant relationships to the Low Reach. In the post-logging summer, 5 piezometers exhibited Spearman correlations above the critical value of 0.490, but none in the pre-logging period exceeded the critical value of 0.738 based on the number of observations. This result suggests that hydraulic gradient was positively but weakly related to discharge for the post-logging summer.

Hydraulic conductivity values generally ranged from about 10^{-6} to 10^{-4} $m \cdot s^{-1}$ (Table 5.5). There were no noticeable patterns in hydraulic conductivity relating to discharge or hydrologic setting throughout the summer of 2005.

5.3.3 Bed temperature patterns in relation to vertical water flux

In the pre-logging summer, bed temperatures at 10 cm depth were greater than the seep temperature and lower than stream temperature on warm summer days (Figure 5.8). Bed temperatures exhibited diurnal fluctuations of about 0.5 °C, similar to that for seep temperature but less than the 2 °C fluctuation exhibited by stream temperature. The UW/N location showed the lowest 10-cm bed temperatures, while the L2 DW site had the highest 10-cm bed temperatures. Stream temperature was measured upstream of L1 and therefore was not affected by the lateral inflow, which may explain the lag in the timing of maximum temperatures between the stream and the bed.

In the post-logging summer, seep and stream temperatures remained the lowest and highest, respectively. However, bed temperatures at the L1 and L2 locations were similar to stream temperature during the coolest portion of the diurnal cycle. The diurnal variation in all the measured bed temperatures increased dramatically in the post-harvest summer and showed fluctuations of 1 - 2 °C. Location L3, an UW/N site, remained the coolest of the thermocouple locations. Location L4, a down-welling site that had essentially the same diurnal variability as the other sites in the pre-logging summer, became notably more responsive to diurnal heating, rising and peaking in concert with stream temperature.

5.3.4 Paired-catchment analysis of bed temperature response to logging

For the pre-harvest regressions, the order of significant residual autocorrelation was either 3 or 1 with daily minimum temperatures only requiring 1 day, and with mean and maximum requiring mostly 3 days of lag. Degrees of freedom ranged from 201 to 355 for the regressions (Table 5.6).

Harvesting appeared to increase daily maximum bed temperatures by no more than 2 °C despite increases in stream temperature of up to 5 °C (Figure 5.10). As shown in Table 5.6, there were only small increases in the post-logging summer for daily maximum temperatures, with little difference between depth and hydrologic setting. Daily mean temperature showed an almost uniform temperature increase of between 0.3 to 0.4 °C in the DW zone. In the up-welling zone, increases in mean temperature ranged from 0.51 °C at 5 cm to 0.19 °C at 30 cm. For daily

minimum temperatures, there appeared to be no treatment effect at the down-welling site but a variable response at the up-welling site, with a slight warming at 5 cm and slight cooling at deeper levels.

5.3.5 Principal component analysis

Principal component analysis was conducted on bed temperature data from 5 thermocouple locations from 2 July to 24 August, 2004, and 1 July to 11 September, 2005. In the pre- and post-logging periods there were 7625 and 10319 observations for each period respectively. Time series of principal component scores show that the first PC in each summer represented the variation of the seasonal temperature changes as well as some proportion of the diurnal cycle, incorporating 94.6% in the pre- and 92.3% of the variation in the post-logging summers (Figure 5.11). The second PC represented the remainder of the diurnal variation, accounting for 5.2% in the pre-logging period and 5.8% in the post-logging summer. Eigenvalues in the pre- and post-logging period were (4.4, 0.9) and (4.4, 1.1) for the first two PC's, respectively.

The ordination of the first and second PC loadings shows different patterns in the pre- and post-logging summers (Figure 5.12). In the pre-logging period, there was no clear pattern associated with depth (Figure 5.12, top left panel). However, there appeared to be some pattern associated with site. For each site, the points tended to fall along a set of lines with positive slope (Figure 5.12, bottom left panel). The deeper locations tend to be in the lower left and shallower points in the upper right. Points for sites L1, L4 and L5 fall along one line, while points for site L2 fall along a separate line, shifted down. The points for site L3 fall along a third, even lower line, and are closely clustered in the lower right corner of the graph.

For the post-logging summer, the ordination reveals a strong relation between the PC 2 loading and depth (Figure 5.12, top right panel). Deeper thermocouples were associated with positive loadings for PC 2, and shallower thermocouples with negative loadings for PC 2. The contrast between up-welling and down-welling had a more subtle effect than for the Low Reach. For example, comparing points for L4 (down-welling) and L5 (up-welling) for the same depth reveals that Location L5 showed higher loadings in the second PC when compared to the respective depth of L4, indicating that the UW/N zone plotted higher along the second PC loading axis than its DW counterpart.

5.3.6 Cross-correlation analysis

Cross-correlation analyses were conducted on two consecutive clear and cloudy sky days in the pre-and post-logging periods. Stream temperature and seep temperatures were used as independent variables and the time step was 10 minutes (Appendix F). As for the Low Reach, cross-correlations with stream temperature were high at the surface and decreased with depth. The reverse pattern held for cross-correlations with seep temperature (Figure 5.13). The lag associated with the maximum cross-correlation showed an inverse relation with correlation coefficient and decreased with increasing correlation (Appendix F).

In the pre-logging period the most noticeable pattern was the high cross-correlations with seep temperature for locations below 10 cm depth. This pattern was present regardless of location or sky condition, especially in the UW/N locations L3 to L5. Cross-correlations with stream temperature were generally weaker than for the Low Reach, but varied with location and sky condition. Under clear skies, cross-correlations with stream temperature were high for L2 at 5 cm, but decreased rapidly with depth, while locations L3 to L5 had weak cross-correlations at all levels, including 5 cm. Under cloudy skies L2 showed high correlations at the surface and higher correlations compared to the clear sky conditions at depth. Thermocouple locations L3 to L5 showed a reduced range of correlation coefficients compared to the clear sky condition, from 0.50 to 0.66. The contrast between up-welling and down-welling sites, as reflected in the contrast between L4 (DW) and L5 (UW/N), was weaker than that observed at the Low Reach.

For the post-logging summer, cross-correlations with stream temperature generally increased for clear sky conditions at all depths, compared to pre-logging conditions, while cross-correlations with seep temperature decreased. Patterns at L2 were no longer distinct from those at the other sites. The contrast between L4 and L5 was similar to that for the pre-harvest period.

5.4 DISCUSSION

5.4.1 Hydrologic characteristics

The two reaches were hydrologically distinct in terms of the magnitude of lateral inflow within the reach and the role of step-pool structures in creating zones of down-welling and up-welling flow. The Mid Reach received a greater proportion of its downstream discharge from lateral inflow compared to the Low Reach, which appeared to lose flow on three measurement dates. These losing periods followed extended periods of low precipitation, except for the measurement on 9 September, 2005, which was conducted after a 6.5 mm event on the preceding day. The Mid Reach on that day showed significant gains and derived 40% of its downstream

flows from lateral inflow. The slopes bounding the Mid Reach appeared to respond relatively rapidly to precipitation events under dry antecedent conditions, in contrast to the slopes bounding the Low Reach, which showed little or no response.

Hydraulic gradients were variable throughout each reach, with the Low Reach exhibiting more DW zones while the Mid Reach contained more piezometers reading positive or slightly fluctuating hydraulic gradients. Vertical hydraulic gradients in DW zones were greater and thus could be measured more accurately compared to the UW/N areas in either reach. There was little variation throughout each year or between logging periods in terms of the direction and magnitude of gradients. Hydraulic gradients showed very weak positive relationships to discharge for both reaches; however, not enough piezometers showed this trend to definitively accept that there is a correlation between discharge and hydraulic gradients.

In general, UW/N zones were found in pools with low elevations below log or rock jams, especially in the Low Reach where these were the only locations UW/N zones were found. In the Mid Reach, UW/N zones were confined to pools only upstream of the groundwater seep; below the seep, UW/N zones were more common and not as confined to low-lying channel morphologies. These results contrast with recent research on hyporheic exchange in mountain channels in the Oregon Cascades, where up-welling zones were generally not observed even in non-losing reaches where they should be present [*Anderson et al.*, 2005; *Gooseff et al.*, 2005; *Wondzell*, 2005]. The measurable UW zones in Griffith Creek may be a result of the relatively consistent lateral inflow that was measured in the two study reaches, causing positive hydraulic gradients from groundwater inflow. This is especially true of the Mid Reach, which generally showed more UW zones than the Low Reach and exhibited larger contributions from lateral inflow throughout the study period. This relation between the presence/absence of lateral inflow and the occurrence of up-welling flow is also supported by the contrast between the portion of Mid Reach upstream of the seep from the portion below.

The relatively consistent gradients that were measured may be an artefact of the depth of the hyporheic zone and the depth at which hydraulic gradients were measured in piezometers in Griffith Creek. If the piezometers were too deep, they might be characterizing the flow system linking the hillslopes to the channel rather than a true hyporheic flow system. Consequently, the observed up-welling zones might actually be related to lateral inflow rather than discharging hyporheic water. This suggestion is supported by results from the cross-correlation of the Low Reach, which shows the strong disconnection of the 20 cm depth bed temperature from the

stream temperature and the strong correlation with seep temperature compared to the DW zones and the other bed temperature depth correlations.

5.4.2 Thermal characteristics

In the Low Reach, bed temperatures were strongly controlled by their hydrologic setting. Temperatures at UW/N sites were lower than at DW sites at equivalent depths during summer. This temperature difference between areas of subsurface exchange is consistent with much research over the past two decades [*Alexander and Caissie*, 2003; *Constantz et al.*, 1998; *Curry et al.*, 2002; *Malcolm et al.*, 2002; *Moore et al.*, 2005c; *Silliman and Booth*, 1993; *White et al.*, 1987]. In the Mid Reach, this effect of vertical water flux on bed temperature was weaker, likely due to the complicated hydrologic pattern and the fact that distinctive zones of up-welling and down-welling were not as apparent. The weaker contrast between up-welling and down-welling sites at Mid Reach could also reflect the greater influence of the lateral inflow, as suggested by the relatively strong cross-correlations between bed and seep temperatures in the pre-harvest summer.

The degree to which bed temperatures responded to logging was strongly dependent on the hydrologic setting. In the Low Reach, the maximum post-logging increases in bed temperatures at DW zones were similar to, though smaller than, the maximum changes in stream temperature. Post-logging increases in bed temperatures also occurred at UW/N sites, though they were smaller than those at DW zones. Bed temperature increases were greatest near the surface and decreased with depth. In the Mid Reach, there were smaller increases in post-logging summer bed temperatures for both hydrologic settings. In part, the smaller post-harvest increases could reflect the smaller change in stream temperature that occurred at Mid Reach (e.g., compare the top graphs in Figure 5.10 and Figure 5.4), although it might also reflect the stronger influence of lateral inflow on bed temperatures. At the Low Reach, the mean increase in bed temperature was greatest for the daily maximum temperature; at the Mid Reach, the mean increase was greatest for daily mean temperature. For both reaches, mean post-logging temperature increases generally decreased with depth, except for the mean change in mean daily temperature at Mid Reach.

The results for Low Reach indicate that the stream bed will likely not warm uniformly following logging, but the magnitude of change will be controlled by the direction of flow into or out of the bed and the thermal signature of the source water. The results for Mid Reach, particularly the tendency to a more uniform increase in temperature with depth, suggest that

vertical heat transport, via conduction and advection, was not the only process causing temperature increases, and that horizontal heat advection via lateral inflow may have played a role.

Effects of hydrologic setting on the bed temperature patterns were also detectable using PCA. Ordination of the loadings for the Low Reach bed temperatures showed that the combined effects of hydrologic setting and depth were expressed by the second principal component for both the pre- and post-logging periods. The second PC accounted for more variance in the post-logging period (11.6% vs 3.5%), possibly reflecting the fact that the effect of logging was more strongly expressed at DW sites and at shallow depths, effectively strengthening the pre-harvest pattern of bed temperature contrasts.

Ordination did not show as clear a picture for the Mid Reach. In the pre-logging period, the horizontal location appeared to account for more of the structure in the ordination plot than the depth. In the post-logging period, the ordination dominantly represented the effect of depth via the second PC, similarly to the pre-logging plots. However, the proportion of variance accounted for by the second PC did not increase after logging at Mid Reach, as it did at Low Reach. Therefore, it appears that, after logging, the effect of depth displaced the effect of horizontal location as a second-order influence on temperature variability. One interpretation of these results is that vertical heat transport in the bed was relatively small in the pre-logging period and the thermal signature of the groundwater seep had a larger influence on the bed temperature patterns. However, with removal of the canopy in the post-logging period, increased solar radiation influenced the bed temperatures through heat conduction associated with the increased insolation at the surface of the bed. This would explain the pattern with depth being established in the post-logging period.

The points in Figures 5.6 and 5.12 exhibit a horseshoe pattern. This pattern is common when conducting PCA and is debated by authors to its meaning. Detrended correspondence analysis (DCA) can be used to correct the shape [*Chang and Gauch*, 1986]. However, it is not clear if DCA will rectify the distortion in the analysis and may even add to it [*Kenkel and Orloci*, 1986]. A critique even suggests that the shape is simply an artifact of the data that are used in the analysis and does not affect the results [*Wartenberg et al.*, 1987]. Due to these differing opinions it is believed that the results from the PCA are not distorted. The fact that the ordination patterns can be interpreted in relation to plausible changes in heat transport processes following harvest supports their validity.

Cross-correlation analyses were consistent with the results of PCA. The Low Reach showed especially consistent results, with the easily identifiable UW/N and DW zones showing higher correlations with seep and stream temperatures, respectively. However, where the cross-correlation results assisted interpretation was in the Mid Reach with its complicated thermal patterns. In the pre-logging period, the high correlations with seep temperature for the L3, L4, and L5 thermocouple locations, which are downstream of the seep, and the different patterns at the L1 and L2 locations, are broadly consistent with the effect of horizontal location that is present in the pre-harvest ordination. The CCA are also consistent with the contrasting changes in mean daily temperature for L4 (DW) and L5 (UW/N). Cross-correlations with seep temperature exceeded 0.5 at all depths at L5, while at L4 they dropped below 0.5 in the top 10 cm, consistent with the stronger influence of vertical heat transport from the surface via down-welling flow at that site.

An example of the potential role that UW/N zones have on stream temperature is illustrated in the pre-logging portion of Figure 5.2. This figure shows that stream temperature was lower than bed temperatures in the DW zone but higher than those in the UW/N zone. Water temperature data loggers were placed in pools throughout the stream to ensure that they would be submerged during summer low flow periods. This particular water temperature probe was located approximately 1 m downstream of the S1D bed temperature site, therefore being in a location where it was receiving a mixture of stream surface water and water that discharged from the bed, giving it an intermediate temperature signature. The S3 site showed similar temperature contrasts between DW and UW/N sites, suggesting that this pattern of stream water mixing below steps may be a common phenomenon, consistent with previous studies [*Bilby*, 1984; *Moore et al.*, 2005c; *Story et al.*, 2003]. This pattern was not present in the post-logging period, likely as a result of the increased solar radiation warming the water mixture before it reached the water temperature probe.

5.4.3 Biological implications

Griffith Creek is non-fish bearing; however, these results are consistent with other research that local UW zones and groundwater discharge provide cooler water temperature locations and can be areas of refuge for fish in extreme summer warm periods [*Power et al.*, 1999]. The lower magnitude of post-logging warming in the UW/N zone also suggests that UW zones may retain their cool water properties and may be able to provide areas of thermal refuge in fish-bearing reaches. However, the post-harvest data from the Low Reach suggested that stream

water did heat shortly after emerging from the bed, and thus that the area or volume of cool-water zones in a stream may be reduced.

These findings also have implications for the distribution and abundance of benthic communities, which are strongly influenced by their thermal environment [*Vannote and Sweeney*, 1980]. Research conducted on stream invertebrates showed that daily temperature fluctuations of 10 °C decreased the mean temperature required to cause lethal results in mayfly *Deleatidium autumnale* by up to 2 °C [*Cox and Rutherford*, 1999]. This may be of concern when considering the increased amplitude of daily bed temperatures in the post-logging period and the greater proportion of the stream bed that exhibited DW flows compared to UW flows in the Low Reach. Although Griffith Creek did not approach these increased mortality ranges it should be noted that benthic communities may be reduced in abundance because UW/N zones, which may be required for optimal growth and fecundity of invertebrates in post-logging conditions, may not be as abundant as the less favourable DW zones in the post-logging period.

Table 5.1 Griffith Creek Low Reach discharge values in Ls^{-1}. UB and LB are the reach upper and lower boundary, respectively, and S2 and S3 are locations of step-pool sequences.

	30/5/ 2005	24/6/ 2005	22/7/ 2005	25/7/ 2005	2/8/ 2005	5/8/ 2005	5/9/ 2005	17/9/ 2005	8/10/ 2005	29/10/ 2005
UB	0.83	2.50	1.03	0.82	0.24	0.31	0.18	0.30	9.54	3.08
S2	0.85				0.24				9.54	3.08
S3	0.9				0.26				9.69	3.11
LB	0.98	2.48	0.99	0.83	0.28	0.31	0.17	0.31	10.01	3.15
S2 - UB	0.02				0.00				0.00	0.00
S3 - S2	0.05				0.02				0.15	0.03
LB - S3	0.08				0.02				0.32	0.04
LB - UB	0.15	-0.02	-0.04	0.01	0.04	0.00	-0.01	0.01	0.47	0.07
Lateral Inflow Percent	15.3	-0.8	-4.0	1.2	14.3	0.0	-5.9	3.2	4.7	2.2

Table 5.2 Hydraulic conductivities measured at Griffith Creek Low Reach. CI indicates approximate 68% confidence intervals.

Piezometer	Hydraulic Conductivity ($m\ s^{-1}$)							Lower CI	Geometric Mean	Upper CI
2 (UW/N)	NA	NA	2.4E-05	3.5E-05	2.3E-05	5.9E-05	4.2E-05	1.3E-05	4.2E-05	1.4E-04
3 (UW/N)	NA	NA	1.6E-04	6.8E-04	1.0E-04	8.6E-04	4.0E-04	9.3E-05	4.0E-04	1.7E-03
4 (DW)	1.7E-07	NA	9.0E-06	1.7E-05	1.2E-05	1.6E-05	6.7E-06	2.0E-07	6.7E-06	2.2E-04
6 (UW/N)	1.7E-04	1.9E-04	9.0E-05	1.7E-04	1.4E-04	2.4E-04	1.6E-04	1.1E-04	1.6E-04	2.4E-04
8 (UW/N)	2.0E-04	7.5E-04	1.1E-04	4.0E-04	1.6E-04	1.2E-04	2.5E-04	9.9E-05	2.5E-04	6.1E-04
12 (DW)	7.4E-05	6.5E-05	8.1E-05	7.4E-05	6.4E-05	5.5E-05	6.7E-05	5.5E-05	6.7E-05	8.2E-05
Sample Date	2/8/ 2005	5/8/ 2005	15/8/ 2005	5/9/ 2005	3/10/ 2005	8/10/ 2005	29/10/ 2005			

Table 5.3 Mean differences between observed and predicted temperatures for the pre- and post-logging periods, for one down-welling (DW) and one up-welling/neutral (UW/N) site in the low reach. s_e of residuals is the standard error of the pre-logging regression, d.f. is the pre-logging degrees of freedom, and k is the order of the residual autocorrelation.

Temperature Variable	Period	DW 1 cm	DW 5 cm	DW 10 cm	DW 15 cm	UW/N 1 cm	UW/N 5 cm	UW/N 10 cm	UW/N 20 cm
Daily Maximum	Pre-logging	0.09	0.09	0.04	0.06	0.00	0.01	0.03	0.14
	Post-logging	1.20	1.03	0.99	0.76	1.08	0.81	0.62	0.42
s_e of residuals		0.60	0.58	0.45	0.48	0.44	0.48	0.53	0.79
d.f.		143	143	143	143	143	143	143	143
K		3	3	2	2	2	3	3	3
Daily Mean	Pre-logging	0.01	-0.02	-0.02	0.00	0.02	0.02	0.04	0.08
	Post-logging	0.75	0.62	0.47	0.36	0.56	0.45	0.33	0.26
s_e of residuals		0.48	0.48	0.51	0.55	0.51	0.53	0.57	0.61
d.f.		143	143	143	139	143	143	143	143
K		2	2	2	2	2	2	2	1
Daily Minimum	Pre-logging	-0.01	0.00	0.01	0.02	0.00	0.00	0.01	0.07
	Post-logging	0.35	0.29	0.11	0.02	0.25	0.12	-0.01	-0.08
s_e of residuals		0.48	0.48	0.51	0.55	0.51	0.53	0.57	0.61
d.f.		143	143	143	143	143	143	143	143
K		2	2	2	2	2	2	2	1

Table 5.4 Measured streamflow at Griffith Creek Mid Reach (Ls^{-1}). UB and LB are the reach upper and lower boundaries, respectively. Location of L5 is shown on Figure 4.8.

	6/6/ 2005	24/6/ 2005	18/7/ 2005	22/7/ 2005	25/7/ 2005	5/8/ 2005	5/9/ 2005	17/9/ 2005	8/10/ 2005	24/10/ 2005	29/10/ 2005
UB	1.43	2.06	0.95	0.86	0.57	0.12	0.09	0.14	8.31	5.65	2.48
L5	1.95		1.15						8.78	5.85	2.73
LB	2.17	2.08	1.23	0.94	0.65	0.26	0.15	0.24	8.99	6.02	2.82
L5 - UB	0.52		0.20						0.47	0.20	0.25
LB - L5	0.22		0.08						0.21	0.17	0.09
LB - UB	0.74	0.02	0.28	0.08	0.08	0.14	0.06	0.10	0.68	0.37	0.34
Lateral Inflow Percent	34.1	1.0	22.8	8.5	12.3	53.8	40.0	41.7	7.6	6.2	12.1

Table 5.5 Hydraulic conductivities measured at Griffith Creek Mid Reach. CI indicates approximate 68% confidence intervals.

Piezometer	Hydraulic Conductivity (m s^{-1})						Lower CI	Geometric Mean	Upper CI
2 (UW/N)	2.5E-05	1.3E-05	1.5E-04	1.2E-04	9.0E-05	5.8E-05	1.1E-05	5.8E-05	3.1E-04
6 (UW/N)	NA	2.4E-05	8.8E-05	7.4E-06	4.3E-06	1.2E-05	7.0E-07	1.2E-05	2.2E-04
8 (UW/N)	NA	9.2E-06	2.3E-05	1.0E-05	1.0E-05	1.1E-05	4.8E-06	1.1E-05	2.7E-05
9 (UW/N)	NA	1.6E-05	4.4E-05	4.7E-05	5.8E-05	3.8E-05	1.4E-05	3.8E-05	1.0E-04
10 (DW)	NA	3.3E-05	1.3E-05	1.1E-05	1.0E-05	1.4E-05	4.9E-06	1.4E-05	4.0E-05
11 (UW/N)	4.3E-06	NA	6.4E-05	7.5E-05	8.2E-05	4.3E-05	3.4E-06	4.3E-05	5.5E-04
12 (DW)	NA	6.3E-05	1.8E-04	6.2E-05	9.0E-05	8.9E-05	3.2E-05	9.0E-05	2.5E-04
13 (DW)	NA	NA	2.8E-05	1.6E-04	2.4E-05	4.0E-05	4.9E-06	4.0E-05	3.2E-04
Sample Date	5/08/ 2005	15/08/ 2005	5/09/ 2005	3/10/ 2005	8/10/ 2005	29/10/ 2005			

Table 5.6 Mean differences between observed and predicted temperatures for the pre- and post-logging periods, for one down-welling (DW) and one up-welling/neutral (UW/N) site in the mid reach. s_e of residuals is the standard error of the pre-logging regression, d.f. is the pre-logging degrees of freedom, and k is the order of the residual autocorrelation

Temperature Variable	Period	DW 5 cm	DW 10 cm	DW 15 cm	DW 30 cm	UW/N 5 cm	UW/N 10 cm	UW/N 15 cm	UW/N 30 cm
Daily Maximum	Pre-logging	0.08	0.08	0.07	0.04	0.02	0.05	0.07	0.05
	Post-logging	0.15	0.17	0.20	0.18	0.33	0.03	0.09	0.14
s_e of residuals		0.81	0.74	0.67	0.52	0.58	0.65	0.59	0.51
d.f.		355	355	336	344	201	324	355	355
K		3	3	3	3	1	3	3	1
Daily Mean	Pre-logging	0.09	0.08	0.07	0.04	0.04	0.05	0.07	0.08
	Post-logging	0.37	0.34	0.36	0.34	0.51	0.22	0.27	0.19
s_e of residuals		0.84	0.78	0.71	0.57	0.59	0.69	0.60	0.62
d.f.		355	355	336	344	201	324	355	355
K		3	3	3	3	1	3	3	3
Daily Minimum	Pre-logging	0.08	0.07	0.06	0.04	0.04	0.07	0.08	0.08
	Post-logging	0.02	0.02	-0.01	-0.02	0.15	-0.17	-0.12	-0.04
s_e of residuals		0.86	0.77	0.70	0.66	0.66	0.73	0.65	0.61
d.f.		355	355	336	344	201	324	355	355
K		1	1	1	1	1	1	1	1

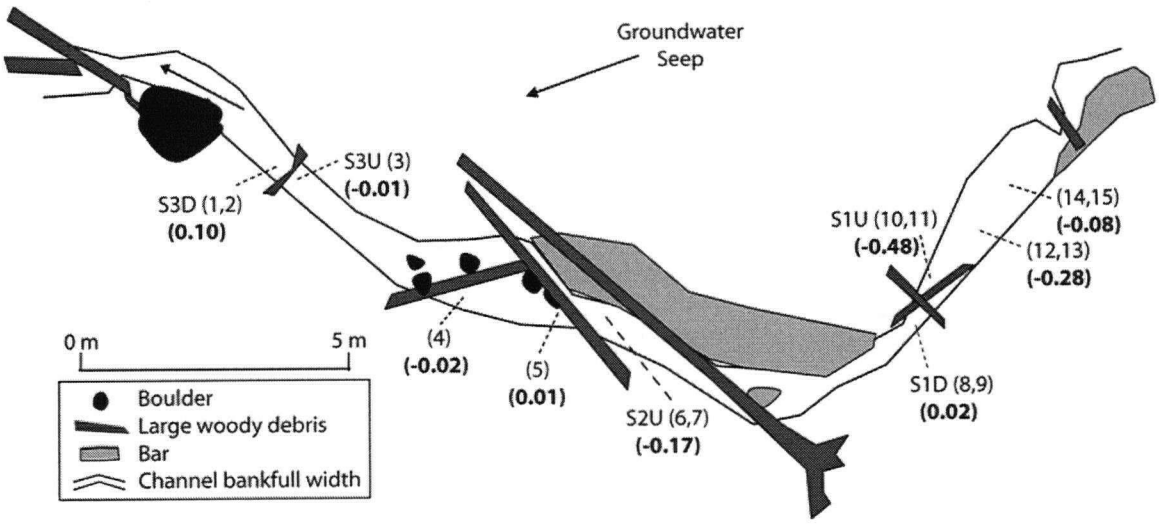

Figure 5.1 Map of Griffith Creek Low Reach, showing locations of thermocouple nests (S1U, S1D, S2U, S3U, S3D), groundwater seep location, and piezometer locations (numbers in brackets). Bold numbers indicate study period average hydraulic gradients (negative values indicating flow into the stream bed). Stream flows according to arrow.

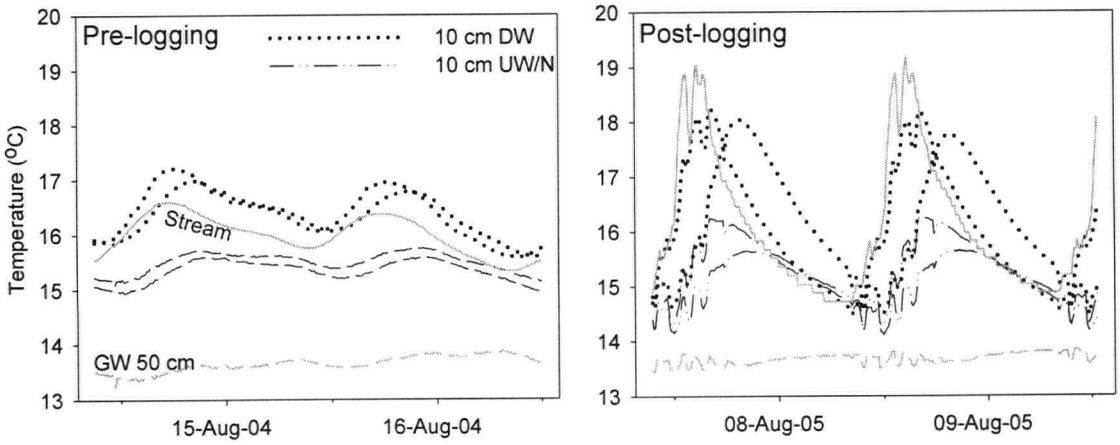

Figure 5.2 Bed temperatures of S1 and S3 down-welling (DW) and up-welling/neutral (UW/N) sites at 10 cm depth in the Low Reach, with stream and 50 cm depth groundwater seep temperatures for two warm days in pre- (left) and post-logging (right) summers.

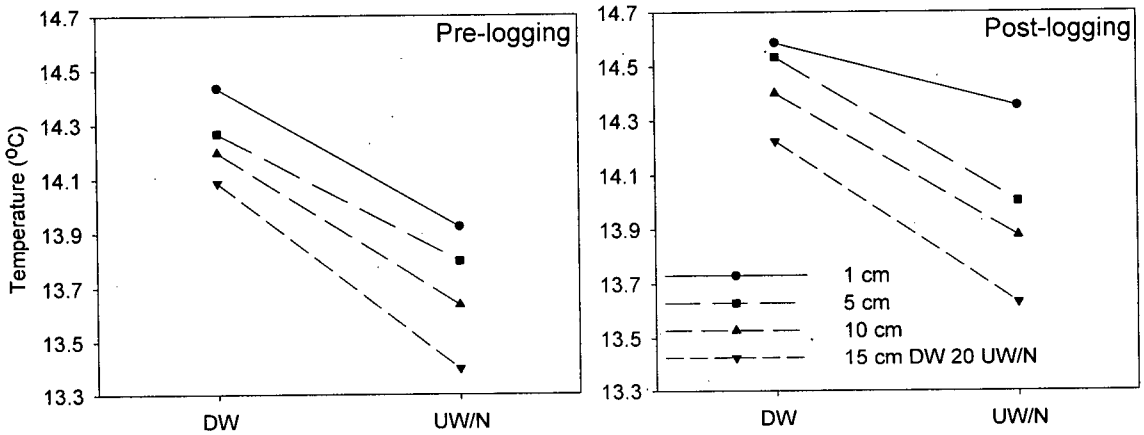

Figure 5.3 Means of mean seasonal bed temperatures grouped by hydrologic setting and depth for 3 down-welling and 2 up-welling sites in the pre- and post-logging summers (13/7/2004 – 12/9/2004 and 10/7/2005 – 9/9/2005).

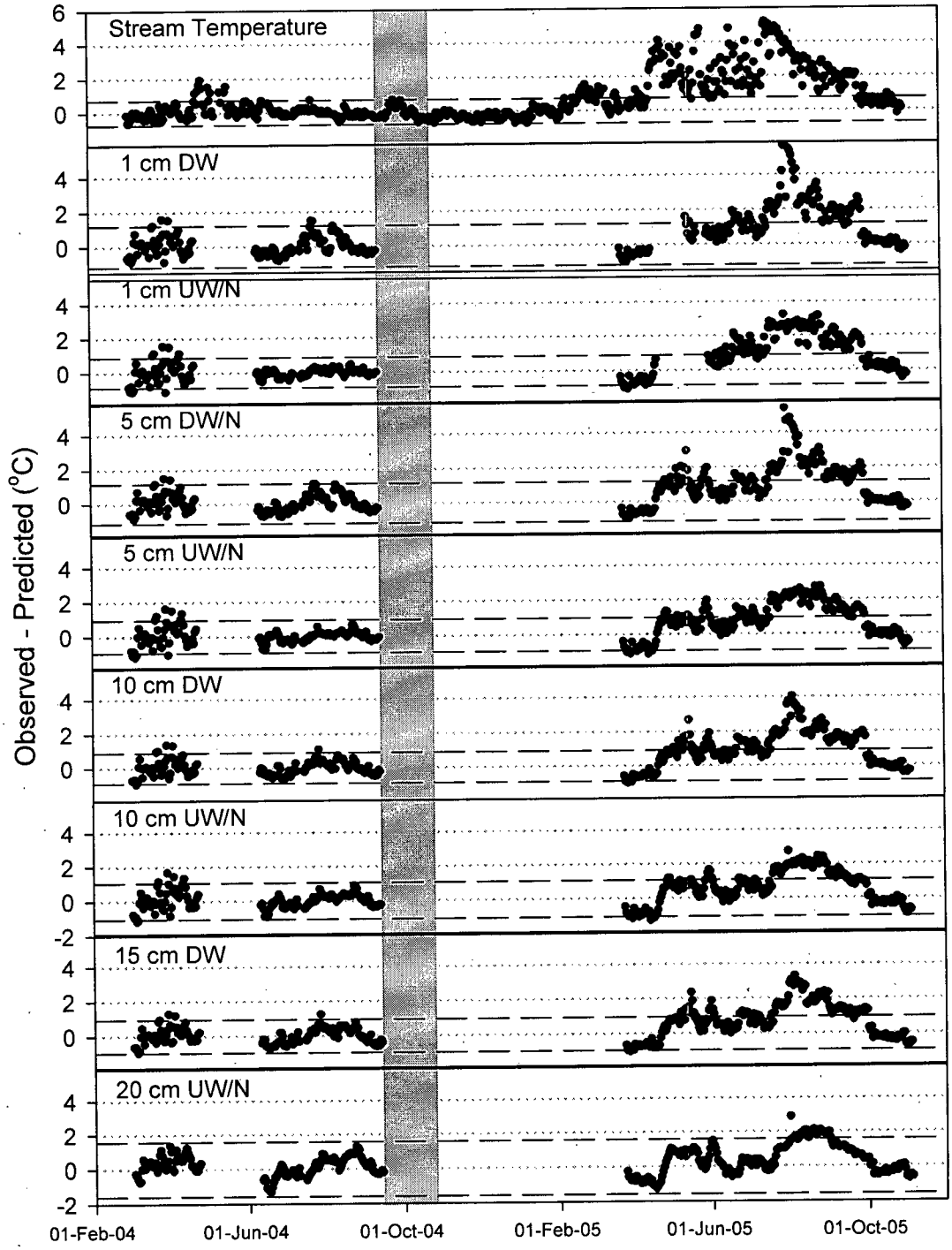

Figure 5.4 Difference between observed and predicted daily maximum stream and bed temperatures in the low reach. Bed temperatures are shown for one down- (DW) and one up-welling/neutral (UW/N) location. Vertical lines indicate logging period (Sep 04 – Nov 04). Horizontal dashed lines indicate 2 times the s_e of residuals from the pre-logging regression. Bed temperature data are missing from 22 April to 8 June 2004 due to a malfunction of the data logging system, and no data were recorded between 11 September 2004 and 23 March 2005.

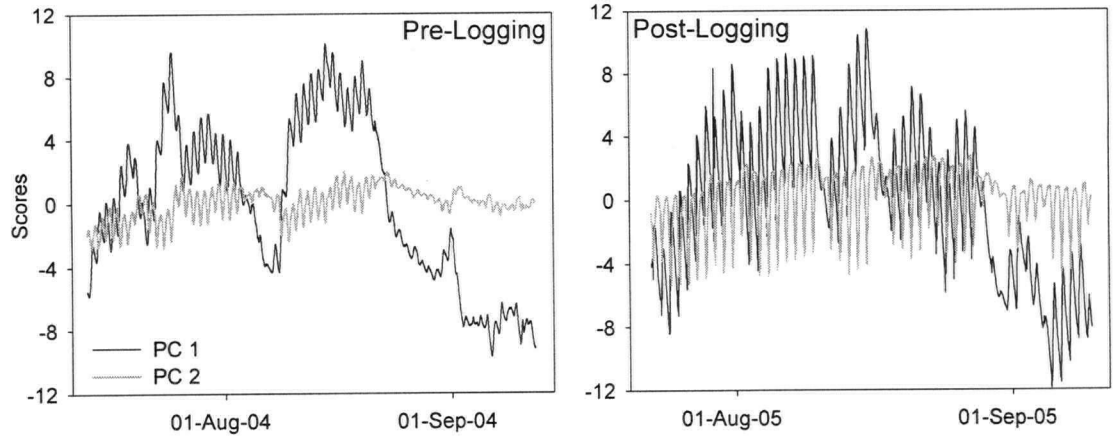

Figure 5.5 Time series of principal component scores from PCA of Low Reach bed temperatures for pre- (left) and post-logging (right) periods. Scores are plotted for the first two principal components.

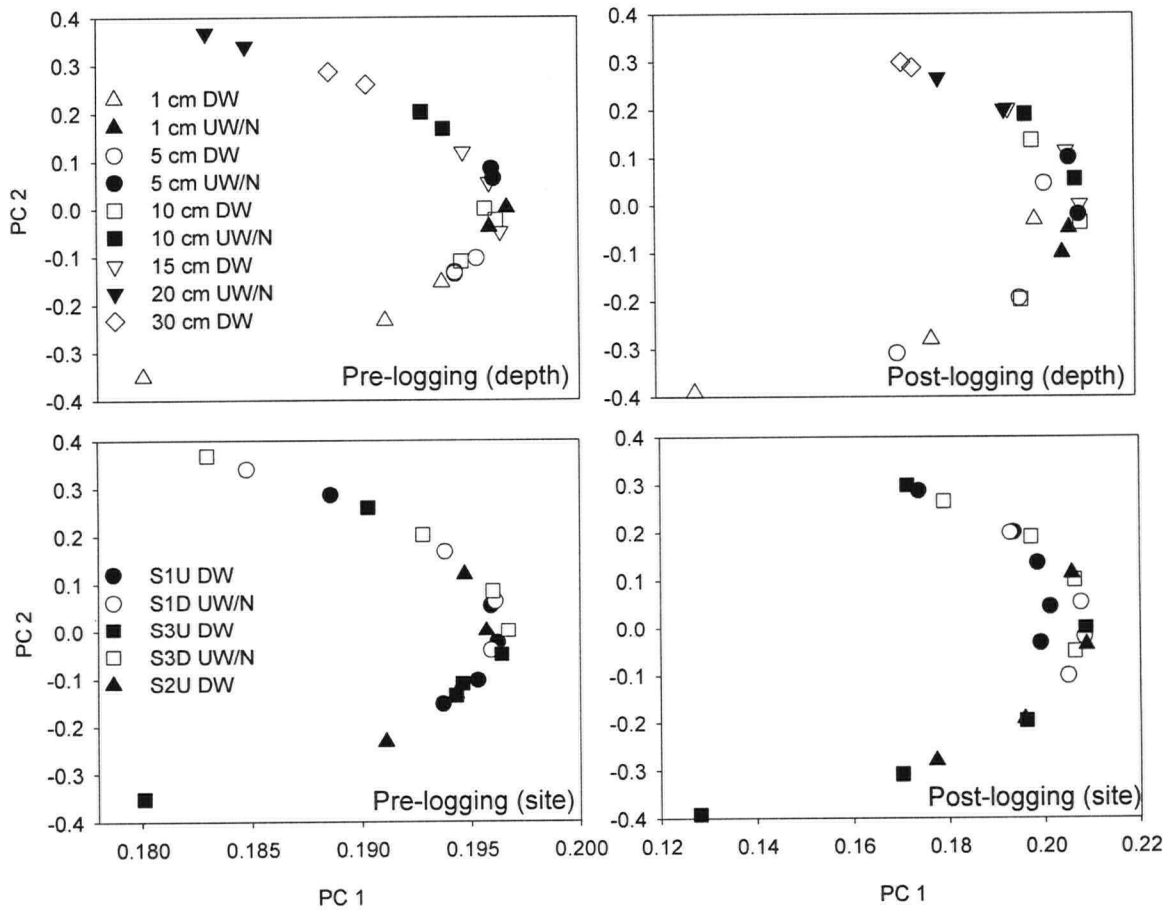

Figure 5.6 Ordination of first and second principal components for pre-logging (left) and post-logging (right) bed temperature data by depth (top) and site (bottom). DW and UP/N indicates down-welling and up-welling/neutral sites respectively.

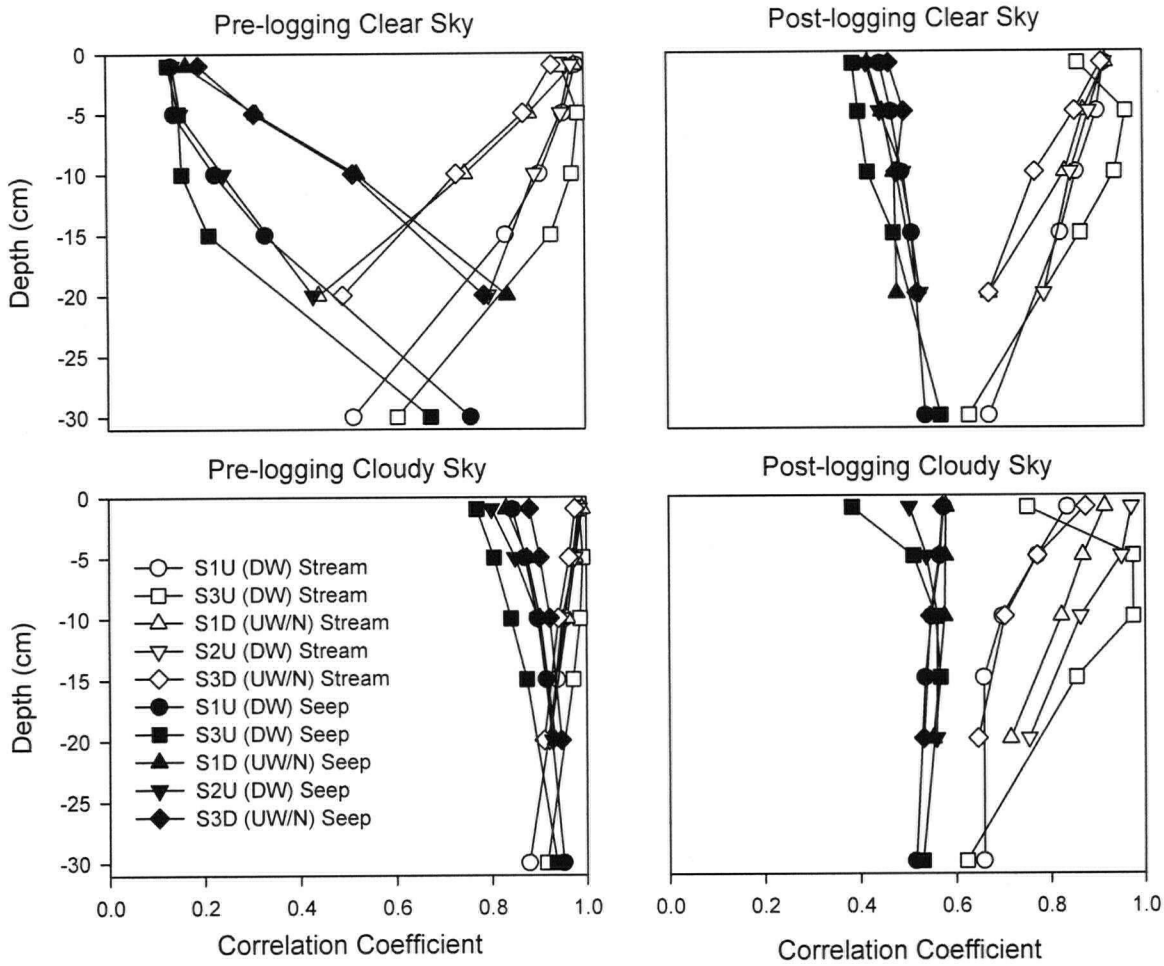

Figure 5.7 Low Reach cross correlation coefficients of bed temperature versus stream and seep temperatures plotted against bed temperature depth for two consecutive clear (top) and cloudy (bottom) sky days in the pre- (left) and post-logging (right) period.

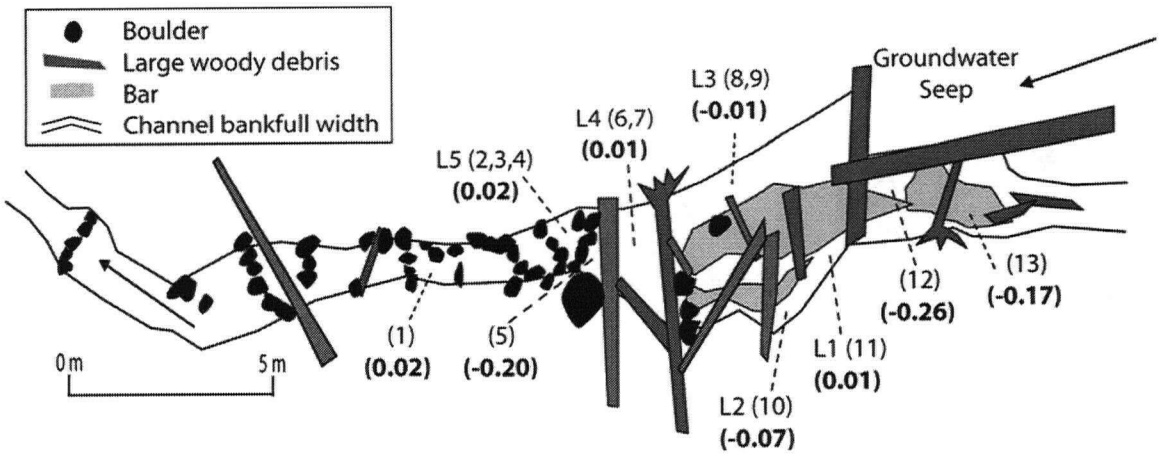

Figure 5.8 Map of Griffith Creek Mid Reach, showing locations of thermocouple nests (L1-L5), groundwater seep location, and piezometer locations (numbers in brackets). Bold numbers indicate study period average hydraulic gradients (negative values indicating flow into the stream bed). Stream flows according to arrow.

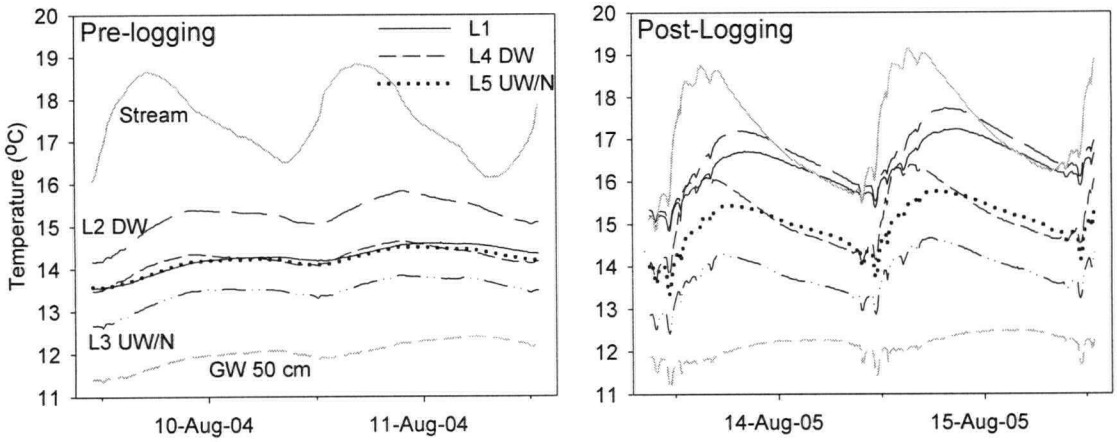

Figure 5.9 Bed temperatures at 10 cm depth in the mid reach, with stream and 50 cm depth groundwater seep temperatures for two warm days in pre- (left) and post-logging (right) summers.

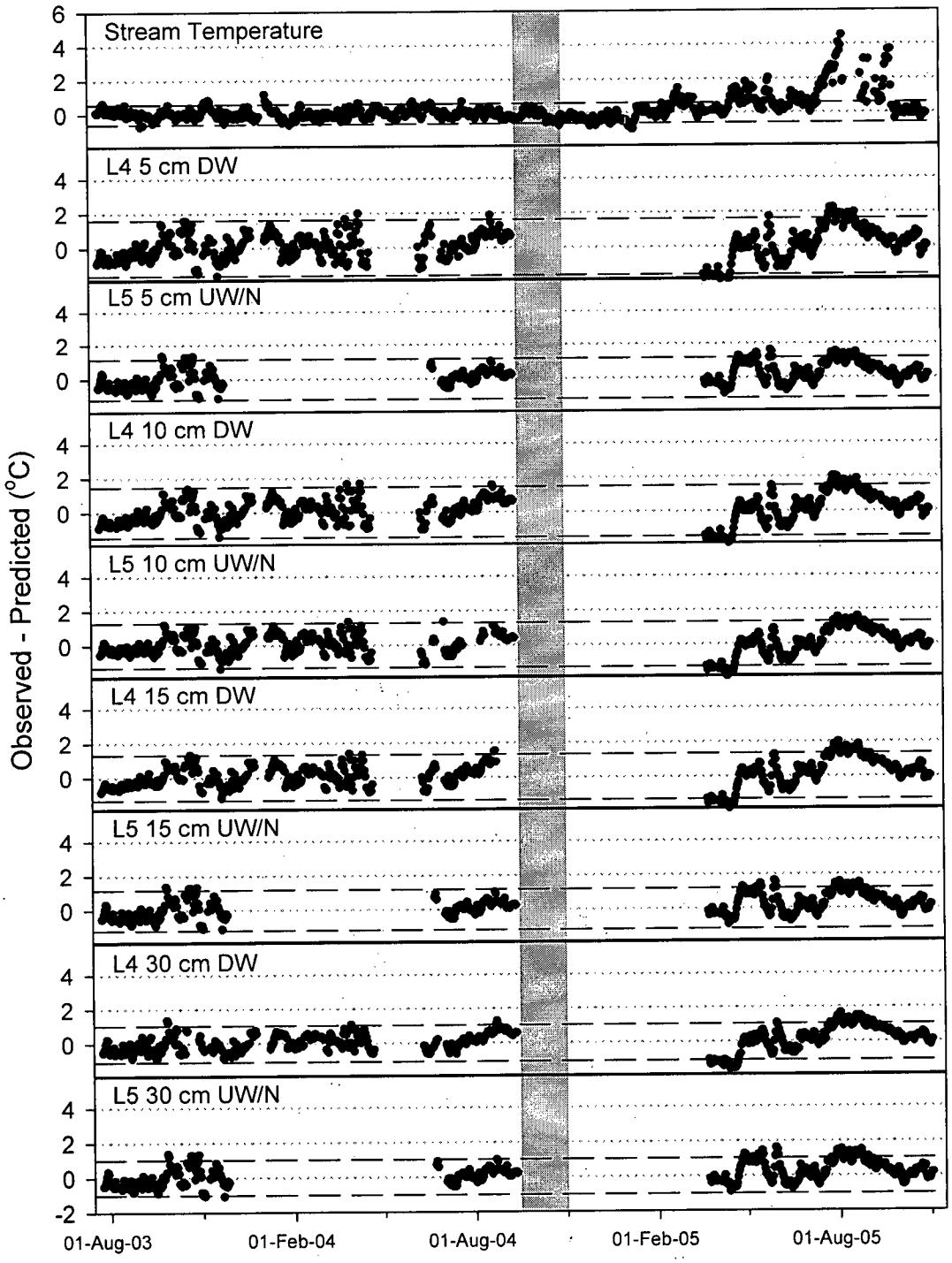

Figure 5.10 Difference between observed and predicted daily maximum stream and bed temperatures in the mid reach. Bed temperatures are shown for one down- (DW) and one up-welling/neutral (UW/N) location. Vertical lines indicate logging period (Sep 04 – Nov 04). Horizontal dashed lines indicate 2 times the s_e of residuals from the pre-logging regression. Bed temperature data are missing from 22 April to 8 June 2004 due to a malfunction of the data logging system, and no data were recorded between 11 September 2004 and 23 March 2005.

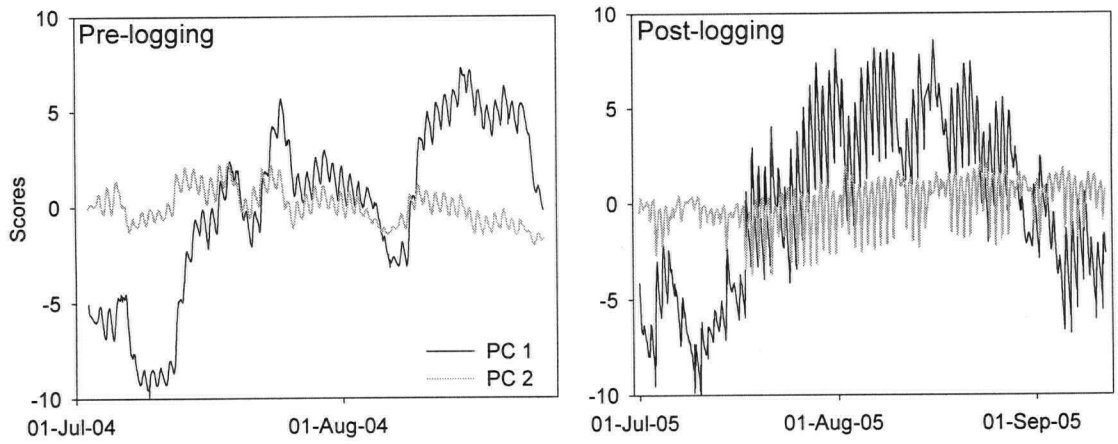

Figure 5.11 Time series of principal component scores from PCA of Mid Reach bed temperatures for pre- (left) and post-logging (right) periods. Scores are plotted for the first two principal components.

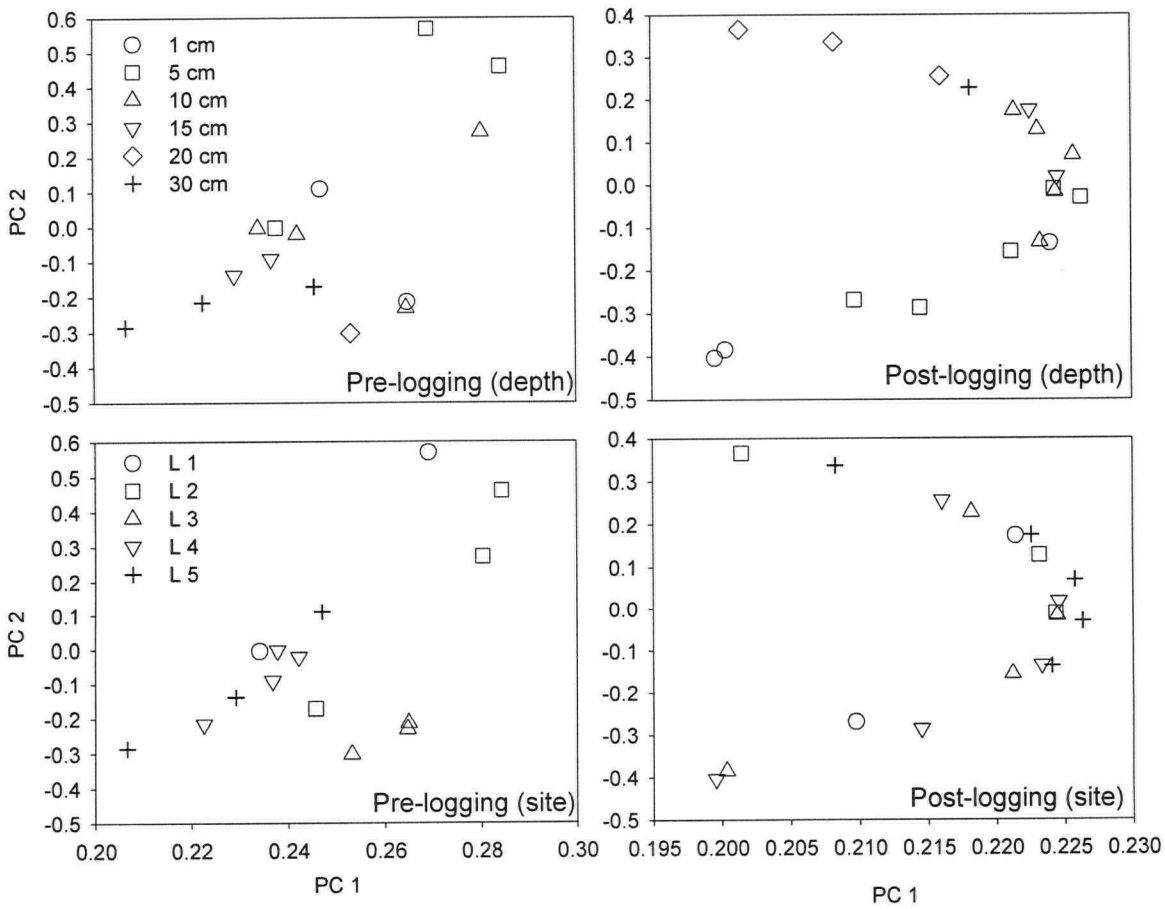

Figure 5.12 Ordination of first and second principal components for pre-logging (left) and post-logging (right) bed temperature data by depth (top) and location in the stream (bottom).

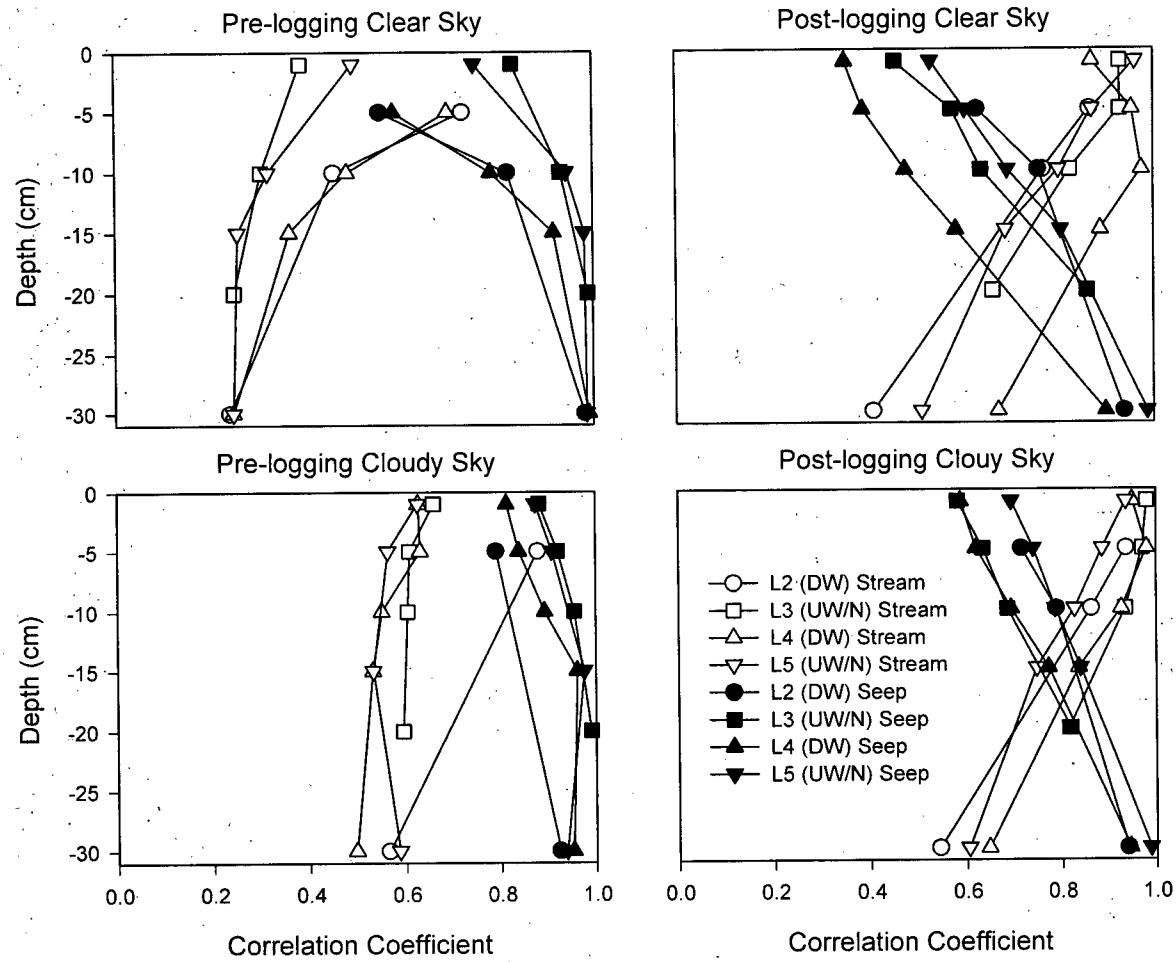

Figure 5.13 Mid Reach cross correlation coefficients of bed temperature versus stream and seep temperatures plotted against bed temperature depth for two consecutive clear (top) and cloudy (bottom) sky days in the pre- (left) and post-logging (right) period.

CHAPTER SIX

EFFECTS OF FOREST HARVESTING ON STREAM HEAT BUDGETS: AN EXPERIMENTAL APPROACH

6.1 INTRODUCTION

Stream temperatures reflect the influences of a variety of energy fluxes, which can be classed as being atmospheric or terrestrial. Atmospheric energy exchanges include solar radiation, longwave radiation, sensible heat, and latent heat. Terrestrial fluxes include bed heat conduction, heat from groundwater discharge, and hyporheic heat exchanges. Heat budgets have been used to understand stream temperature dynamics in a variety of settings; however most of these studies were not conducted in the context of forest harvesting [*Evans et al.*, 1998; *Webb and Zhang, 1997*]. The earliest heat budget study focused on forest harvesting was conducted by Brown [1969]; since then, only Story *et al.* [2003], Johnson [2004] and Moore *et al.* [2005b] appear to have estimated heat budgets for forestry-influenced streams.

None of those studies applied heat budgets in both pre- and post-logging conditions at the same site, making the analysis of which processes are responsible for stream temperature increases more difficult to assess. This chapter will focus on the results of the application of a heat budget analysis to two study reaches both before and after a 50% dispersed retention logging treatment along the stream. Analysis will focus on the identification of the processes which are responsible for creating the thermal regime of the stream in the post-logging environment. Methods have been described in detail in chapter two.

6.2 OVERVIEW OF PERIODS USED FOR HEAT BUDGET ANALYSIS

Heat budgets were calculated for two days in July and August of both the pre- and post-logging period. The pre-logging summer was warmer and drier than the post-logging summer (Figure 6.1 and 6.2, and chapter 3). The two-day periods used in the heat budget were similar between pre- and post-logging summers. Daily maximum air temperature was greater in 2004 for both the July and August two-day periods, with daily maximum temperature near 30°C compared to 25°C in the post-logging summer. Minimum air temperatures were similar for both periods, with values ranging between 10 °C and 15 °C. This pattern was reversed for stream temperatures: the post-logging summer was warmer by at least 1 °C compared to the respective

period of the pre-logging summer. Discharge also was greater in the post-logging summer compared to 2004, with values averaging one order of magnitude greater than the pre-logging summer.

6.3 SOLAR RADIATION MODELLING

Solar radiation for the heat budget was modelled using hemispheric canopy images taken above the stream to map the distribution of canopy gaps in relation to the sun's position. Modelled solar radiation was compared to measured data to calibrate the darkness threshold of the images in both the pre- and post-logging periods. For the pre-logging period, the calibration was based on hourly averages of solar radiation for three pyranometers located directly over Griffith Creek. For the post-logging period, data were only available for one location over the stream. The calibration periods for both the pre- and post-logging conditions consisted of generally clear sky conditions. Calibration emphasized clear sky conditions due to the proportions of these conditions during the summer months when stream heating occurred.

Calibration in the pre-logging period was relatively accurate, with only small deviations present between the modelled and below canopy measurements (Figure 6.3). The post-logging calibration was not as accurate, with the modelled radiation exhibiting a lower peak but greater amounts of radiation in the morning and evening compared to the measured below canopy observations. However, the daily radiation totals were approximately equal between observed and modelled data.

6.4 HEAT BUDGET RESULTS FOR THE LOW REACH

In the pre-logging period, the primary positive flux was net radiation during the day time, with sensible and latent heat contributing small quantities irregularly for latent heat (Figure 6.4 and 6.5). Bed heat conduction and hyporheic heat exchange were the dominant day time cooling fluxes, accounting for almost 60% and 40% of the heat losses in the pre-logging period, respectively. Groundwater discharge contributed consistently small magnitudes near 2 W m^{-2}; these negative fluxes were strongest during daytime and decreased at night. All fluxes were relatively small in magnitude, ranging from about 70 to -40 W m^{-2}.

The heat fluxes exhibited some contrasts between the July and August periods in the pre-logging period. In July, most heat fluxes became negligible at night, with the exception of bed heat conduction, which was a heat source, and latent heat which acted as cooling fluxes. In

August, net radiation remained positive at night, while bed heat conduction became a heat sink. Hyporheic exchange also became a nocturnal heat sink in August.

The agreement between observed and modelled rates of temperature change varied. In July, the heat budget predicted almost continuous cooling, in contrast to the observed pattern of diurnal warming and nocturnal cooling. In August 2004, the modelled temperature changes were in reasonable agreement with observations at night, with both indicating weak cooling. However, the heat budget predicted cooling through the morning in contrast to observed warming, and warming in the late afternoon, when weak cooling actually occurred.

In the post-logging period, energy fluxes were generally greater than in the pre-logging period, ranging from 390 to -50 W m^{-2} in July and 380 to -110 W m^{-2} in August (Figure 6.6 and 6.7). Fluxes were lower in July compared to August, similar to the pre-logging situation. The relative magnitudes of most of the energy fluxes were similar to those during the pre-logging period, with net radiation remaining the dominant daytime warming flux and sensible heat adding small amounts. In contrast to the pre-logging period, groundwater discharge assumed a stronger role as a daytime cooling flux. Latent heat changed sign in the post-logging period, and remained continuously negative and accounted for almost 25% of the cooling. Hyporheic exchange, bed heat conduction, and groundwater discharge accounted for, on average, 40, 25, and 10% of the cooling in the two post-logging study periods, respectively. One exception to this pattern occurred in the evening after a warm day in August, when bed heat conduction and hyporheic heat exchange became positive (Figure 6.7).

Consistent with the increased heat inputs after logging, observed rates of temperature change exceeded 1 °C/hr, in contrast to maximum pre-logging warming rates of about 0.3 °C/hr. The observed and modelled rates of temperature change showed better agreement than for the pre-logging period, particularly at night. However, the heat budget over-predicted warming in the morning and late afternoon, and over-predicted cooling in the early evening.

For the pre-logging period, increasing the stream depth used in the heat budget calculations improved the agreement between predicted and observed temperature change to some degree by dampening the modelled rate of temperature change, but there were still notable discrepancies. Increasing stream depth for the post-logging period greatly increased the agreement between predicted and observed temperature changes. However, some of the short term fluctuations were not represented by the heat budget model. This is supported by root mean squared error (RMSE) values which showed that model agreement with observed values increased when water column depth was increased, with RMSE values decreasing 0.20 and 0.12

for July and August of the pre-logging period and 0.46 and 0.45 in July and August of the post-logging period (Table 6.1).

6.5 HEAT BUDGET RESULTS FOR THE MID REACH

Energy fluxes showed similar patterns in the Mid Reach as for the Low Reach in both the pre- and post-logging periods (Figure 6.8 to 6.11). Inputs of energy were dominated by net radiation, and in the pre-logging July period, latent and sensible heat added energy to the stream during day time. Negative fluxes in the pre-logging period were dominated by bed heat conduction, accounting for approximately 50% of the heat loss, as well as groundwater discharge, hyporheic exchange, and latent heat, accounting for approximately 25, 20 and 5% of the heat loss, respectively. In the post-logging period, all terms except net radiation were negative fluxes. Bed heat conduction, latent heat, groundwater discharge, and hyporheic exchanges each accounted for approximately 25% of the day time cooling fluxes in the Mid Reach.

In the July example for the pre-logging period, the modelled temperature changes captured the observed diurnal warming and nocturnal cooling, but greatly exaggerated the rates, particularly for nocturnal cooling. In the August example, the modelled temperature changes were strongly biased toward cooling. In the post-logging period, modelled temperature changes dramatically over-predicted day time warming and night time cooling. As with the Low Reach, the heat budget generally overestimated daytime heating and underestimated a short period after sunset.

Agreement between modelled and observed rates of temperature change increased for both pre- and post-logging periods by increasing stream depth (Figures 6.8 to 6.11). Calculated RMSE values for the two modelled depths reduced when depth was increased with values decreasing from 0.42 to 2.69 (Table 6.2). Depth had to be increased more in the Mid Reach than the Low Reach to achieve agreement with observed data.

The improved agreement between modelled and observed rates of temperature change with increased stream depth suggests that the conceptualization of hyporheic exchange in the heat budget model may not be appropriate. Figure 6.12 illustrates the rates of temperature change for the model without the hyporheic heat exchange component. Depth was set to achieve the best fit to daytime heating. This revised model underestimated rates of cooling in the early evening. Modelled rates of temperature change were reasonable for the cloudy day. The fit was not as

precise in comparison to that of Figure 6.7, where hyporheic exchange was included in the heat budget.

6.6 DISCUSSION

Modelled rates of temperature change did not agree well with observed rates in the pre-logging period. In particular, the heat budget appeared to be biased toward cooling, in contrast to the consistently observed daytime warming. However, all fluxes were small, and thermal differences used to compute heat fluxes were on the order of ± 0.2 °C, the same as the measurement error. Modelled and observed rates of temperature change agreed better after logging, at least at the Low Reach, when stronger thermal contrasts dominated. The heat budget model performed better in the Low Reach than in the Mid Reach.

A major source of error in the heat budget estimates could be the difficulty in accurately modelling solar radiation in such complex shade environments. For example, the overestimation of dT/dt on overcast days, when all fluxes but net radiation were minor, suggests that net radiation has been overestimated (Figure 6.6, July 2, 2005). Similarly, the overestimation of dT/dt in the morning and late afternoon could result from underestimation of shading at lower sun angles. However, the improved agreement with observed dT/dt when reach average water column depth was increased suggests that our depth estimates are too low. Moore et al. [2005c] observed similar results, with doubling the water column depth creating much better agreement with the observed rate of temperature change. This result suggests either that the reach-average water column depth was underestimated, or that the volume of water involved in stream heating and cooling is not only constrained to that of the water column. While uncertainty does exist in the estimated depths, it is not likely to be large enough to account for the depth increases that were required to match modelled and observed rates of temperature change.

These results suggest that our conceptualization of hyporheic exchange flows may not be accurate, especially since we focused on parameterizing the effects of vertical exchanges. This parameterization is based on the notion that hyporheic residence times are on the order of hours, so that the temperature of discharging hyporheic water is out of phase with stream temperature. However, this conceptualization does not account for short duration hyporheic exchange through steps and lateral flow paths through point bars and across the stream banks. These exchanges effectively increase the active water volume that is heated and cooled, but without the effects of a significant temperature difference between downwelling and discharging water. Tracer studies conducted on Griffith Creek's Low and Mid Reach showed that the transient storage zone

represented a mean depth of approximately 7 cm for both reaches (Gomi, unpublished data). This value is somewhat lower than differences between measured water column depths and those used to achieve a good fit in the heat budgets, which were 6 cm for the Low and 13 cm for the Mid Reach.

Errors in solar radiation and water column depth cannot account for all of the discrepancies between modelled and observed temperature change. For example, the overestimation of late-afternoon cooling (e.g., Figure 6.7, August 8, 2005) suggests that some of the cooling fluxes have been inaccurately estimated, specifically evaporation and hyporheic exchange. The comparison of the Penman equation with measured pan evaporation suggests that the calculated evaporation does tend to be too high. Hyporheic exchange is a difficult term to estimate, as it depends on correct estimation of the hydrologic flux as well as the temperature of discharging hyporheic water. The spatial resolution of our temperature measurements in the water column and the stream bed was likely insufficient to represent accurately the temperatures and temperature gradients driving hyporheic heat exchange and bed heat conduction. This was especially true for the Mid Reach, which exhibited a more complex hydrology and thermal regime compared to the Low Reach (see Chapter 5). Additionally, the relatively heavy concentration of measurements in the Mid Reach near and in areas that were influenced by the groundwater seep may have influenced the spatial distribution of bed and hyporheic exchange measurements. Errors in sensible heat are likely small since the calculated values were negligible, and the evaporation pan measurements indicate that the Penman equation tends to over-estimate turbulent exchange in this environment. (Figure 3.8).

The results presented in this study are broadly consistent with previous research on forest streams by Story et al. [2003], Johnson [2004], and Moore et al. [2005c]. Hyporheic heat exchange was reported by Moore et al. [2005c] to be approximately 25% of the net radiation, lower than in the Low Reach but of similar magnitude to that in the Mid Reach. Bed heat conduction was estimated to be approximately 25% of net radiation in both reaches of Griffith Creek, which was higher than Moore et al. [2005c], but of similar magnitudes to those estimated by Brown [1969] for conduction in a bedrock stream. The high rates of bed heat conduction at Griffith Creek are likely a result of the relatively large quantities of lateral inflow and the interaction of groundwater in the streambed, which creates steep thermal gradients and larger energy fluxes for both bed heat conduction and hyporheic heat exchanges. Latent and sensible heat fluxes were negligible in the pre-logging period, but they increased to account for 25% and a small proportion of the cooling in the post-logging periods, respectively. Previous studies have

noted that sensible and latent heat exchanges tend to be an order of magnitude lower than net radiation [*Johnson*, 2004; *Moore et al.*, 2005], which is in a similar range for both the Low and Mid Reach post-logging results.

The results of this study demonstrate that net radiation is the dominant flux driving post-logging warming. Sensible heat flux was negligible before harvesting and became a small cooling flux in the post-harvest period, indicating that advection of warm air from the harvested area cannot be invoked as a cause of stream heating. Similarly, although the temperature of lateral inflow (shallow groundwater) did increase by about 2 °C after logging, it remained lower than stream temperature during the day time and thus did not contribute to stream warming. It is possible, however, that the warming of lateral inflow could have influenced daily minimum temperatures, which increased by up to about 2 °C during summer . Latent heat accounted for about 25% of the calculated cooling fluxes. The remainder was contributed by hyporheic exchange, bed heat conduction and, to a lesser extent in the Low Reach, groundwater discharge.

Table 6.1 RMSE of heat budget reach-average temperature change rates for two water column depths in Griffith Low Reach.

Date	Water Column Depth (cm)	RMSE	Water Column Depth (cm)	RMSE
July 2004	4.0	0.45	8.0	0.25
August 2004	1.8	0.31	3.0	0.19
July 2005	8.2	0.65	20.0	0.18
August 2005	4.2	0.73	10.0	0.28

Table 6.2 RMSE of heat budget reach-average temperature change rates for two water column depths in Griffith Mid Reach.

Date	Water Column Depth (cm)	RMSE	Water Column Depth (cm)	RMSE
July 2004	2.0	0.74	18.0	0.05
August 2004	2.3	0.53	10.0	0.11
July 2005	7.3	0.72	25.0	0.15
August 2005	2.3	3.04	15.0	0.34

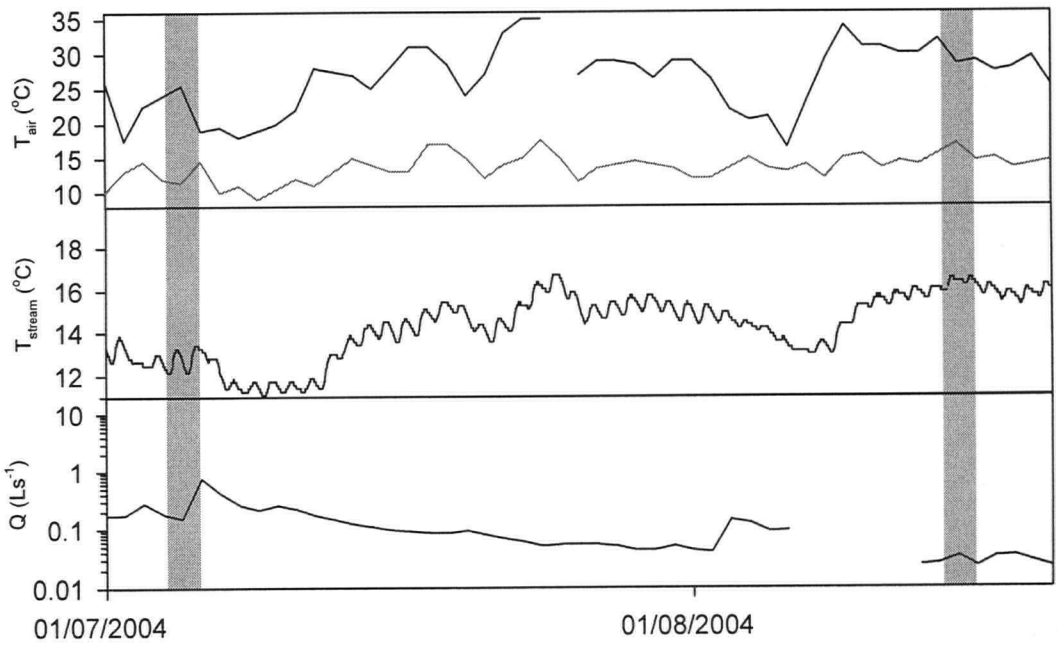

Figure 6.1 Air and stream temperatures and streamflow for July and August 2004. From top to bottom: daily maximum and minimum air temperature, Griffith Creek stream temperature and discharge. The shaded portion indicates the periods for the Heat Budgets.

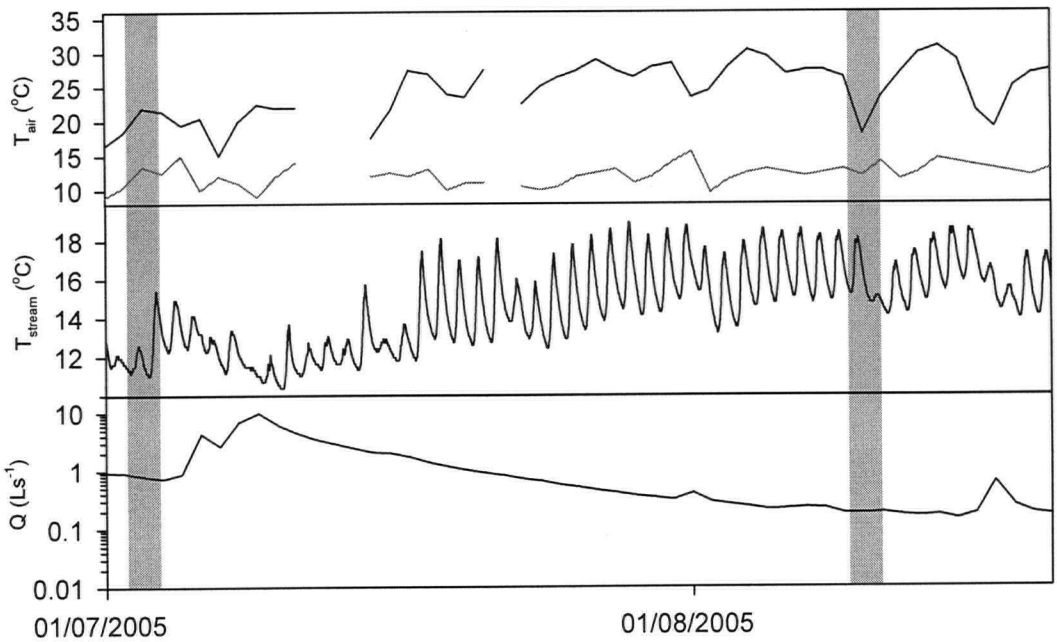

Figure 6.2 Air and stream temperatures and streamflow for July and August 2005. From top to bottom: daily maximum and minimum air temperature, Griffith Creek stream temperature and discharge. The shaded portion indicates the periods for the Heat Budgets.

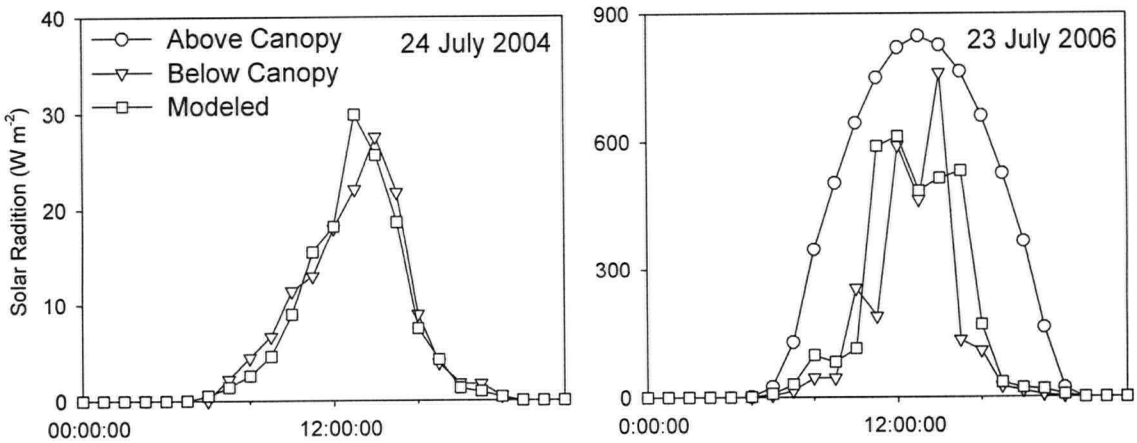

Figure 6.3 Modelled and observed solar radiation for pre- and post-logging conditions above Griffith Creek.

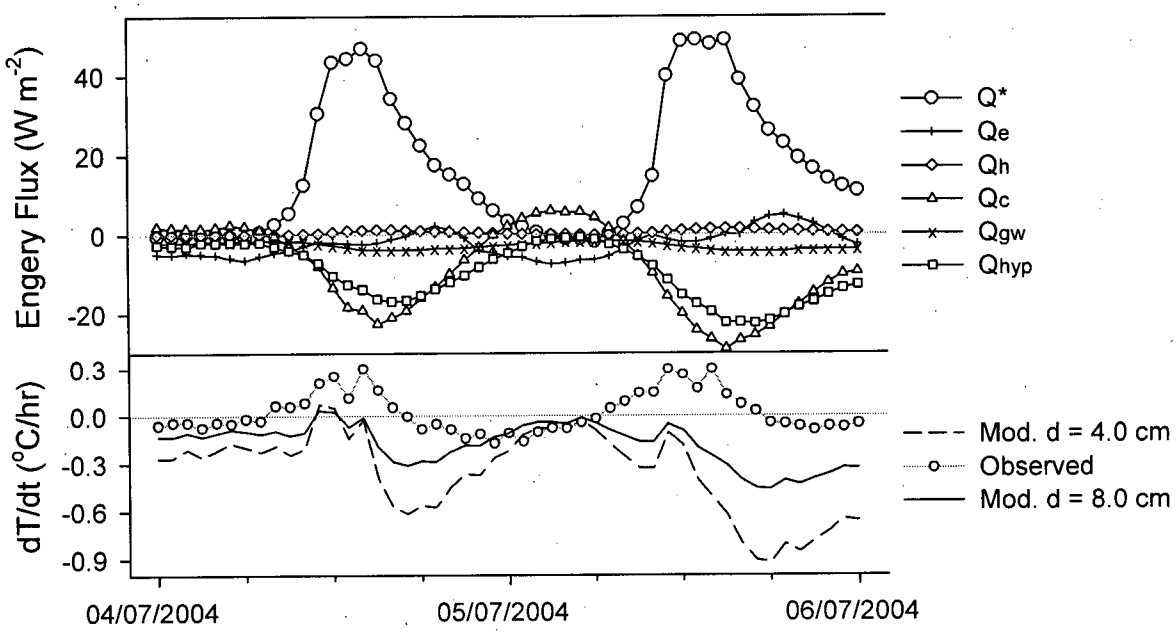

Figure 6.4 Energy fluxes and reach-average observed and modelled temperature change rates for two water column depths for July 5 and 6, 2004, in Griffith Low Reach.

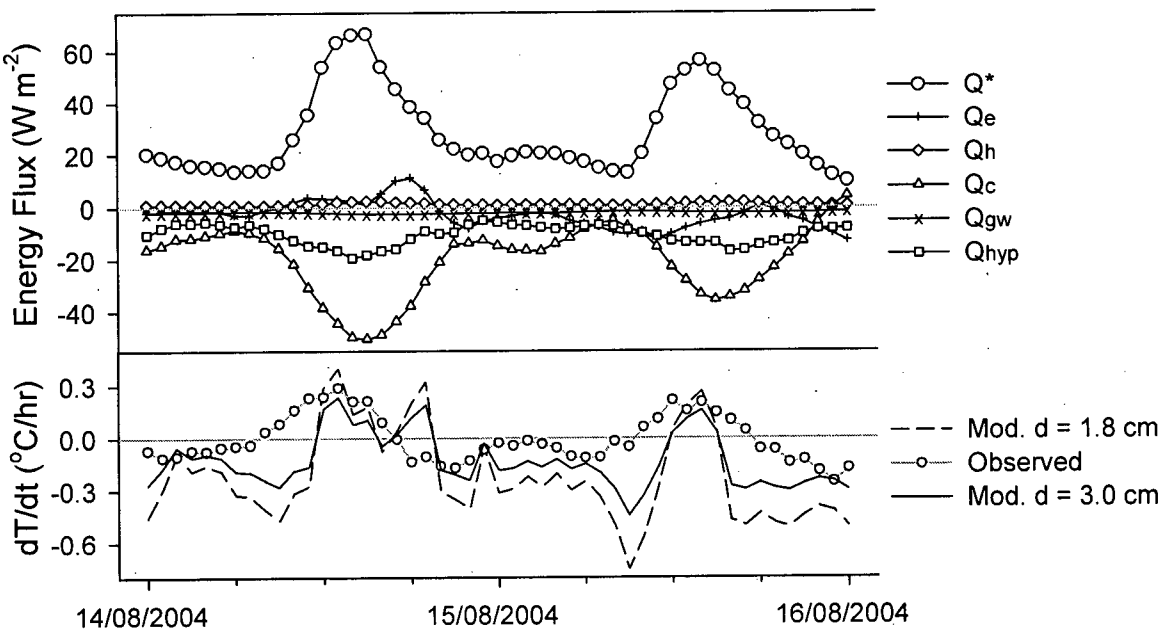

Figure 6.5 Energy fluxes and reach-average observed and modelled temperature change rates for two water column depths for August 15 and 16, 2004 in Griffith Low Reach.

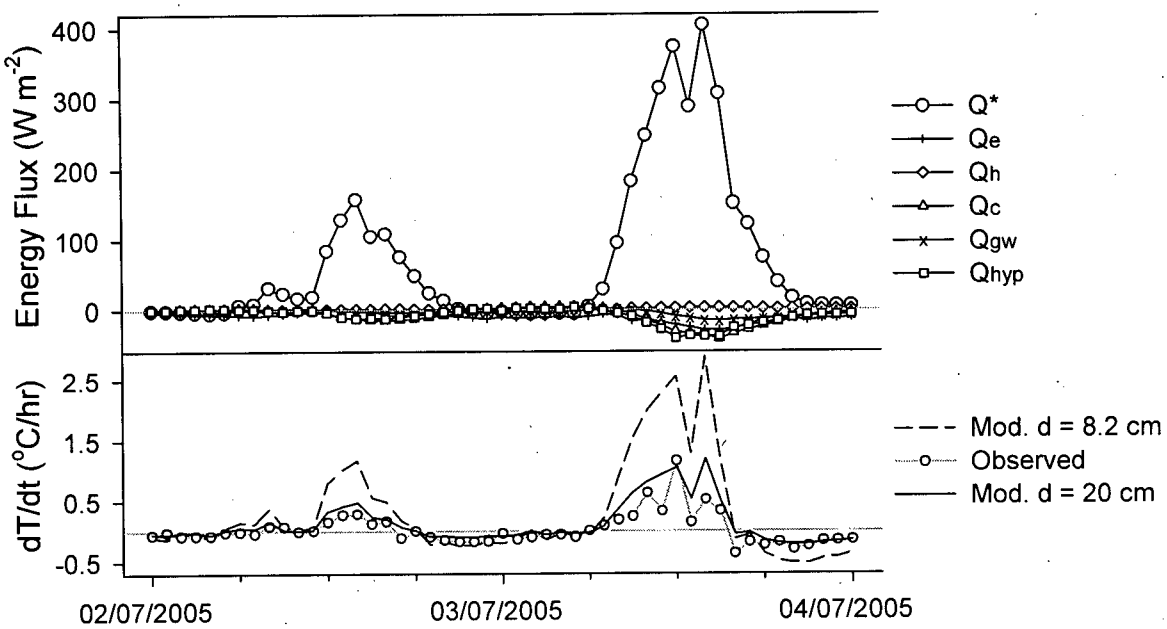

Figure 6.6 Energy fluxes and reach-average observed and modelled temperature change rates for two water column depths for July 3 and 4, 2005 in Griffith Low Reach.

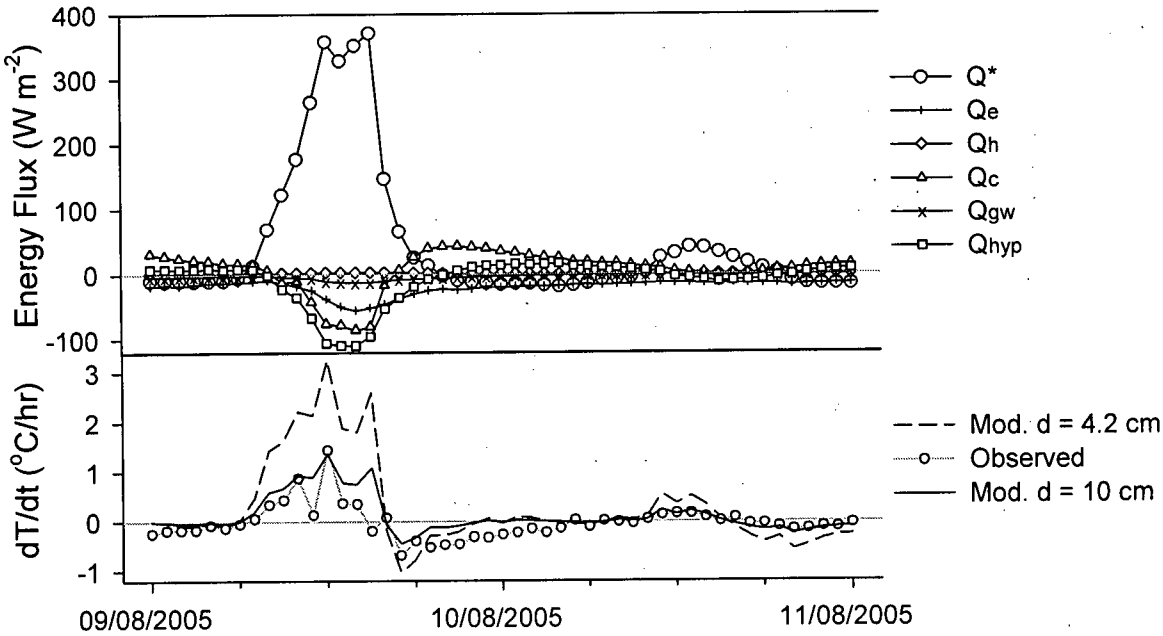

Figure 6.7 Energy fluxes and reach-average observed and modelled temperature change rates for two water column depths for August 10 and 11, 2005 in Griffith Low Reach.

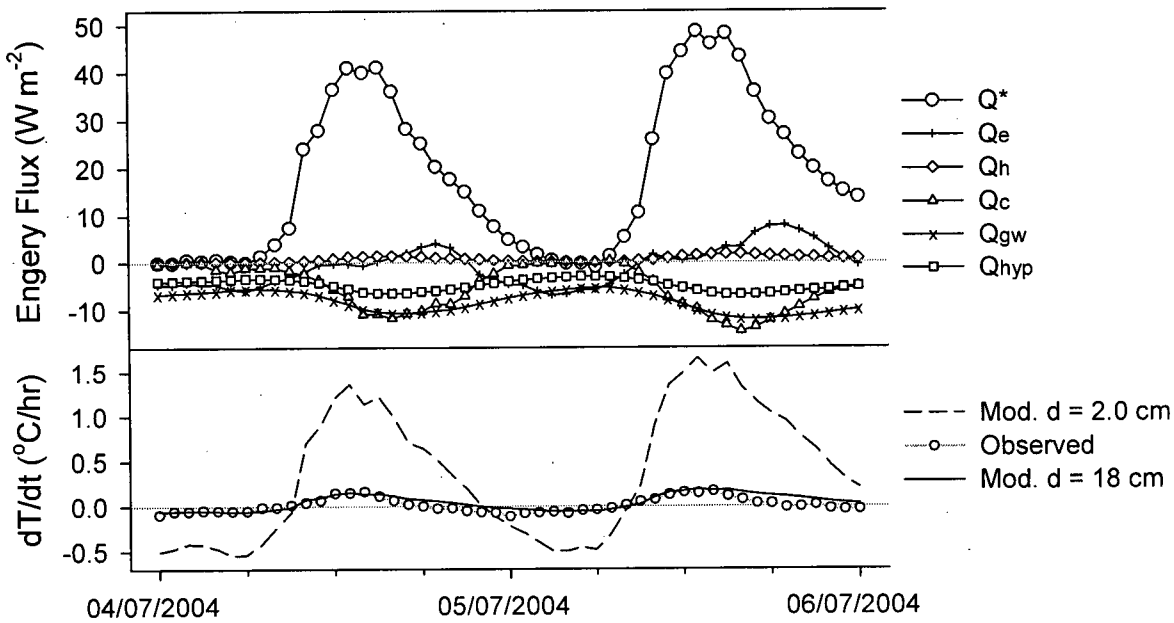

Figure 6.8 Energy fluxes and reach-average observed and modelled temperature change rates for two water column depths for July 5 and 6, 2004 in Griffith Mid Reach.

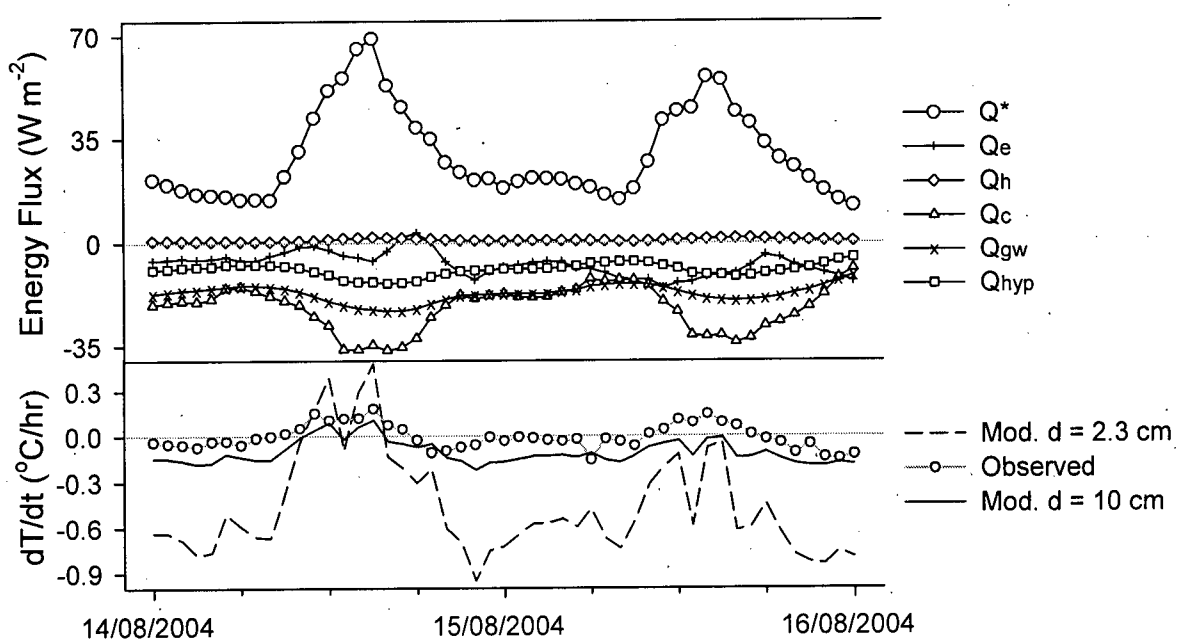

Figure 6.9 Energy fluxes and reach-average observed and modelled temperature change rates for two water column depths for August 15 and 16, 2004 in Griffith Mid Reach.

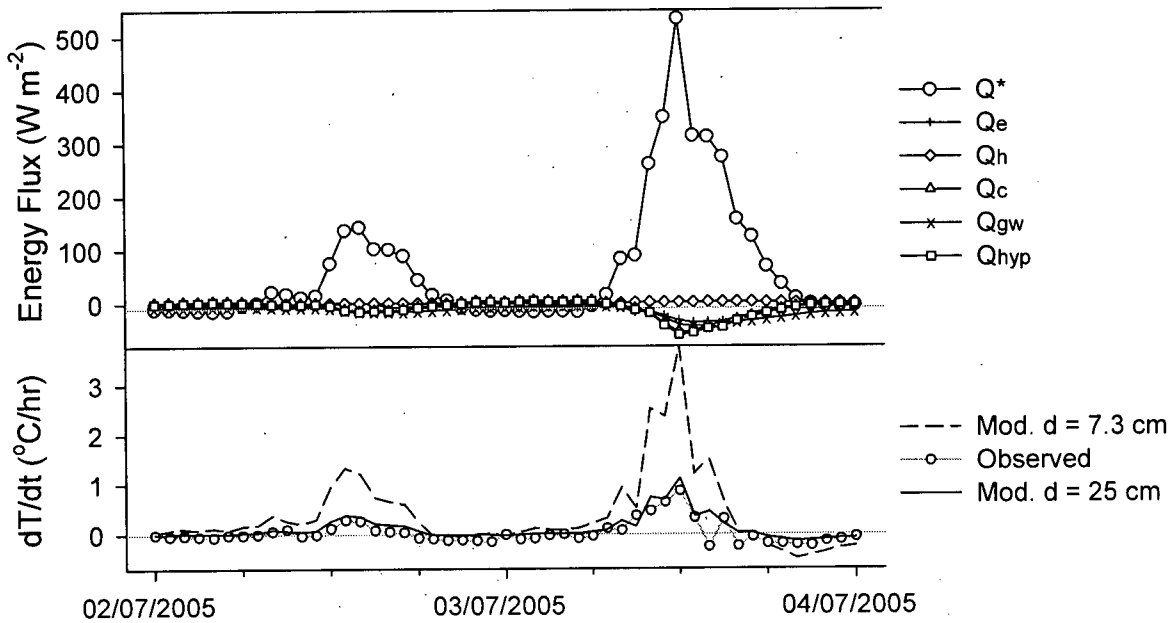

Figure 6.10 Energy fluxes and reach-average observed and modelled temperature change rates for two water column depths for July 3 and 4, 2005 in Griffith Mid Reach.

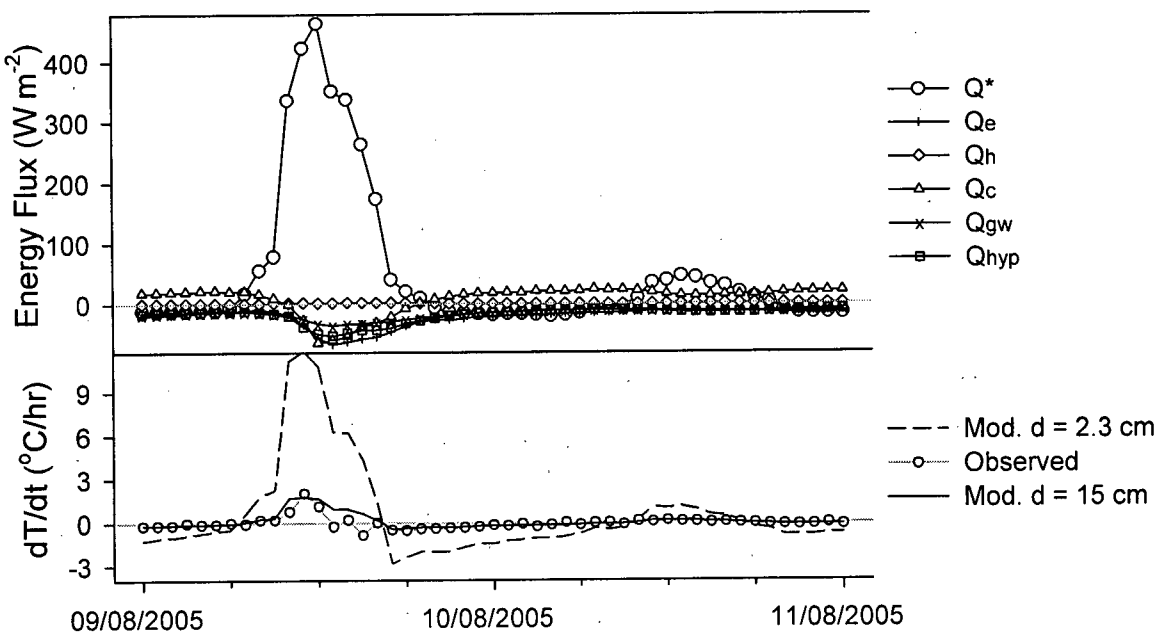

Figure 6.11 Energy fluxes and reach-average observed and modelled temperature change rates for two water column depths for August 10 and 11, 2005 in Griffith Mid Reach.

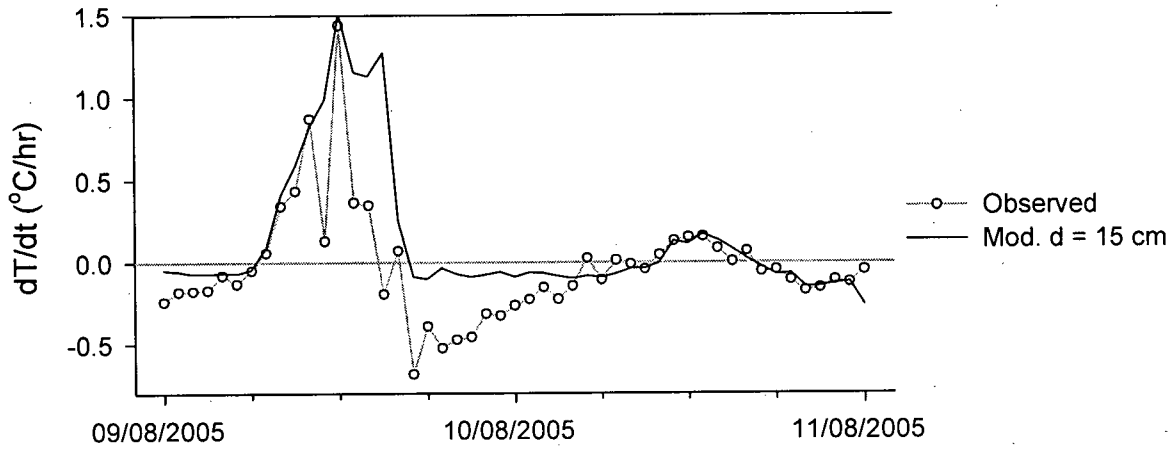

Figure 6.12 Reach-average observed and modelled temperature change rates for August 10 and 11, 2005 in Griffith Low Reach.

CHAPTER SEVEN

CONCLUSIONS

7.1 SUMMARY OF MAIN FINDINGS

7.1.1 Stream temperature response to a dispersed retention logging treatment

Warming was greatest in spring and summer, with no apparent warming in winter. The largest treatment effects occurred in spring and not during the period of seasonal peak temperatures, consistent with results from the Oregon Cascades [*Johnson and Jones*, 2000] and at other sites at MKRF [*Gomi et al.*, 2006]. While seasonal means of the daily mean and maximum temperatures increased with downstream distance through the cut block, post-logging changes in daily maximum temperature did not consistently increase with downstream distance. The greatest change in daily maximum temperature, 8 °C, occurred 200 m above the lower end of the cut block, suggesting that daily maximum temperatures can respond to local variations in heat exchanges, and not just the accumulation of heat as water flows through the cut block. The magnitude of warming was positively correlated to air temperature and negatively related to discharge. Daily minimum temperatures increased slightly in the summer months but showed no decreases in the two post-logging years.

Despite the considerable amount of shade provided by the dispersed retention within the cut block, the magnitude of warming at Griffith Creek is similar to or greater than that found for a number of streams subject to clear-cut logging with no riparian buffer, both in Malcolm Knapp Research Forest [*Gomi et al.*, 2006] and at other sites in the Pacific Northwest [Moore et al., 2005b]. One explanation is that Griffith Creek has a small catchment (12 ha) and thus low summer flows compared to many of the streams examined in previous studies. These low flows, combined with Griffith Creek's weakly incised channel and low banks, yield low surface water depths, increasing Griffith Creek's sensitivity to increased energy inputs. Therefore, it is difficult to assess the extent to which the 50% dispersed retention treatment protected Griffith Creek from stream warming through comparisons with other streams, without explicitly accounting for inherent differences in sensitivities through the use of a physically based heat budget model.

7.1.2 Hydrology and thermal regime of the stream bed

Bed temperature patterns differed between upwelling/neutral and downwelling zones. Temperatures responded to the logging treatment less dramatically in UW/N areas compared to DW areas, which showed similar maximum increases to those for stream water. The UW/N zones were better correlated with groundwater temperature patterns, while DW areas showed stronger correlations with surface water temperatures. Lateral inputs had a large influence on the thermal regime of the stream bed and almost overpowered the thermal patterns produced by vertical hyporheic exchange at some locations. Overall this study showed that bed temperature response to the logging treatment was not uniform and depended strongly on the direction of hyporheic exchange flows.

Post-logging bed temperature increases did not appear to be great enough to cause mortality of benthic invertebrates, based on published temperature thresholds for species found in Griffith Creek. However, the bed temperature changes could influence rates of growth and/or development and also timing of emergence. Because the post-logging thermal response varied with the direction of hyporheic exchange flows, the biological response to such changes should also exhibit distinctive spatial patterns. Such patterns should be considered in future attempts to assess the ecological influence of post-logging stream warming.

7.1.3 Heat budget analysis before and after logging

Net radiation was the dominant input of energy to the stream in both the pre- and post-logging periods. Latent and sensible heat was occasionally positive in the pre-logging period, and became negative fluxes in the post-logging summer. Therefore, advection of warm air from cut blocks does not appear to be a viable mechanism for explaining post-logging stream warming, reinforcing the dominant consensus that increased solar radiation following logging is the main driver of stream warming. Heat losses were dominated by groundwater, bed heat conduction, and hyporheic heat exchange. These terrestrial fluxes comprised 75% of the total heat loss from the stream, with evaporation being the main atmospheric heat loss.

The large differences between observed and modelled rates of temperature change in the pre-logging period were likely a result of small thermal gradients, which were near measurement errors for the temperature probes. The post-logging period showed better correspondence between observed and modelled temperature change, although the heat budget exhibited systematic errors, particularly by overestimating daytime warming. The good agreement between modelled and observed rates of temperature change with increased water column depth suggests

that rapid flow of water through the hyporheic zone increases the active volume of stream water engaged in heating and cooling. If this is the case, then the conceptualization of the thermal influence of the hyporheic zone used in this study, and by Moore *et al.* [2005c] should be reassessed.

7.2 RECOMMENDATIONS FOR FUTURE REASEARCH

This study revealed significant variability in bed temperatures, which undoubtedly introduced significant error into the calculated bed heat conduction and the heat exchange associated with hyporheic flows (which used bed temperatures to estimate the temperature of discharging hyporheic water). Bed temperatures were influenced by vertical advection via hyporheic exchange, as well as by advection via lateral inflow. To reduce uncertainties in the terrestrial heat fluxes, further research is required on water fluxes between a stream and its bed and banks, particularly the interactions between hyporheic flow paths and lateral inflow. Given the difficulties of studying these processes in complex headwater streams, it may be useful to study these processes through the use of numerical groundwater models and through physical models (e.g., flumes with step-pool structures). Understanding the processes in simplified systems may assist in designing sampling schemes to better measure the processes in complex streams.

While variations in surface water temperatures were not sampled to the same degree as bed temperatures, there was evidence of significant heterogeneity. For example, water temperatures in one pool were found to vary by up to 2 °C, and stream warming did not consistently display a systematic downstream pattern. Furthermore, water temperatures differed between areas of the stream bed influenced by different vertical hyporheic exchange flows. Because most of the energy flux computations involve stream temperature, it is critical to specify it accurately. A more detailed study of the variability of surface water temperatures in both time and space would help address some of the errors in the heat budget calculations, especially in a hydrologically complex reach such as the Mid Reach.

Given the significance of solar radiation as the dominant driver of post-logging warming, it is crucial to be able to estimate accurately how much insolation reaches the stream surface. Further research should focus on validating the use of canopy photographs for modelling solar radiation under complex canopies, particularly in relation to developing robust guidelines for setting thresholds for distinguishing sky from foliage.

This study has helped to answer questions related to how much stream temperatures change after logging and which processes are responsible. However, further research is required to examine how these temperature changes influence biological and ecological processes, and thus answer questions about their broader significance.

REFERENCES

Alexander, M. D., Caissie, D. (2003), Variability and comparison of hyporheic water temperatures and seepage fluxes in a small Atlantic salmon stream, *Ground Water*, *41*, 72-82.

Allen, J. D. (1995), Stream ecology: Structure and function of running waters, Chapman & Hall, New York, 388 pp.

Anderson, J. K., Wondzell, S.M., Gooseff, M.N., and Haggerty, R. (2005), Patterns in stream longitudinal profiles and implications for hyporheic exchange flow at the H.J. Andrews Experimental Forest, Oregon, USA, *Hydrological Processes*, *19*, 2931-2949.

Bao, Z. H., Cho, H.R., and Ye, H.C. (2002), Multi-temporal scale variations of summer precipitation in wet seasons over China and their association with 500 mb geopotential height, *Climate Research*, *20*, 107-122.

Baxter, C., Hauer, F.R., and Woessner, W.W. (2003), Measuring groundwater-stream water exchange: New techniques for installing minipiezometers and estimating hydraulic conductivity, *Transactions of the American Fisheries Society*, *123*, 493-502.

Beese, W. J., Dunsworth, B.G., Zielke, K., and Bancroft, B. (2003), Maintaining attributes of old-growth forests in coastal B.C. through variable retention, *Forestry Chronicle*, *79*, 570-578.

Beschta, R. L., Bilby, R.E., Brown, G.W., Holtby, L.B., and Hofstra, T.D. (1987), Stream temperature and aquatic habitats: fisheries and forestry interactions, in *Streamside management: forestry and fishery interactions.*, edited by C. E.O. Salo, T.W., pp. 191-232, Institute of Forest Resources, University of Washington, Seattle.

Bilby, R. E. (1984), Characteristics and frequency of cool-water areas in a western Washington stream, *Journal of Freshwater Ecology*, *2*, 593-602.

Bogan, T., Mohseni, O., and Stefan, H.G. (2003), Stream temperature-equilibrium temperature relationship, *Water Resources Research*, *39*, Art. No. 1245.

Bornette, G., and Amoros, C. (1991), Aquatic vegetation and hydrology of a braided river floodplain, *Journal of Vegetation Science*, *2*, 497-512.

Bourque, C. P. A., and Pomeroy, J.H. (2001), Effects of forest harvesting on summer stream temperatures in New Brunswick, Canada: an inter-catchment, multiple-year comparison, *Hydrology and Earth System Sciences*, *5*, 599-613.

Brittain, J. E., Saltveit, S.J., Castella, E., Bogen, J., Bonsnes, T.E., Blakar, I., Bremnes, T., Haug, I., and Velle, G. (2001), The macroinvertebrate communities of two contrasting Norwegian glacial rivers in relation to environmental variables, *Freshwater Biology*, *46*, 1723-1736.

Brosofske, K. D., Chen, J.Q., Naiman, R.J., and Franklin, J.F. (1997), Harvesting effects on microclimatic gradients from small streams to uplands in western Washington, *Ecological Applications*, *7*, 1188-1200.

Brown, G. W., and Krygier, J.T. (1970), Effects of clear-cutting on stream temperature, *Water Resources Research*, *6*, 1133-1139.

Brown, G. W. (1969), Predicting temperautre of small streams, *Water Resources Research*, *5*, 68-75.

Brunke, M., and Gonser, T. (1997), The ecological significance of exchange processes between rivers and groundwater, *Freshwater Biology*, *37*, 1-33.

Burton, T. M., and Likens, G.E. (1973), Effect of strip-cutting on stream temperatures in Hubbard Brook Experimental Forest, New Hampshire, *Bioscience*, *23*, 433-435.

Chang, D. H. S., and Gauch, H.G. (1986), Multivariate analysis of plant communities and environmental factors in Ngari, Tibet, *Ecology*, *67*, 1568-1575.

Constantz, J. (1998), Interaction between stream temperature, streamflow, and groundwater exchanges in alpine streams, *Water Resources Research*, *34*, 1609-1615.

Cox, T. J., and Rutherford, J.C. (1999), Thermal tolerances of two stream invertebrates exposed to diurnally varying temperature, *New Zealand Journal of Marine and Freshwater Research*, *34*, 209-215.

Cozzetto, D., McKnight, D., Nylen, T., and Fountain, A. (2006), Experimental investigation into processes controlling stream and hyporheic temperatures, Fryxell Basin, Antarctica, *Advances in Water Resources*, *29*, 130-153.

Crisp, D. T. (1988), Prediction, from temperature, of eyeing, hatching and swim-up times for salmonid embryos, *Freshwater Biology*, *19*, 41-48.

Crisp, D. T. (1990), Water temperature in a stream gravel bed and implications for salmonid incubation, *Freshwater Biology*, *23*, 601-612.

Curry, R. A., and Devito, K.J. (1996), Hydrogeology of brook trout (Salvelinus fontinalis) spawning and incubation implications for forestry and land use development, *Canadian Journal of Forest Research*, *26*, 767-772.

Curry, R. A., Scruton, D.A., and Clarke, K.D. (2002), The thermal regimes of brook trout incubation habitats and evidence of changes during forestry operations, *Canadian Journal of Forest Research*, *32*, 1200-1207.

Evans, E. C., McGregor, G.R., and Petts, G.E. (1998), River energy budgets with special reference to river bed processes, *Hydrological Processes*, *12*, 575-595.

Feller, M. C. (1981), Effect of clearcutting and slashburning on stream temperature in southwestern british columbia, *Water Resources Bulletin*, *17*, 863-867.

Freeze, R. A., and Cherry, J.A. (1979), *Groundwater*, Prentice-Hall, Englewood Cliffs, NJ.

Findlay, S. (1995), Importance of surface-subsurface exchange in stream ecosystems - the hyporheic zone, *Limnology and Oceanography*, *40*, 159-164.

Frazer, G. W., Canham, C.D., and Letzman, K.P. (1999), *Gap Light Analyser (GLA), Version 2.0: Imaging Software to extract structure and gap light transmission indices from true-colour fisheye photographs, users manual and program documentation.* Simon Fraser University, Bunaby, B.C. and the Institute of Ecosystem Studies, Millbrook, New York.

Gomi, T., Moore, R.D., and Dhakal, A.S. (2006), Headwater stream temperature response to clear-cut harvesting with different riparian treatments, coastal British Columbia, *Water Resources Research*, *42*, Art. No. W08437.

Gooseff, M. N., Anderson, J.K., Wondzell, S.M., LaNier, J., and Haggerty, R. (2005), A modelling study of hyporheic exchange pattern and the sequence, size, and spacing of stream bedforms in mountain stream networks, *Hydrological Processes*, *19*, 2915-2929.

Harris, D. D. (1977), *Hydrologic Changes After Logging in Two Small Oregon Coastal Watersheds*, U.S. Geologic Survey, Washington, 31 pp.

Hartman, G. F., and Scrivener, J.C. (1990), Impacts of forestry practices on a coastal stream ecosystem, Carnation Creek, British Columbia, *Canadian Bulletin of Fisheries and Aquatic Sciences*, *223*, 148 pp.

Harvey, J. W., and Bencala, K.E. (1993), The effect of streambed topography on surface-subsurface water exchange in mountain catchments, *Water Resources Research*, *29*, 89-98.

Hendricks, S. P., and White, D.S. (1991), Physicochemical patterns within a hyporheic zone of a northern Michigan River, with comments on surface-water patterns, *Canadian Journal of Fisheries and Aquatic Sciences*, *48*, 1645-1654.

Herlihy, A. T., Gerth, W.J., Li, J., and Banks, J.L. (2005), Macroinvertebrate community response to natural and forest harvest gradients in western Oregon headwater streams, *Freshwater Biology*, *50*, 905-919.

Hewlett, J. D., and Fortson, J.C. (1982), Stream temperature under an inadequate buffer strip in the southeast Piedmont, *Water Resources Bulletin*, *18*, 983-988.

Hill, A. R., Labadia, C.F., and Sanmugadas, K.H. (1998), Hyporheic zone hydrology and nitrogen dynamics in relation to the streambed topography of a N-rich stream, *Biogeochemistry*, *42*, 285-310.

Holtby, L. B. (1988), Effects of logging on stream temperatures in Carnation Creek, British Columbia, and associated impacts on the Coho Salmon (Oncorhynchus-Kisutch), *Canadian Journal of Fisheries and Aquatic Sciences*, *45*, 502-515.

Holtby, L. B., and Newcombe, C.P. (1982), A preliminary analysis of logging-related temperature changes in Carnation Creek, British Columbia. pp, 81-99, Department of Fisheries and Oceans, Pacific Biological Station, Nanaimo B.C.

Hutchens, J. J., Batzer, D.P., and Reese, E. (2004), Bioassessment of silvicultural impacts in stream and wetlands of the eastern United States, *Water Air and Soil Pollution Focus*, *4*, 37-53.

Hutchinson, D. G., and Moore, R.D. (2000), Throughflow variability on a forested slope underlain by compacted glacial till, *Hydrological Processes*, *14*, 1751-1766.

Idso, S. B. (1981), A set of equations for full spectrum and 8-14 μm and 10.5-12.5 μm thermal radiation from cloudless skies, *Water Resources Research*, *17*, 295-304.

Ihaka, R., and Gentleman, R. (1996), R: a language for data analysis and graphics, *Journal of Computational and Graphical Statistics*, *5*, 299-314.

Johnson, S. L., and Jones, J.A. (2000), Stream temperature responses to forest harvest and debris flows in western Cascades, Oregon, *Canadian Journal of Fisheries and Aquatic Sciences*, *57*, 30-39.

Johnson, S. L. (2004), Factors influencing stream temperatures in small streams: substrate effects and a shading experiment, *Canadian Journal of Fisheries and Aquatic Sciences*, *61*, 913-923.

Jolliffe, I. T. (1990), Principal component analysis: A beginner's guide - 1. Introduction and application, *Weather*, *45*, 375-382.

Kasahara, T., and Wondzell, S.M. (2003), Geomorphic controls on hyporheic exchange flow in mountain streams, *Water Resources Research*, *39*, Art. No. 1005.

Kenkel, N. C., and Orloci, L.H. (1986), Applying metric and nonmetric multidimensional-scaling to ecological studies - some new results, *Ecology*, *67*, 919-928.

Kiffney, P. M., Richardson, J.S., and Bull, J.P. (2003), Responses of periphyton and insects to experimental manipulation of riparian buffer width along forest streams, *Journal of Applied Ecology*, *40*, *19-21*.

Lapham, W. (1989), Use of temperature profiles beneath streams to determine rates of vertical ground-water flow and vertical hydraulic conductivity, *U.S. Geological Survey Water-Supply Paper 2337*.

Leggett, W. C., and Carscadden, J.E. (1978), Latitudinal variation in reproductive characteristics of American shad (*Alosa sapidissima*): evidence of population specific life history strategies in fish, *Journal of the Fisheries Research Board of Canada*, *35*, 1469-1478.

Levno, A., and Rothacher, J. (1967), Increases in maximum stream temperatures after logging in old-growth Douglas-Fir watersheds, *USDA Forest Services Research Note PNW 65, Portland*, *65*.

Loftis, J. C., MacDonald, L.H., Streett, S., Iyer, H.K., and Bunte, K. (2001), Detecting cumulative watershed effects, the statistical power of pairing, *Journal of Hydrology*, *251*, 49-64.

Macdonald, J. S., MacIsaac, E.A., and Herunter, H.E. (2003), The effect of variable-retention riparian buffer zones on water temperatures in small headwater streams in sub-boreal forest ecosystems of British Columbia, *Canadian Journal of Forest Research*, *33*, 1371-1382.

Malard, F., Mangin, A., Uehlinger, U., and Ward, J.V. (2001), Thermal heterogeneity in the hyporheic zone of a glacial floodplain, *Canadian Journal of Fisheries and Aquatic Sciences*, *58*, 1319-1335.

Malcolm, I. A., Soulsby, C.H., and Youngson, A.F. (2002), Thermal regime in the hyporheic zone of two contrasting salmonid spawning streams: ecological and hydrological implications, *Fisheries Management and Ecology*, *9*, 1-10.

Mantua, N. J., Hare, S.R., Zhang, Y., Wallace, J.M., and Francis, R.C. (1997), A Pacific interdecadal climate oscillation with impacts on salmon production, *Bulletin of the American Meteorological Society*, *78*, 1069-1079.

Mellina, E., Moore, R.D., Hinch, S.G., Macdonald, J.S., and Pearson, G.H. (2002), Stream temperature responses to clearcut logging in British Columbia: the moderating influences of groundwater and headwater lakes, *Canadian Journal of Fisheries and Aquatic Sciences*, *59*, 1886-1900.

Mohseni, O., Stefan, H.G., and Erickson, T.R. (1998), A nonlinear regression model for weekly stream temperature, *Water Resources Research*, *34*, 2685-2692.

Moore, R. D. (2005a), Introduction to salt dilution gauging for streamflow measurement Part 2: Constant-rate injection, *Streamline Watershed Management Bulletin*, *8*, 11-14.

Moore, R. D., Spittlehouse, D.L., and Story, A. (2005b), Riparian microclimate and stream temperature response to forest harvesting: A review, *Journal of the American Water Resources Association*, *41*, 813-834.

Moore, R. D., Sutherland, P., Gomi, T., and Dhakal, A. (2005c), Thermal regime of a headwater stream within a clearcut, coastal British Columbia, Canada, *Hydrological Processes*, *19*, 2591-2608.

Power, G., Brown, R. S., Imhof, J. G. (1999), Groundwater and fish-Insights from northern North America, *Hydrological Processes*, *13*, 401-422.

Ringler, N.H., and Hall, J.D. (1975). Effects of Logging on Water Temperature and Dissolved Oxygen in Spawning Beds. Transactions of the American Fisheries Society 104:111-121.

Rutherford, J. C., Blackett, S., Blackett, C., Saito, L., and Davies-Colley, R.J. (1997), Predicting the effects of shade on water temperature in small streams, *New Zealand Journal of Marine and Freshwater Research*, *31*, 707-721.

Shieh, S. H., and Yang, P.S. (2000), Community structure and functional organization of aquatic insects in an agricultural mountain stream of Taiwan: 1985-1986 and 1995-1996, *Zoological Studies*, *19*, 191-202.

Silliman, S. E., and Booth, D.F.H. (1993), Analysis of time-series measurements of sediment temperature for identification of gaining vs losing portions of Juday Creek, Indiana, *Journal of Hydrology*, *146*, 131-148.

Sridhar, V., Sansone, A.L., LaMarche, J., Dubin, T., and Lettenmaier, D.P. (2004), Prediction of stream temperature in forested watersheds, *Journal of the American Water Resources Association*, *40*, 197-213.

Storey, R. G., and Cowley, D.R. (1997), Recovery of three New Zealand rural streams as they pass through native forest remnants, *Hydrobiologia*, *353*, 63-76.

Story, A., Moore, R.D., and Macdonald, J.S. (2003), Stream temperatures in two shaded reaches below cutblocks and logging roads: downstream cooling linked to subsurface hydrology, *Canadian Journal of Forest Research*, *33*, 1383-1396.

Termonia, P. H. (2001), On the removal of random variables in data sets of meteorological observations, *Meteorology and Atmospheric Physics*, *78*, 143-156.

Titcomb, J. (1926), Forests in relation to fresh water fishes, *Transactions of the American Fish Society*, *56*, 122-129.

Vannote, R. L., and Sweeney, B.W. (1980), Geographic analysis of thermal equilibria - a conceptual model for evaluating the effect of natural and modified thermal regimes on aquatic insect communities, *American Naturalist*, *115*, 667-695.

Wartenberg, D., Ferson, S., and Rohlf, F.J. (1987), Putting things in order - a critique of detrended correspondence analysis, *American Naturalist*, *129*, 434-448.

Ward, J. V., and Stanford, J.A. (1992), Thermal response in the evolutionary ecology of aquatic insects, *Annual Reviews of Entomology*, *27*, 97-117.

Watson, F., Vertessy, R., McMahon, T., Rhodes, B., and Watson, I. (2001), Improved methods to assess water yield changes from paired-catchment studies: application to the Maroondah catchments, *Forest Ecology and Management*, *143*, 189-204.

Webb, B. W., and Zhang, Y. (1997), Spatial and seasonal variability in the components of the river heat budget, *Hydrological Processes*, *11*, 79-101.

White, D. S., Elzinga, C.H., Hendricks, S.P. (1987), Temperature patterns within the hyporheic zone of a northern Michigan river, *Journal of the North American Benthological Society*, *6*, 85-91.

Wondzell, S. M. (2005), Effect of morphology and discharge on hyporheic exchange flows in two small streams in the Cascade Mountains of Oregon, USA, *Hydrological Processes*, *20*, 267-287.

Zwieniecki, M., and Newton, M. (1999), Influences of streamside cover and stream features on temperature trends in forested streams of Western Oregon, *Western Journal of Applied Forestry*, *14*, 106-113.

APPENDIX A. Hydraulic gradients measured in Griffith Creek Low Reach during 2004. r_s are Spearman Correlation between discharge and hydraulic gradients, DW and UW/N indicates seasonally down- and up-welling/neutral hydraulic gradients, respectively. Columns are arranged from left to right in order of decreasing discharge.

Piezometer	Hydraulic Gradient								r_s	Hydrologic Setting
1	0.03	0.00	0.02	-0.02	0.00	0.02	0.00	-0.03	0.58	UW/N
2	-0.03	0.00	0.00	-0.03	0.00	0.00	0.00	0.00	-0.51	UW/N
3	-0.14	-0.08	0.00	-0.03	-0.03	-0.03	-0.09	-0.09	0.09	DW
4	-0.04	-0.06	-0.06	0.00	-0.08	-0.04	0.00	-0.02	-0.45	DW
5	0.00	0.06	0.00	0.00	0.00	0.03	0.07	0.07	-0.69	UW/N
6	-0.10	-0.09	-0.08	0.00	-0.28	-0.07	-0.15	-0.16	0.34	DW
7	-0.33	-0.37	-0.13	NA	-0.21	NA	-0.39	-0.43	0.55	DW
8	0.00	0.03	0.00	0.00	0.00	0.00	0.00	-0.05	0.62	UW/N
9	0.00	0.04	0.00	0.00	0.00	0.00	0.04	0.02	-0.38	UW/N
10	-0.13	-0.59	-0.59	-0.63	0.00	-0.72	-0.74	-0.74	0.76	DW
11	-0.49	-0.48	-0.47	-0.52	-0.65	-0.53	-0.56	-0.54	0.77	DW
12	-0.28	-0.08	-0.25	-0.26	0.00	-0.39	-0.36	-0.45	0.57	DW
13	-0.18	-0.29	-0.15	-0.16	-0.37	-0.17	-0.12	-0.12	-0.55	DW
Discharge Ls^{-1}	0.58	0.15	0.15	0.09	0.07	0.05	0.03	0.03		
Sample Date	24/8/ 2004	13/7/ 2004	3/8/ 2004	6/8/ 2004	22/7/ 2004	28/7/ 2004	13/8/ 2004	16/8/ 2004		

APPENDIX B. Hydraulic gradients measured in Griffith Creek Low Reach during 2005. r_s are Spearman Correlation between discharge and hydraulic gradients, DW and UW/N indicates seasonally down- and up-welling/neutral hydraulic gradients, respectively. Columns are arranged from left to right in order of decreasing discharge.

Piezometer	Hydraulic Gradient																	r_s	Hydrologic Setting
1	0.17	0.15	0.15	0.23	0.09	0.15	0.15	0.18	0.14	0.19	0.17	0.17	0.19	0.22	0.20	0.11	0.17	-0.24	UW/N
2	0.00	0.00	0.00	0.00	-0.03	-0.02	-0.02	0.00	-0.02	0.00	0.00	-0.04	0.00	0.00	0.00	-0.04	-0.03	0.33	UW/N
3	0.00	0.00	0.00	0.00	0.04	0.13	-0.05	0.10	-0.02	0.07	-0.04	0.05	-0.03	0.00	-0.02	0.00	-0.05	0.32	UW/N
4	0.02	0.00	0.03	0.02	-0.07	-0.10	-0.08	-0.08	0.03	-0.09	0.00	-0.09	0.07	0.00	0.00	0.10	-0.09	0.07	DW
5	0.02	0.00	0.00	0.00	0.00	-0.02	-0.02	-0.02	0.00	0.00	-0.03	-0.03	0.00	-0.03	0.03	0.00	0.00	0.17	UW/N
6	0.00	0.00	-0.02	0.07	0.00	-0.02	-0.02	-0.02	-0.04	-0.02	-0.04	-0.04	-0.03	-0.04	0.00	0.02	-0.04	0.43	UW/N
7	-0.15	-0.15	-0.14	-0.06	-0.35	-0.35	-0.33	-0.35	-0.30	-0.40	-0.20	-0.36	-0.33	-0.26	-0.29	-0.33	-0.33	0.36	DW
8	0.00	0.02	0.00	0.03	0.02	0.00	0.00	0.00	0.03	0.09	0.00	0.03	0.00	0.00	-0.03	-0.02	0.03	0.15	UW/N
9	0.00	0.00	0.00	0.01	0.00	0.02	0.02	0.00	0.02	0.02	0.00	0.00	0.00	0.00	0.00	0.00	0.04	-0.07	UW/N
10	-0.57	-0.58	-0.49	-0.33	-0.60	-0.58	-0.59	-0.63	-0.63	-0.61	-0.59	-0.58	-0.61	-0.62	-0.60	-0.60	-0.61	0.59	DW
11	-0.41	-0.43	-0.30	-0.28	-0.45	-0.45	-0.45	-0.50	-0.49	-0.44	-0.47	-0.45	-0.45	-0.45	-0.45	-0.44	-0.44	0.55	DW
12	-0.33	-0.32	-0.41	-0.27	-0.33	-0.35	-0.29	-0.36	-0.37	-0.36	-0.35	-0.34	-0.36	-0.35	-0.35	-0.36	-0.34	0.36	DW
13	-0.28	-0.24	-0.20	-0.26	-0.14	-0.11	-0.11	-0.14	-0.16	-0.12	-0.17	-0.17	-0.16	-0.16	-0.21	-0.12	-0.22	-0.21	DW
14	-0.11	-0.11	-0.10	-0.09	NA	NA	NA	NA	-0.12	NA	-0.14	NA	-0.14	-0.14	-0.14	-0.15	-0.17	0.89	DW
15	-0.02	-0.11	0.00	0.00	NA	NA	NA	NA	0.00	NA	-0.05	NA	-0.05	-0.05	-0.02	-0.05	-0.02	0.18	DW
Discharge $L\ s^{-1}$	6.82	5.53	4.84	3.68	2.76	0.83	0.72	0.55	0.52	0.36	0.33	0.28	0.28	0.26	0.24	0.22	0.15		
Sample Date	8/10 /2005	3/10 /2005	29/10 /2005	24/10 /2005	6/6 /2005	22/7 /2005	30/5 /2005	25/7 /2005	5/9 /2005	29/7 /2005	17/9 /2005	2/8 /2005	2/9 /2005	10/9 /2005	26/9 /2005	5/8 /2005	15/8 /2005		

APPENDIX C. Cross-correlation coefficients and lags in minutes for bed temperatures on two clear and cloudy sky days in the pre- and post-logging period in the Low Reach. CC is the Cross-correlation coefficient. DW and UW mean down- and up-welling flows, respectively.

Location and depth (cm)	Pre-Logging Period								Post-Logging Period							
	Clear Sky				Cloudy Sky				Clear Sky				Cloudy Sky			
	Stream Temperature		Seep Temperature		Stream Temperature		Seep Temperature		Stream Temperature		Seep Temperature		Stream Temperature		Seep Temperature	
	CC	Lag	CC	Lag	CC	Lag	CC	Lag	CC	Lag	CC	Lag	CC	Lag	CC	Lag
S1U 1 (DW)	0.98	0	0.14	770	0.98	0	0.85	0	0.92	-190	0.45	580	0.84	-20	0.58	520
S1U 5 (DW)	0.96	-50	0.14	690	0.97	0	0.87	0	0.90	-230	0.47	550	0.77	0	0.57	510
S1U 10 (DW)	0.91	-120	0.23	230	0.95	0	0.90	0	0.86	-280	0.49	480	0.70	0	0.55	510
S1U 15 (DW)	0.83	-180	0.33	190	0.94	0	0.92	0	0.82	-340	0.51	430	0.66	0	0.54	480
S1U 30 (DW)	0.51	-390	0.76	0	0.88	0	0.95	0	0.67	-500	0.54	320	0.66	0	0.52	440
S1D 1 (UW)	0.98	0	0.17	750	0.99	0	0.83	0	0.92	-90	0.42	650	0.92	0	0.58	640
S1D 5 (UW)	0.88	-110	0.31	240	0.98	0	0.88	0	0.87	-120	0.45	610	0.87	-20	0.58	540
S1D 10 (UW)	0.75	-170	0.52	140	0.96	0	0.90	0	0.83	-190	0.48	550	0.82	-50	0.58	510
S1D 20 (UW)	0.44	-320	0.84	50	0.92	0	0.93	0	0.67	-340	0.48	480	0.72	-80	0.55	490
S2U 1 (DW)	0.97	-10	0.14	740	0.99	0	0.80	0	0.92	10	0.42	780	0.97	0	0.50	710
S2U 5 (DW)	0.95	-70	0.16	680	0.98	0	0.85	0	0.89	-20	0.45	700	0.95	0	0.54	640
S2U 10 (DW)	0.90	-130	0.24	200	0.95	0	0.90	0	0.85	-170	0.49	590	0.86	-20	0.56	540
S2U 20 (DW)	0.80	-200	0.43	150	0.92	0	0.93	0	0.79	-250	0.53	490	0.76	-40	0.56	510
S3U 1 (DW)	0.95	90	0.13	890	0.99	0	0.77	0	0.86	80	0.39	870	0.75	60	0.38	860
S3U 5 (DW)	0.99	0	0.15	780	0.99	0	0.81	0	0.96	0	0.40	820	0.98	0	0.51	780
S3U 10 (DW)	0.97	-30	0.16	740	0.99	0	0.84	0	0.94	-70	0.42	720	0.98	0	0.56	640
S3U 15 (DW)	0.93	-90	0.21	270	0.97	0	0.87	0	0.87	-180	0.47	570	0.86	-10	0.57	520
S3U 30 (DW)	0.61	-290	0.68	50	0.92	0	0.94	0	0.63	-460	0.57	330	0.62	-110	0.53	440
S3D 1 (UW)	0.93	-80	0.19	290	0.98	0	0.88	0	0.91	-160	0.47	620	0.88	0	0.57	540
S3D 5 (UW)	0.87	-130	0.31	210	0.96	0	0.90	0	0.86	-230	0.50	550	0.77	0	0.57	510
S3D 10 (UW)	0.73	-210	0.51	130	0.94	0	0.92	0	0.77	-340	0.48	340	0.70	0	0.55	500
S3D 20 (UW)	0.49	-350	0.79	20	0.91	0	0.95	0	0.67	-440	0.52	230	0.65	0	0.53	440

APPENDIX D. Hydraulic gradients measured in Griffith Creek Mid Reach during 2004. r_s are Spearman Correlation between discharge and hydraulic gradients, DW and UW/N indicates seasonally down- and up-welling/neutral hydraulic gradients, respectively. Columns are arranged from left to right in order of decreasing discharge.

Piezometer	Hydraulic Gradient								r_s	Hydrologic Setting
1	0.00	-0.10	-0.03	-0.05	-0.03	0.00	-0.03	0.00	-0.25	DW
2	0.01	0.01	0.01	0.01	0.02	-0.01	0.01	0.01	0.11	UW/N
3	0.09	0.05	0.09	0.05	0.09	0.05	0.05	0.05	0.57	UW/N
4	0.09	0.09	0.06	0.03	0.00	0.00	0.03	0.03	0.71	UW/N
5	-0.61	-0.52	-0.53	-0.50	-0.50	-0.46	-0.53	-0.50	-0.52	DW
6	0.00	0.04	0.00	0.01	0.01	0.00	0.00	0.00	0.28	UW/N
7	0.00	0.00	0.00	0.00	0.00	0.06	0.00	0.00	-0.25	UW/N
8	-0.01	0.00	-0.12	-0.02	-0.02	-0.02	-0.02	-0.02	0.35	UW/N
9	-0.05	-0.07	-0.07	-0.07	-0.10	-0.07	-0.07	-0.10	0.63	DW
10	0.02	0.02	0.05	0.02	0.09	0.02	0.00	0.02	0.36	UW/N
11	0.00	0.10	0.00	0.03	0.00	0.00	0.00	0.00	0.34	UW/N
12	NA	NA	NA	NA	NA	NA	NA	NA	NA	NA
13	-0.19	-0.25	-0.22	-0.25	-0.19	-0.25	-0.25	-0.22	0.31	DW
Discharge $L \cdot s^{-1}$	0.41	0.09	0.09	0.05	0.04	0.02	0.01	0.01		
Sample Date	24/8 /2004	13/7 /2004	3/8 /2004	6/8 /2004	22/7 /2004	28/7 /2004	13/8 /2004	16/8 /2004		

APPENDIX E. Hydraulic gradients measured in Griffith Creek Mid Reach during 2005. r_s are Spearman Correlation between discharge and hydraulic gradients, DW and UW/N indicates seasonally down- and up-welling/neutral hydraulic gradients, respectively. Columns are arranged from left to right in order of decreasing discharge.

Piezometer	Hydraulic Gradient																	r_s	Hydrologic Setting
1	0.11	0.09	0.04	0.06	0.06	0.02	0.05	0.04	0.02	0.04	0.00	0.05	0.00	0.05	0.00	0.00	0.05	0.57	UW/N
2	0.05	0.11	0.00	0.08	-0.05	0.00	0.03	-0.06	0.03	-0.06	0.00	-0.06	0.03	0.06	0.00	0.13	0.03	0.04	UW/N
3	0.05	0.00	0.06	0.06	0.03	NA	0.00	0.03	0.04	0.00	0.00	0.04	0.04	0.00	0.04	-0.04	-0.04	0.51	UW/N
4	-0.06	-0.08	0.00	0.00	-0.02	NA	-0.03	0.00	0.00	-0.03	-0.06	0.00	-0.03	0.00	0.00	-0.06	-0.06	-0.03	DW
5	0.00	0.02	0.05	0.02	-0.08	NA	-0.04	-0.04	-0.02	-0.09	-0.07	-0.09	-0.05	-0.05	-0.05	-0.11	-0.02	0.60	DW
6	0.00	-0.05	0.02	0.05	-0.02	0.00	0.00	0.09	0.02	0.02	0.05	0.00	0.05	0.02	0.00	0.00	0.02	-0.21	UW/N
7	-0.02	0.00	0.02	0.00	0.00	NA	-0.03	0.00	0.05	0.00	0.05	-0.03	-0.03	0.03	0.00	0.00	0.03	-0.19	UW/N
8	0.00	0.02	0.02	0.00	-0.02	0.00	-0.02	-0.15	0.02	0.00	-0.02	0.00	-0.02	0.04	0.00	-0.02	0.02	0.04	UW/N
9	0.07	0.02	0.02	0.00	0.07	0.04	0.05	0.05	0.06	0.05	0.00	0.02	0.03	0.03	0.03	0.02	0.02	0.26	UW/N
10	-0.11	-0.11	-0.12	-0.03	-0.11	-0.16	-0.16	-0.17	-0.06	-0.19	-0.18	-0.17	-0.18	-0.06	-0.16	0.26	-0.24	0.31	DW
11	0.02	0.04	0.04	0.04	0.04	0.02	0.08	0.02	-0.13	0.02	0.02	0.02	0.02	-0.09	0.00	-0.02	0.00	0.71	UW/N
12	-0.22	-0.65	-0.24	-0.12	-0.51	-0.43	-0.51	-0.12	-0.07	-0.37	-0.13	-0.34	-0.04	-0.09	-0.19	-0.32	-0.13	0.71	DW
13	-0.12	-0.13	-0.08	-0.04	-0.13	NA	-0.16	-0.17	-0.15	-0.19	-0.15	-0.19	-0.11	-0.17	-0.20	-0.17	-0.19	0.71	DW
Discharge $L \cdot s^{-1}$	6.79	5.34	4.59	3.36	2.42	1.13	0.52	0.39	0.36	0.23	0.22	0.18	0.18	0.17	0.15	0.14	0.09		
Sample Date	8/10 /2005	3/10 /2005	29/10 /2005	24/10 /2005	6/6 /2005	18/7 /2005	30/5 /2005	25/7 /2005	5/9 /2005	29/7 /2005	17/9 /2005	2/8 /2005	2/9 /2005	10/9 /2005	26/9 /2005	5/8 /2005	15/8 /2005		

APPENDIX F. Cross-correlation coefficients and lags in minutes for bed temperatures on two clear and cloudy sky days in the pre- and post-logging period in the Mid Reach. CC is the Cross-correlation coefficient. DW and UW mean down- and up-welling flows, respectively.

Location and Depth (cm)	Pre-Logging Period								Post-Logging Period							
	Clear Sky				Cloudy Sky				Clear Sky				Cloudy Sky			
	Stream Temperature		Seep Temperature		Stream Temperature		Seep Temperature		Stream Temperature		Seep Temperature		Stream Temperature		Seep Temperature	
	CC	Lag	CC	Lag	CC	Lag	CC	Lag	CC	Lag	CC	Lag	CC	Lag	CC	Lag
L1-5	0.90	-60	0.39	450	0.93	-30	0.73	320	0.96	10	0.45	430	0.99	20	0.60	440
L1-10	0.24	-470	0.98	0	0.60	-380	0.97	0	0.70	-190	0.80	100	0.82	-190	0.82	170
L2-5	0.73	-120	0.55	210	0.88	-90	0.79	240	0.87	-80	0.63	220	0.94	-80	0.72	280
L2-10	0.46	-260	0.82	40	NA	NA	NA	NA	0.77	-130	0.76	120	0.86	-160	0.79	180
L2-30	0.24	-690	0.98	0	0.57	-510	0.92	-20	0.41	-510	0.94	0	0.54	-470	0.94	0
L3-1	0.39	-250	0.83	10	0.66	-210	0.88	80	0.93	0	0.46	390	0.98	10	0.58	430
L3-5	NA	NA	NA	NA	0.61	-250	0.92	40	0.93	-10	0.58	300	0.97	-20	0.64	340
L3-10	0.31	-350	0.93	0	0.61	-300	0.96	10	0.82	-30	0.64	220	0.94	-90	0.69	270
L3-20	0.25	-510	0.99	0	0.60	-410	0.99	0	0.66	-220	0.86	0	0.82	-220	0.82	110
L4-1 (DW)	NA	NA	NA	NA	0.63	-80	0.81	210	0.87	50	0.35	530	0.95	50	0.59	490
L4-5 (DW)	0.69	-120	0.58	210	0.63	-130	0.84	190	0.96	0	0.39	480	0.98	0	0.62	380
L4-10 (DW)	0.48	-220	0.79	60	0.55	-230	0.89	60	0.98	-10	0.48	360	0.93	-40	0.69	290
L4-15 (DW)	0.36	-340	0.92	0	0.53	-320	0.96	0	0.89	-90	0.58	280	0.84	-130	0.77	190
L4-30 (DW)	0.25	-560	0.99	0	0.50	-450	0.95	0	0.67	-270	0.90	0	0.65	-310	0.94	0
L5-1 (UW)	0.50	-210	0.75	60	0.63	-190	0.87	120	0.96	0	0.53	310	0.94	-30	0.70	320
L5-5 (UW)	NA	NA	NA	NA	0.56	-250	0.91	40	0.87	-30	0.60	280	0.89	-100	0.74	250
L5-10 (UW)	0.32	-370	0.94	0	NA	NA	NA	NA	0.80	-100	0.69	100	0.83	-140	0.79	180
L5-15 (UW)	0.26	-470	0.98	0	0.53	-410	0.98	0	0.69	-190	0.81	0	0.75	-210	0.84	110
L5-30 (UW)	0.25	-670	0.99	0	0.59	500	0.94	-10	0.51	-380	0.99	0	0.61	-370	0.99	0